ETHYLENEDIAMINETETRAACETATE AND NITRILOTRIACETATE DEGRADATION BY BACTERIUM BNC1: BIOCHEMICAL CHARACTERIZATION OF THE SUBSTRATE UPTAKE SYSTEM AND CLONING OF THE ENTIRE EDTA-DEGRADING GENE CLUSTER IN *ESCHERICHIA COLI*

By

JACOB PAUL HERMAN

A dissertation submitted in partial fulfillment of
the requirements of the degree of

DOCTOR OF PHILOSOPHY
(MICROBIOLOGY)

WASHINGTON STATE UNIVESITY
School of Molecular Biosciences

AUGUST 2004

To the Faculty of Washington State University:

The members of the Committee appointed to examine the dissertation of JACOB PAUL HERMAN find it satisfactory and recommend that it be accepted.

_____
Chair

_____

_____

_____

_____

ACKNOWLEDGMENTS

I would like to thank my committee, Drs. Luying Xun, Michael Kahn, Linda Thomashow, James Petersen, and Harvey Bolton Jr. for their advice, ideas, and assistance in research project development during my graduate studies. I would like to especially thank Dr. Luying Xun, my mentor, for his patience, understanding, and friendship during my training. He has helped me become the scientist that I am, and I am forever indebted to him. I would also like to thank all the members of the lab, past and present, including Dr. Tai Man Louie, Dr. Yong Lui, Dr. Mian Cai, Dr. Geoffrey Puzon, and Michelle Gisi for their consistent advice and help in all areas of my research. Finally, I would like to especially thank Chris Webster for enduring many years of in depth scientific discussions and helping with many of my experiments.

ETHYLENEDIAMINETETRAACETATE AND NITRILOTRIACETATE DEGRADATION BY BACTERIUM BNC1: BIOCHEMICAL CHARACTERIZATION OF THE SUBSTRATE UPTAKE SYSTEM AND CLONING OF THE ENTIRE EDTA-DEGRADING GENE CLUSTER IN *ESCHERICHIA COLI*

Abstract

By Jacob Paul Herman, Ph. D.
Washington State University
August 2004

Chair: Luying Xun

Ethylenediaminetetraacetate (EDTA) and nitrilotriacetate (NTA) possess a remarkable ability to form stable, water-soluble complexes with many metal ions. The industrial uses of EDTA and NTA are numerous, ranging from bleach stabilizers to preventing oxidations catalyzed by metal ions. The synthetic chelating agents also have been used for decontamination of nuclear material and processing nuclear waste, resulting in the co-disposal with radionuclides. The presence of complexing agents in waste promotes the formation of strong complexes with radionuclides, increasing the mobility of radionuclides and toxic metals in the subsurface environment. Bacterial degradation of EDTA and NTA eliminates the enhanced mobility.

The studies presented in this dissertation focus on the EDTA and NTA transport system (EppABCD) of bacterium BNC1. Whole cell analysis of BNC1 demonstrates that

metal-EDTA and metal-NTA complexes with low stability constants are preferentially transported into the cell and metabolized. The transporter consists of four proteins: EppA, a periplasmic binding protein, and the other three proteins are membrane proteins involved in the transport. I have shown that EppA preferentially binds $CaEDTA^{2-}$, $MgEDTA^{2-}$, $CaNTA^{-}$ and $MgNTA^{-}$, but not $CuEDTA^{2-}$ and $CuNTA^{-}$, which also are stable complexes. The specificity of cellular uptake of different metal-EDTA/-NTA complexes correlates well with the preferential binding of these complexes by EppA and explains why some stable metal-EDTA and metal-NTA complexes are not metabolized. To further study this system, I cloned the entire 12-kb EDTA/NTA transport and metabolism gene cluster into *Escherichia coli* W3110. The engineered organism was able to metabolize metal-EDTA and metal-NTA complexes in a manner similar to BNC1, providing *in vivo* evidence that EppABCD is a specific transporter for EDTA and NTA and that the introduced metabolism genes *emoA*, *emoB*, *emoR*, and *idaA* are responsible for their mineralization. These data contribute greatly to our understanding of EDTA and NTA transport and metabolism by bacterium BNC1, and provide scientific guidance for developing a field applicable microorganism directly targeted to mixed wastes containing EDTA and NTA.

TABLE OF CONTENTS

LIST OF TABLES

CHAPTER TWO

CHAPTER THREE

LIST OF FIGURES

DEDICATION

This work is dedicated to my parents Cherry and Paul Herman, who have dedicated their lives to their children and have helped me through everything. I would also like to dedicate this dissertation to my sister and best friend, Rachel Herman, the strongest woman I know. Finally, I would like to especially dedicate this work to Dr. Luying Xun, Dr. Tim Doyle, and Chris Webster, who have supported me relentlessly through this entire experience.

CHAPTER ONE

INTRODUCTION AND BACKGROUND

Chelating agents

The term chelate originates from the Greek term "chele", meaning lobster claw. Chelating agents are multidentate ligands that bind metal ion(s), similar to a claw holding a small object. Many biological processes rely on chelated metals tightly positioned within the complexes. Familiar biological complexes include heme for oxygen transport, cytochromes for electron transport, chlorophylls for photosynthesis, vitamin B12 involved in C-1 metabolism, and siderophores produced by microorganisms for trace metal sequestration.

In the environment, chelating agents are abundant. Essential trace metals often exist as biologically available chelated complexes in aqueous environments (23). The chelating agents involved in these complexes are produced by microorganisms, fungi, algae, and plants for trace metal sequestration by specific uptake systems.

Synthetic chelating agents also are present in the environment due to their use in household and agricultural products and in many industrial processes (46). These chelating agents are developed for specific purposes, to bind metals with different affinity or selectivity. An important group of synthetic chelating agents are the aminopolycarboxylic acids (APCAs). APCAs are composed of one or more carboxylate groups bound to one or more nitrogen atoms (11). Synthetic APCAs originally were produced for analytical purposes; the first such compound was nitrilotriacetate (NTA), synthesized in 1862 from the reaction of monochloroacetic acid and ammonium (11). In

the mid 1930s the German firm I.G. Farbenidustrie introduced ethylenediaminetetraacetate (EDTA), under the trade name Trilon B. EDTA possessed a remarkable ability to form very stable, water-soluble complexes with many metal ions including alkaline earth metals (19), and originally was marketed in conjunction with an analytical method to determine the hardness of water. In 1945, Shwarzenbach and co-workers began fundamental studies of the complex-forming ability of these substances from a physiochemical point of view, and developed a sound theory based on values of the ionization constants of acids and the stability constants of the complexes in which they form (57). A number of preliminary studies indicated a variety of useful practical applications, including water softeners and dyeing assistants. The studies have revealed that EDTA and NTA forms 1:1 complexes with metal substrates, an ideal situation for complexiметric titrimetry, because problems arising from the stepwise formation of complexes are avoided (44). The significance of APCAs is due to the fact that few substances form stable complexes with alkaline earth metals, especially calcium and magnesium. The structure of NTA allows for a total of four possible ligand sites, and that of EDTA allows for a total of six (Fig. 1) (41). The properties of EDTA and other synthetic APCAs have led to their use in a multitude of industrial processes, other than only complexiметric titrimetry. To date, APCAs have been used in order to: "(i) prevent the formation of metal precipitates, (ii) to hinder unwanted chemical reactions caused by metal ion catalysis, (iii) to remove ions from systems, or (iv) to make metal ions more available by keeping them in solution" (11).

Today EDTA is produced industrially by the reaction of ethylenediamine with sodium cyanide and formaldehyde under alkaline conditions at an elevated temperature

(60). A partial vacuum is used to remove ammonium, which is the by-product. Exact amounts of EDTA and NTA produced annually each year are unknown, but the amounts used by the United States and Western Europe in 1981 totaled 95,900 metric tons (11). NTA based detergents have been used in the United States, Canada, Finland, Sweden and Switzerland and account for approximately 15% of laundry detergents released in wastewater systems in Canada (11). EDTA is banned for use in detergents by many countries, but is still used extensively in foodstuffs (46). The widespread use of these compounds has raised major concerns with the amounts of APCAs that are released to the environment (46). Reports of the exact environmental concentrations of NTA and EDTA differ depending on the sample location. Past environmental NTA concentrations reported were: 2500 $\mu g\ l^{-1}$ at sewage treatment plants in Canada (56); 100-1000 $\mu g\ l^{-1}$ at Swiss municipal wastewater treatment plants (2); 50 $\mu g\ l^{-1}$ in Canadian streams (61); up to 20 $\mu g\ l^{-1}$ in European rivers (22); 10 $\mu g\ l^{-1}$ in Swiss lakes (22); between 1 and 10 $\mu g\ l^{-1}$ in Swiss ground and drinking water (17); and approximately 1-2 g^{-1} in mixed waste soils at the Department of Energy's Hanford site in Washington State (52). Past environmental EDTA concentrations reported are: 10 to 500 $\mu g\ l^{-1}$ at Canadian sewage treatment plants (1, 2); up to 60 $\mu g\ l^{-1}$ in European rivers (22); 100 $\mu g\ l^{-1}$ in some German and Swiss rivers (25); 1-4 $\mu g\ l^{-1}$ in Swiss lakes (22); 60-1170 $\mu g\ l^{-1}$ in sediment cores from Lake Greifensee, Switzerland (39); 15 $\mu g\ l^{-1}$ in Swiss groundwater and 25 $\mu g\ l^{-1}$ in some Swiss drinking water (17); and approximately 9 g^{-1} in mixed waste soils at the Department of Energy's Hanford site (52).

NTA is eliminated by most wastewater treatment processes, and is not persistent in the environment (11). However, EDTA is recalcitrant to both chemical and biological

wastewater treatment processes (46). The environmentally measurable concentrations and recalcitrance of EDTA has raised concern about the environmental fate of EDTA. NTA and EDTA are reported to be relatively non-toxic, but nothing is known about the impact of sustained exposure to NTA and EDTA on the entire eukaryotic life cycle (46). It also has been speculated that EDTA can enhance the toxic effects of heavy metals and radionuclides (46).

Chemical properties of EDTA and NTA

Metal chelates are considered organometallic complexes, but they possess properties that distinguish them from conventional "organometallics" (8). Metal chelate complexes are commonly inert, and usually remain unchanged throughout chemical and physical operations (8). The chelate ligand acts as a Lewis base (electron donor) and the metal acts as a Lewis acid (electron acceptor); the donation of an electron pair creates a metal-chelator bond (8).

The chemistry of metal chelates is complicated due to the different properties of the metal ions. These properties include the electronic structure, coordination number, stereochemistry, and variable oxidation states (8). Different metal ions have specific coordination numbers, or the number of bonds which can be linked to the metal (8). The coordination number of the metal determines the type and strength of the chelate that can bind it. Further, metal ion size plays an important role in the properties of the metal-chelate complex (8).

The NTA molecule has four possible binding sites, and acts best as a tetradentate ligand with a pentagonal bypyrimid coordination geometry (13, 47), although several

tridentate complexes also have been reported (13). The insufficient number of coordination groups of NTA make it unable to efficiently bind transition metals, especially Zn^{2+} and Fe^{3+} (8). Therefore, the metal must fill the empty coordination sites with water molecules. The stability constants of metal-NTA complexes are several orders of magnitude lower than those of their metal-EDTA counterparts, which contain additional coordinates (32).

EDTA has six possible binding sites and acts as a sexdentate ligand (8). The stereochemistry of metal-EDTA complexes is affected by the metal ion size. EDTA can form an octahedral coordination with small sized metal ions such as Mg^{2+} and Ca^{2+} (8). $MgEDTA^{2-}$ is seven-coordinate with a monocapped trigonal prism stereochemistry but $CuEDTA^{2-}$ is a six-coordinate pentadentate complex (8). Therefore, EDTA does not always fulfill its donor capacity, and the coordination of the metal can be completed with a water molecule.

Uses of EDTA and NTA

The industrial uses of EDTA and NTA are numerous, ranging from bleach stabilizers to preventing metal-catalyzed oxidation. In addition, the synthetic chelating agents also have been used for metal processing (7, 43), decontamination of nuclear material (7, 43) and processing nuclear waste (33), resulting in their co-disposal with radionuclides.

The co-disposal of the APCAs with radioactive wastes can pose major problems (52). The presence of complexing agents in the waste, including organic chelates used in decontamination operations and natural organic acids from soil,promotes the formation of

strong complexes with radionuclides (34), which are soluble and mobile in groundwater (14, 35). EDTA and NTA have been used at several Department of Energy sites in nuclear waste processing (33) and decontamination procedures (7, 43). The co-disposal of EDTA with radionuclides has been shown to enhance the transport of Pu and ^{60}Co in the groundwater (14, 34, 45) at Oak Ridge National Laboratory (34), Chalk River Nuclear Laboratories (12) and Maxey Flats (14). Approximately 220,000 kg of EDTA (4, 27) and 240-381 kg of plutonium (4, 20) were discharged to single shell tanks at Hanford from 1944-1975, and 67 of the tanks have leaked or are suspected of leaking (4, 20). It has been shown that the co-disposal of PuO_2 and EDTA promotes the formation of soluble $Pu(OH)_2EDTA^{2-}$ complexes (10). The complexes may enhance Pu transport in groundwater under aerobic conditions (10). Due to these problems and the fact it has reached measurable concentrations in many surface and drinking waters (37), the presence of EDTA has become a concern of public health. Thus, microbial degradation of EDTA and other chelating agents has been studied for the purpose of bioremediation.

Remediation processes of ETDA and NTA

EDTA and NTA differ drastically in their environmental biodegradability. NTA is readily degraded in soils, natural waters and during wastewater treatment processes, but EDTA is not (11). Complete degradation of NTA in aquifer and soil settings has been reported (28, 50), while NTA degradation at wastewater treatment plants occurs in oxidation ponds, activated sludge and trickling filter processes (5). EDTA, on the other hand, is not eliminated during the same processes. For example, influent and effluent concentrations of EDTA at wastewater treatment plants remains approximately the same

(2, 26, 29). EDTA also is recalcitrant to biodegradation in soil (3, 48). Thus, efforts to bioremediate EDTA waste by using specific microorganisms have been investigated. These studies have led to the isolation of pure bacterial cultures able to utilize both EDTA and NTA as carbon and nitrogen sources.

NTA-metabolizing microorganisms include both gram-positive and gram-negative species, and have been isolated from a variety of environments (6, 24, 55). These NTA degrading organisms have been divided into three groups, depending on morphology and substrate range (11). The first group contains "obligate aerobic, motile rods which are mostly pleomorphic and can utilize sugars and other substrates including methylated amines, hence indicating their ability to assimilate C1 units" (11). Phylogenetically, these organisms are *Agrobacterium-Rhizobium* species, and had been collectively been named as *Chelatobacter* sp., but have been renamed *Aminobacter aminovorans* (24). The second group are "obligately aerobic, non-motile short rods or diplococci unable to grow on sugars" (11). They have been assigned as a new genospecies, *Chelatococcus asaccharovorans* (6). The third group "consists of only one strain (TE11) that is facultatively denitrifying" (11). The substrate range for these groups includes NTA and iminodiacetate (IDA), but not EDTA (6, 55).

The isolation of EDTA-degrading microorganisms has been more difficult due to the recalcitrance of EDTA to microbial degradation. A mixed EDTA-degrading culture was enriched from an industrial wastewater treatment plant sludge that had been receiving large amounts of EDTA (49). Pure cultures were not obtained from the mixed culture (which contained *Methylobacterium*, *Variovorax*, *Enterobacter*, *Aureobacterium*,

and *Bacillus*) (49), but the mixed culture was reported to be able to metabolize up to 60% of the Fe(III)EDTA in the culture media (49).

The first pure culture that could support growth on a metal-EDTA chelate was reported as an *Agrobacterium species* isolated by Lauff et al. (30). The EDTA was oxidized at a high initial concentration of approximately 30 mM, but consumption of the substrates ceased when the concentration decreased to approximately 3 mM (36). Another *Agrobacterium species* (40) could oxidize the Fe(III)EDTA chelate, however residual concentrations of more than 40% of the initial content remained in the culture fluid (37). A mixed culture (49) utilized Fe(III), Cu, Co, Ni, and CdEDTA as substrates for growth, but the oxidation rates were slow and decreased significantly at relatively high concentrations (37). Strain DSM 9103, which is classified as an *Agrobacterium-Rhizobium* species, is able to degrade EDTA up to an initial concentration of 3.5 mM (59). Strain BNC1, isolated from EDTA containing sludge, is able to degrade EDTA when present at a 16 mM concentration (38). The genome of BNC1 recently has been sequenced, and BNC1 is temporarily named *Mesorhizobium* sp. BNC1.

Characterization of the EDTA and NTA metabolic pathways

The biochemistry of NTA metabolism is well studied. The pathway proposed 25 years ago (15, 16, 18, 51) has since been confirmed by the isolation, purification, and characterization of the specific enzymes from *Chelatobacter heintzii* (54) (renamed as *Aminobacter aminovorans*) and *C. asaccharovorans* (53). An NTA monooxygenase (NTA MO) catalyzes the conversion of NTA to IDA and glyoxylate, with the

consumption of $FMNH_2$ and oxygen (62), and IDA is converted to glyoxylate and glycine by IDA dehydrogenase (IDA DH) (53).

The biochemistry of EDTA metabolism also has been elucidated at the molecular level, and will be discussed in reference to BNC1. The EDTA monooxygenase (EmoA) catalyzes the first two steps of EDTA metabolism (42). EmoA oxidizes EDTA to ethylenediaminetriacetate (ED3A), and ED3A to ethylenediaminediacetate (EDDA); both reactions occur at the expense of $FMNH_2$ and oxygen, which is provided by EmoB, an $NADH_2$:FMN oxidoreductase (42). The iminodiacetate oxidase (IdaA) catalyzes the last two steps of EDTA degradation. IdaA oxidizes EDDA to ethylenediaminemonoacetate (EDMA), and EDMA to ethylenediamine (ED), with the co-production of glyoxylate and H_2O_2 (31). EmoA also oxidizes NTA to IDA, and IdaA converts IDA to glycine (42); therefore, BNC1 possesses the ability to metabolize both EDTA and NTA by the same enzymes.

BNC1 whole cells are able to metabolize metal-EDTA complexes with relatively low stability constants ($K \leq 10^{13.81}$, eg. Ca, Mg and Mn) but is unable to metabolize complexes with high stability constants ($K \geq 10^{16.26}$, eg., Co and Cu). Purified EmoA is able to catabolize the metal-EDTA complexes of Al, Ca, Co(III), Cu, Fe(III), Mg, and Ni (42). It therefore is speculated that the recalcitrance of certain metal-EDTA complexes is due to the lack of transport into the cell.

During the sequencing of *emoA*, four genes immediately upstream of *emoA* were found to have sequence homology to ABC-type transporter genes (9), indicating that the genes may be responsible for EDTA uptake. Using whole cell assays, Witschel et al. have recently reported that DSM 9103 actively transports EDTA (58). Understanding the

transport system involved in EDTA and NTA degradation in BNC1 is a major goal of this dissertation research.

ABC-type transporters

ABC-type transporters are common transmembrane transport systems found in many prokaryotes and are associated with many important biological functions (21). The transporters require the function of multiple polypeptides, organized in a characteristic fashion (21) (Fig. 2). The typical transporter consists of four membrane-associated components. Two of these components (equivalent to EppB and EppC in Fig. 2) are highly hydrophobic and each consists of six-membrane-spanning segments (21). The components form the channel through which the substrate crosses the membrane, and in large part are believed to determine the substrate specificity of the transporter (21). The other protein, homologous to EppD, (often a homodimer), peripherally located at the cytoplasmic face of the membrane, binds ATP and couples ATP hydrolysis to the transport process (21). Importantly, all bacterial ABC dependent transporters that mediate solute uptake require a substrate binding protein located in the periplasmic space (21). This periplasmic protein is essential for the function of the transporter, conferring substrate specificity. EppA is the periplasmic protein in strain BNC1, and its coding gene is located upstream of *emoA*.

Project goals and significance

BNC1 cells can only degrade selected metal-EDTA complexes (42). We speculated that the inability of BNC1 to metabolize certain metal-EDTA and metal-NTA

complexes was due to the lack of transport of these complexes. To study this hypothesis, we have focused on EppA, the periplasmic binding protein of the hypothetical transporter. Characterization of EppA confirmed that the inability of whole cells to degrade of certain metal-EDTA and -NTA complexes was due to the inability of EppA to bind them for uptake. Unfortunately, the metal-EDTA complexes that cannot be transported into the cell for metabolism are stable complexes, contributing the recalcitrance of EDTA in the environment. I have also demonstrated that *eppABCD* is inducibly co-transcribed with *emoA*, further supporting the hypothesis that the *eppABCD*-encoded ABC transporter system is responsible for EDTA and NTA uptake into bacterium BNC1.

The physiological role of the entire EDTA gene cluster carrying the transporter, metabolism, and regulation genes of EDTA and NTA degradation also has been confirmed by showing that *Escherichia coli* carrying the EDTA-degrading gene cluster was able to grow on EDTA and NTA. The success in transferring the entire EDTA-degrading gene cluster into *E. coli* offers the potential to genetically engineer field adapted microorganisms for the purpose of bioremediation if BNC1 proves unsuitable for treatment in mixed waste sites, or if the engineered microorganisms offers other advantages in field applications.

REFERENCES

1. **Alder, A., H. Siegrist, K. Fent, T. Egli, E. Monar, T. Poiger, C. Schaffner, and W. Gigger.** 1997. The fate of organic pollutants in wastewater and sludge treatment: Significant processes and impact of compound properties. Chimia **51:**922-928.

2. **Alder, A., H. Siegrist, W. Gujer, and W. Giger.** 1990. Behavior of NTA and EDTA in biological wastewater treatment. Water Resour. **24:**733-742.

3. **Allard, A., L. Renberg, and A. Neilson.** 1996. Absence of $^{14}CO_2$ evolution from ^{14}C-labelled EDTA and DTPA and the sediment/eater partition ratio. Chemosphere **33:**577-583.

4. **Allen, G.** 1976. Estimated inventories of chemicals added to underground waste tanks, 1944 through 1975. Atlantic Richfield Hanford Company.

5. **Anderson, R., E. Bishop, and R. Campbell.** 1985. A review of the environmental and mammalian toxicology of nitrilotriacetic acid. Crit. Rev. Toxicol. **15:**1-102.

6. **Auling, G., H. Busse, T. Egli, T. El-Banna, and E. Stackebrandt.** 1993. Description of the Gram-negative, obligately aerobic, nitrilotriacetate (NTA)-utilizing bacteria *Chelatococcus asaccharovorans*, gen. nov., sp. nov. Syst. Appl. Microbiol. **12:**104-112.

7. **Ayers, G.** 1970. Decontamination of Nuclear Reactors and Equipment. The Ronald Press Co., New York, NY.

8. **Bell, C.** 1977. Principles and applications of metal chelation. Oxford University Press, Oxford.

9. **Bohuslavek, J., J. Payne, Y. Liu, H. Bolton, and L. Xun.** 2001. Cloning, sequencing, and characterization of a gene cluster involved in EDTA degradation from the bacterium BNC1. Appl. Environ. Microbiol. **67:**688-695.

10. **Bolton, H., Jr.** 2004. Personal communication.

11. **Bucheli-Witschel, M., and T. Egli.** 2001. Environmental fate and microbial degradation of aminopolycarboxylic acids. FEMS Microbiol. Rev. **25:**69-106.

12. **Champ, D., and D. Robertson.** 1986. Chemical speciation of radionuclides in contaminant plumes at the Chalk River Nuclear Laboratories. Elsevier.

13. **Clegg, W., A. Powell, and M. Ware.** 1984. Structure of trisodium bis(nitrilotriacetato)ferrate(III) pentahydrate, $Na_3[Fe\{N(CH_2CO_2)_2]$.$5H_2O$. Acta Cryst. **C40:**1822-1824.

14. **Cleveland, J., and T. Rees.** 1981. Characterization of plutonium in Maxey Flats radioactive trench leachates. Science **212:**1506-1509.

15. **Cripps, R., and A. Noble.** 1973. The metabolism of nitrilotriacetate by a Pseudomonad. Biochem. J. **136:**1059-1068.

16. **Cripps, R., and A. Noble.** 1972. The microbial metabolism of nitrilotriacetate. Biochem. J. **130:**31P-32P.

17. **de Oude, I.** 1984. NTA-Monitoring - Organisation und Erfahrungen von Knada, USA and den Niederlanden, p. 237-250, NTA: Studie uber die aquatishe Umweltvertaglichkeit von Nitrilotriacetat (NTA). Verlag Hans Richarz, Sankt Augustin.

18. **Firestone, M., and J. Tiedje.** 1978. Pathway of degradation of nitrilotriacetate by *Pseudomonas* species. Appl. Environ. Microbiol. **35:**955-961.

19. **Flackshika, H.** 1959. EDTA Titrations. Pregamon Press, New York, NY.

20. **Gephart, R., and R. Lundgren.** 1996. Hanford tank clean up: a guide to understanding the technical issues. Pacific Northwest National Laboratory.

21. **Higgins, C.** 1992. ABC transporters: from microorganisms to man. Annu. Rev. Cell Biol **8:**67-113.

22. **Houriet, J.** 1996. NTA dans les eaux. Cahier de l'environnement, des forets et du paysage (OFEFP), Bern.

23. **Hughes, M. N., and R. K. Poole.** 1989. Metals and Micro-organisms. Chapman and Hall, New York.

24. **Kampfer, P., A. Neef, M. Salkinoja-Salonen, and H. Busse.** 2002. *Chelatobacter heintzii* (Auling et al. 1993) is a later subjective synonym of *Aminobacter aminovorans* (Urakami et al. 1992). Int. J. Syst. Evol. Microbiol. **52:**835-839.

25. **Kari, F.** 1994. Umweltverhalten von Ethylendiamintetraacetat (EDTA) unter spezieller Berucksichtigung des photochemischen Abaus. Ph.D. Thesis No 10698, Swiss Federal Institute of Technology, Zurich.

26. **Kari, F., and W. Giger.** 1996. Speciation and fate of ethylenediaminetetraacetate (EDTA) in municipal wastewater treatment. Water Resour. **30:**12-20.

27. **Klem, M.** 1988. Inventory of chemicals used at Hanford production plants and support operations (1944-1980). Westinghouse Hanford Company.

28. **Kuhn, E., M. van Loosderecht, W. Giger, and R. Schwarzenback.** 1987. Microbial degradation of nitrilotriacetate (NTA) during river water/groundwater infiltration: laboratory column studies. Water Resour. **10:**1237-1248.

29. **Lahl, U., and H. Burbaum.** 1988. Eincelstoffanalysed im Zu- and Ablauf einerr kommunalen Klaranlage. Korresp. Abwasser **35:**360-364.

30. **Lauff, J., D. Steele, L. Coogan, and J. Breitfeller.** 1990. Degradation of the ferric chelate of EDTA by a pure culture of an *Agrobacterium* sp. Appl. Environ. Microbiol. **56:**3346-3353.

31. **Liu, Y., T. Louie, J. Payne, J. Bohuslavek, H. Bolton, and L. Xun.** 2001. Identification, purification, and characterization of iminodiacetate oxidase from the EDTA-degrading bacterium BNC1. Appl. Environ. Microbiol. **67:**696-701.

32. **Martell, A., and R. Smith.** 1974. Critical Stability Constants, vol. 1. Plenum Press, New York.

33. **McFadden, K.** 1980. Organic components of nuclear wastes and their potential for altering radionuclide distribution when released to soil. National Technical Service, Springfield, VA.

34. **Means, J., and D. Crerar.** 1978. Migration of radioactive wastes: Radionuclide mobilization by complexing agents. Science **200:**1477-1486.

35. **Means, J., T. Kucak, and D. Crerar.** 1980. Relative degradation rates of NTA, EDTA, and DTPA and environmental implications. Environ. Pollut. (Series B) **1:**45-60.

36. **Miyazi, H., S. Suzuki, and K. Imada.** 1997. Isolation and characterization of a bacterium that decomposes EDTA ferrate (IIII) complex. Environ. Sci. **10:**257-262.

37. **Nortemann, B.** 1999. Biodegradation of EDTA. Appl. Microbiol. Biotechnol. **51:**751-759.

38. **Nortemann, B.** 1992. Total degradation of EDTA by mixed cultures and a bacterial isolate. Appl. Environ. Microbiol. **58:**671-676.

39. **Nowack, B., F. Kari, S. Hilger, and L. Sigg.** 1996. Determination of dissolved and adsorbed EDTA species in water and sediment by HPLC. Anal. Chem. **68:**561-566.

40. **Palumbo, A., S. Lee, and P. Boerman.** 1994. The effect of media composition on EDTA degradation by *Agrobacterium* sp. Appl. Biochem. Bioechnol. **45:**811-822.

41. **Pankow, J.** 1991. Aquatic Chemistry Concepts. Lewis Publishers, Chelsa Michigan.

42. **Payne, J., H. Bolton, J. Campbell, and L. Xun.** 1998. Purification and characterization of EDTA monooxygenase from the EDTA-degrading bacterium BNC1. J. Bacteriol. **180:**3823-3827.

43. **Piciulo, P., J. Adams, M. Davis, L. Milian, and C. Anderson.** 1986. Release of organic chelating agents from solidified decontamination wastes. National Technical Information Service, Springfield, VA.

44. **Pribil, J.** 1972. Analytical Applications of EDTA and Related Compounds. Pregamon Press.

45. **Riley, R., and J. Zachara.** 1992. Chemical contaminants on DOE lands and selection of contaminant mixtures for subsurface science research, DOE/ER-0547T. National Technical Information Services, U.S. Department of Commerce.

46. **Sillanpaa, M.** 1997. Environmental fate of EDTA and DTPA. Rev. Environ. Contam. Toxicol. **152:**85-111.

47. **Stanford, R.** 1967. The crystal structure of nitrilotriacetic acid. Acta Cryst. **23:**825-833.

48. **Stumpf, M., T. Ternes, B. Schuppert, K. Haberer, P. Hoffman, and H. Ortner.** 1996. Sorption und Abbau con NTA, EDTA und DTPA wahrend der Bodenpassage. Vom Wasserr **86:**157-171.

49. **Thomas, R., K. Lawlor, M. Bailey, and L. Macaski.** 1998. Biodegradation of metal-EDTA complexes by an enriched microbial population. Appl. Environ. Microbiol. **64:**1319-1322.

50. **Tiedje, J., and B. Mason.** 1971. Biodegradation of nitrilotriacetate (NTA) in soils. Sol. Sci. Am. Proc. **38:**278-283.

51. **Tiedje, J., B. Mason, C. Warren, and E. Malec.** 1973. Metabolism of nitrilotriacetate by cells of *Pseudomonas* species. J. Sci. Lab. Denision Univ. **54:**811-818.

52. **Toste, A., B. Osborn, K. Polach, and T. Lechner-Fish.** 1995. Organic analyses of an actual and simulated mixed waste: Hanford's organic complexant revisited. J. Radioanal. Nucl. Chem. **194:**25-34.

53. **Uetz, T., and T. Egli.** 1993. Characterization of an inducible membrane-bound iminodiacetate dehydrogenase from *Chelatobacter heintzii* ATCC 29600. Biodegradation.

54. **Uetz, T., R. Schneider, M. Snozzi, and T. Egli.** 1992. Purification and characterization of a two-component monooxygenase that hydroxylates nitrilotriacetate from '*Chelatobacter*' strain ATCC 29600. J. Bacteriol. **174:**1179-1188.

55. **Wanner, U., J. Kemmler, H. Weilenmann, T. Egli, T. El-Banna, and G. Auling.** 1990. Isolation and growth of a bacterium able to degrade nitrilotriacetate acid under denitrifying conditions. Biodegradation **1:**31-41.

56. **Wei, N., P. Crescoulo, and B. LeClair.** 1979. Impact of nitrilotriacetic acid (NTA) on an activated sludge plant - a field study Project No. 71-3-3. Environmental Protection Service Environment Canada.

57. **Welcher, D.** 1958. The Analytical Use of EDTA. D. Van. Nostrand Company Inc.

58. **Witschel, M., T. Egli, A. Zehnder, and M. Spycher.** 1999. Transport of EDTA into cells of the EDTA-degrading bacterial strain DSM 9103. Microbiology **145:**973-983.

59. **Witschel, M., H. Weilenmann, and T. Egli.** 1995. Degredation of EDTA by a bacterial isolate. Poster presented at the 54th annual meeting of the Swiss Society of Microbiology, Lugano.

60. **Wolf, K., and P. Gilbert.** 1992. EDTA-Ethylenediaminetetraacetic Acid. Handbook of Environmental Chemistry**:**243-259.

61. **Woodiwiss, C., R. Walker, and F. Brownridge.** 1979. Concentration of nitrilotriacetate and certain metals in Canadian waste-waters and streams: 1971-1975. Water Resour. **13:**599-622.

62. **Xu, Y., M. Mortimer, T. Fisher, M. Kahn, F. Brockman, and L. Xun.** 1997. Cloning, sequencing, and analysis of a gene cluster from *Chelatobacter heintzii* ATCC 29600 encoding nitrilotriacetate monooxygenase and NADH:Flavin mononucleotide oxidoreductase. J. Bacteriol. **179:**1112-1116.

Figure 1. Structures of NTA and EDTA. Me=divalent metal ion, e.g. Mg^{2+}, Ca^{2+}

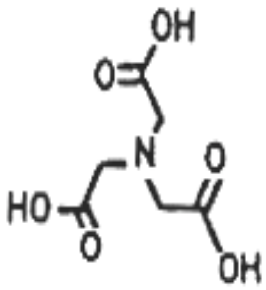

NTA

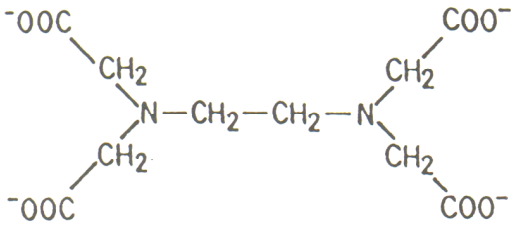

EDTA

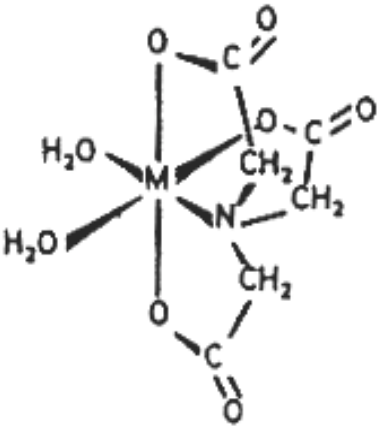

MeNTA

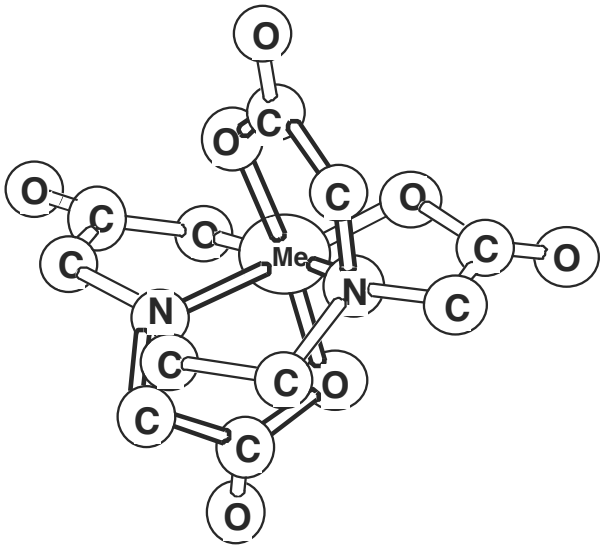

MeEDTA

Figure 2. ABC-type transport system. EDTA is transported into the cell as a metal complex. EppA binds the metal-EDTA complex and shuttles it to the EppB/EppC permease. ATP is hydrolyzed, and metal-EDTA is transported into the cytoplasm.

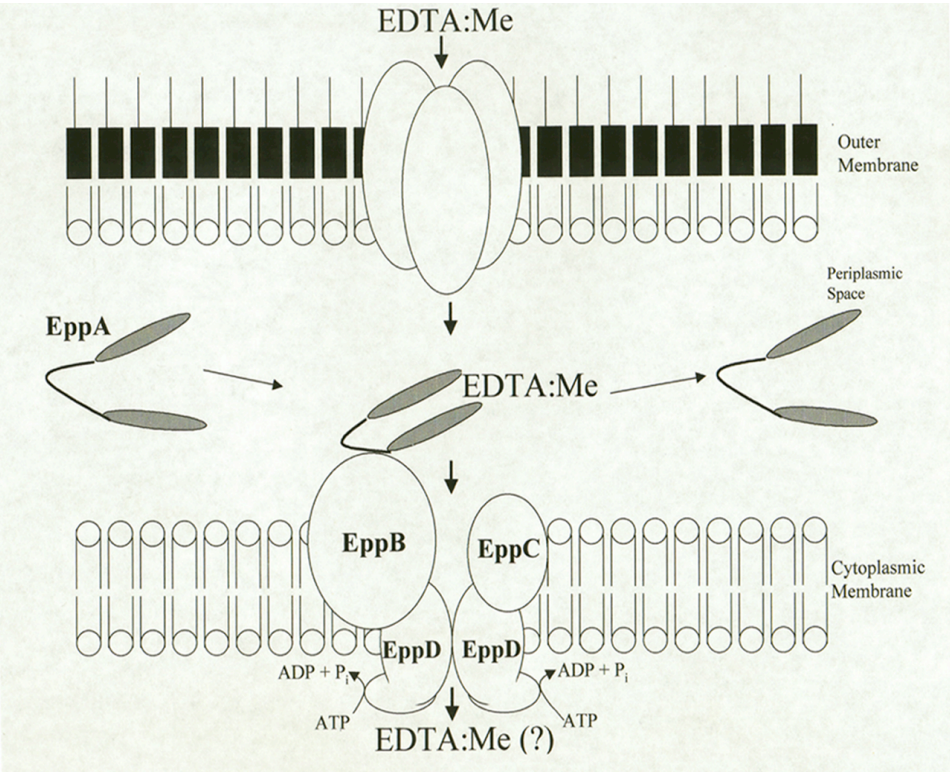
EDTA:Me
Outer
Membrane
Periplasmic
Space
EppA
EDTA:Me
EppB
EppC
Cytoplasmic
Membrane
EppD
EppD
ADP + P$_i$
ADP + P$_i$
ATP
ATP
EDTA:Me (?)

CHAPTER TWO

Characterization of Periplasmic EDTA-Binding Protein (EppA) of an ABC-Type Transporter from EDTA-Degrading Bacterium BNC1

ABSTRACT

Ethylenediaminetetraacetate (EDTA), a common chelating agent, forms stable metal-EDTA complexes, contributing to the recalcitrance of EDTA in the environment. The EDTA-degrading bacterium BNC1 has a gene cluster containing the EDTA-metabolizing genes and hypothetical ABC transporter genes. Reverse transcriptase PCR analysis of the total RNA from cells grown with or without EDTA showed that the genes *eppABCD* and *emoA* were transcribed on the same mRNA and regulated as an operon in response to the presence of EDTA in the growth medium. The gene encoding the periplasmic binding protein (*eppA*) was cloned and expressed in *Escherichia coli*; the recombinant EppA was purified. The purified EppA was shown to bind selected metal-EDTA complexes by using spectrofluorometric, spectrophotometric and microcalorimetric assays. The dissociation constants (K_d) for EppA binding of $CaEDTA^{2-}$, $MgEDTA^{2-}$, and $ZnEDTA^{2-}$, were 0.43, 0.58, and 28.6 μM, respectively. EppA did not bind $CuEDTA^{2-}$. The K_d values suggest that the transport system cannot uptake $CuEDTA^{2-}$, which was confirmed by whole cells studies. BNC1 metabolized $CaEDTA^{2-}$, $MgEDTA^{2-}$, and $ZnEDTA^{2-}$, but not $CuEDTA^{2-}$. The results reveal the biochemical basis of EDTA recalcitrance in the environment, as some stable metal-EDTA complexes, e.g. $CuEDTA^{2-}$, are not transported into bacterial cells for metabolism.

INTRODUCTION

The synthetic aminopolycarboxylic acid, ethylenediaminetetraacetate (EDTA), has a variety of industrial applications because of its high affinity for alkaline earth metals. The annual sale of EDTA in Europe alone was 32,550 metric tons in 1997 (37). Due to improper discharge, EDTA is found with heavy metals and radionuclides at many contaminated sites (7, 50). EDTA increases the solubility of radionuclides and heavy metals, leading to their enhanced mobility in groundwater (9, 33), which may increase the potential exposure to the public of these contaminants. Since EDTA is recalcitrant to biodegradation in the environment (4, 34, 49), it poses a long-term environmental problem. The resistance to biodegradation is intriguing because EDTA is a simple organic compound.

Thus far only three bacterial isolates are known to degrade EDTA (27, 38, 53). The biochemistry and molecular biology of EDTA degradation have been studied with the EDTA-degrading bacterium BNC1 (22, 38). EDTA monooxygenase (EmoA), an $FMNH_2$-utilizing monooxygenase, oxidizes EDTA to ethylenediaminetriacetate and then to ethylenediaminediacetate (3, 40). Iminodiacetate monooxygenase (IdaA) then oxidizes ethylenediaminediacetate to ethylenediamine (30), which is structurally similar to putrescine, a common biological diamine present in bacterial cells (21). The genes corresponding to these enzymes are organized in a gene cluster in the order of *emoA*, *emoB*, *emoR* (a regulatory gene), and *idaA* (3). Immediatly upstream of *emoA* are four genes, *eppABCD,* coding for a hypothetical ABC-type transporter system. Since whole cell studies have shown that EDTA is transported into BNC1 cells by an active uptake system (22), the location of *eppABCD* indicates a potential role of the encoded

transporter system in EDTA uptake. Experimental data are presented here to support the hypothesis that the *eppABCD*-encoded ABC transporter system is responsible for EDTA uptake into bacterium BNC1 and that the system selectively transports specific metal-EDTA complexes. The lack of uptake for some stable metal-EDTA complexes is suggested to contribute to the recalcitrance of EDTA in the environment.

MATERIALS AND METHODS

Bacterial strains and plasmids. The EDTA-degrading bacterium was kindly provided by Bernd Nörtemann (Technical University of Braunshweig, Braunshweig, Germany). BNC1 was cultured with disodium EDTA (0.3 g/liter) in a mineral salts medium (38). BNC1 also was grown in mineral salts media (38) supplemented with NH_3Cl (10 mM) and 1 mM glycerol ($MMNH_3$) and Luria-Bertani (LB) medium. *Escherichia coli* strain BL21(DE3) (Novagen, Madison, WI) was grown in LB medium.

Chemicals. Reagents used were of the highest purity available and were purchased from Sigma Co. (St. Louis, MO), Aldrich Chemical Co. (Milwaukee, WI), or Fisher Scientific Co. (Pittsburgh, PA). All PCR reactions were preformed with *Taq* DNA polymerase (Invitrogen, Carlsbad CA) and primers were purchased from Gibco BRL (Gaithersburg, MD). Restriction endonucleases and DNA-modifying enzymes were purchased from Gibco BRL or New England Biolabs (Beverly, MA).

Radioisotopes and radioactive solutions. Working solutions of ^{14}C-labeled EDTA (173 Mbq $mmol^{-1}$, 98% purity, ICN Pharmaceuticals, Irvine, CA) was prepared by mixing labeled and unlabeled EDTA solutions and buffers as required for the specific experiment. Radioactive solutions contained 10 μM concentration of EDTA and 1 mM $CaCl_2$. The initial concentration of EDTA in each growth experiment was 3.33 μM.

Growth on different metal-EDTA species. Growth on EDTA as a nitrogen source was measured in mineral salts growth medium (38) containing 1.5 mM $MgCl_2$ and 1.5 mM $CaCl_2$, and 0.2% (v/v) glycerol and supplemented with different amounts of Na_2EDTA, ZnEDTA, or CuEDTA. Sterile media were inoculated with 0.1% of EDTA-

grown cells from a later log phase culture. The cultures were grown at 30°C with shaking at 200 rpm. The optical density was analyzed at 600 nm (OD_{600nm}).

Cellular uptake of EDTA. BNC1 cells were grown in the EDTA mineral medium or LB medium to an OD_{600nm} of approximately 0.1 for EDTA-grown cells and 0.2 for LB-grown cells. Cells were harvested, washed three times with ice-cold uptake buffer (10 mM PIPES buffer, pH 7.0, 1 mM $CaCl_2$), and the cells suspended in the PIPES solution to an OD_{600nm} of 0.45. Cell suspensions of 1 ml were then delivered into individual sterile 5-ml test tubes, and each tube was used for each time point. Controls at each time point consisted of uninoculated PIPES solution. A 0.5 ml volume of 10 μM ^{14}C-labeled EDTA was added to each sample with vortexing. Samples were removed after 1, 5, and 15 minutes and the contents were immediately filtered through a 0.2-μm nitrocellulose filter under vacuum. Filters with trapped cells were then washed with 5 ml of ice-cold PIPES solution and transferred to 15 ml of scintillation cocktail for quantification of radioactive signal on a liquid scintillation counter.

Degradation of EDTA by BNC1 cell suspensions. BNC1 cells were grown in EDTA and $MMNH_3$ media to late exponential phase. Cells were harvested and washed twice in 20 mM PIPES buffer (pH 7.5). Experimental reactions were started by adding 1 mM of the respective metal-EDTA complex to the cell suspension. Controls experiments consisted of cell suspensions without the addition of metal-EDTA complexes and the addition of 1 mM of the metal-EDTA complex to cell-free PIPES buffer. The metal-EDTA ratios were 10:1 for Mg and Ca, and 1:1 for Zn and Cu. Additional controls were BNC1 growth experiments in the presence of 1 mM of Zn or Cu to test for the toxicity of

the metals in the $MMNH_3$ medium (NH_3Cl as the nitrogen source and glycerol as the carbon source).

Ammonia concentration was determined using the Krallmann-Wenzel method (23). At specific time points, 0.5 ml samples were removed, centrifuged, and 0.25 ml of the supernatant solution was used for experimental procedures. Added to the sample supernatant was 10 μl of catalyst solution, 0.5 ml of phenol reagent, and 0.25 ml of 1.5 % hypochlorite solution (5). The mixture was incubated for 6 minutes, and the OD_{636nm} was recorded, and converted to ammonium concentration by comparision to a standard concentration curve. This value was compared to a standard calibration curve (1 μM to 5 mM NH_3).

Reverse transcription (RT)-PCR. Total RNA was isolated according to a published method (52) from BNC1 cells grown to mid-log phase in the EDTA or $MMNH_3$ medium. After isolation, RNA was treated with RNase-free DNase (GibcoBRL), and further purified by using the RNeasy Midi Kit (Qiagen, San Diego, CA). RNA samples were screened for DNA contamination by PCR analysis. Samples that yielded no signal contained no DNA and were used for RT-PCR analysis.

RT-PCR reactions were carried out by using a OneStep RT-PCR kit (Gibco BRL) in a 100-μl reaction with 2 ng of RNA, and the products were analyzed on 0.7% agarose gel. Reactions were performed by using various combinations of sequence-specific primers (Table 1) (3, 36).

Construction of pEppA. *eppA* was cloned into the pET30-LIC vector without the leader peptide coding region (nucleotide 1-78) (13), primers MS-6 and MS-7 (Table 1) were designed. PCR yielded a predicted 1739-bp product, which was treated with T4-

DNA polymerase and dATP according to the supplier's instruction (Novagen), and annealed to pET30-LIC to obtain pEppA,. The pEppA plasmid was then electroporated into competent *E. coli* NovaBlue cells for amplification, recovery, and verification by sequencing. The correct pEppA, carrying an N-terminal his-tag fusion *eppA* gene, was transformed into *E. coli* BL21(DE3).

Overproduction and purification of the EppA fusion protein. *E. coli* strain BL21(DE3)(pEppA) was grown at 37ºC in 500 ml of LB with kanamycin to an OD_{600nm} = 0.5. Isopropyl-β-D-thiogalactopyranoside (IPTG) was then added to a final concentration of 0.1 mM, and the culture was incubated for an additional 3 hr. All subsequent steps were performed at 4°C. Cells were harvested by centrifugation at 15,000 × *g* for 10 min and suspended in 10 ml of 20 mM potassium phosphate (KPi) buffer (pH 7) containing freshly prepared 0.5 mM phenylmethylsulfonyl fluoride. The cells were then lysed by using a French pressures cell (model FA-030; Aminco, Urbana, Ill.) three times at 260 MPa. The product was centrifuged at 15,000 × *g* for 20 minutes. The supernatant was recovered and ultracentrifuged at 183,960 × *g* (average) for 1 hr, and was injected onto an Econo-Pac High Q column (Bio-Rad, Hercules, CA) equilibrated with the 20 mM KPi buffer (pH 7) containing 1 mM dithiothreitol (DTT). Proteins were eluted with a step and linear gradient of NaCl (percentages of 1M NaCl in the same buffer: 0%, 10 ml; 20-40%, 15 ml gradient; 100%, 10 ml) by a liquid chromatography (LC) system (Bio-Logic, Bio-Rad). EppA was eluted with a major peak around 35% NaCl. These fractions were pooled, and Ni^{2+}-NTA-agarose matrix was added at 1 ml per 20 mg of protein. After mixing gently for 1 hour, the slurry was loaded onto a small column. The matrix was washed with the first wash buffer (50 mM KPi, 20 mM imidazole, 1 mM DTT) and then

the second wash buffer (50 mM KPi, 40 mM imidazole, 1 mM DTT) for 5 bed volumes each. The target protein was eluted with the same buffer containing 250 mM imidazole. The purity of the protein was analyzed by SDS-PAGE (26). The eluted protein fractions were pooled and dialyzed against 1 L of 20 mM Tris-HCl buffer (pH 7.5) containing 1 mM DTT and 0.05% sodium azide for 4 hours, and then against 1 L of the same buffer overnight. The protein solution was concentrated to approximately 0.5 mg of protein per ml by Centriprep (Millipore, Billerica, Mass.) and stored at –80°C.

Gel Mobility Shift Assay. Ligand dependent gel mobility shift assays were performed as described by Rech et al. (41). Approximately 10 μg of EppA was incubated with 1 mM of the respective metal-EDTA species in 20 mM Tris-HCL for 20 minutes on ice. Samples were loaded on a 7% polyacrylamide gel. Electrophoresis was performed at 250 V at 4° C for 50 minutes. Gels were stained with Gelcode Blue Stain reagent (Pierce, Rockford IL) and analyzed visually.

Difference in UV absorption spectra. Changes in the intrinsic UV absorption of EppA were studied by using a Pharmacia Biotech Ultrospec 4000 UV/visible spectrophotometer. Experiments were conducted at room temperature in 25 mM Tris-HCl pH 7.5. The absorption spectra of EppA (10 μM) in the presence and absence of different metal-EDTA (20 μM) were recorded (18, 54).

Measurement of the dissociation constant. Fluorescence spectroscopy measurements were analyzed to determine the substrate binding for EppA. All measurements were done on an AVIV ATF 105 spectrofluorometer (Protein Solutions, Inc., Lakewood, NJ). Fluorescence emission changes were followed from 300-400 nm using an excitation wavelength of 280 nm. Emission and excitation bandwidths were set

at 2 nm. Prior to fluorescence measurements, the protein sample was dialyzed for three hours at 4° C against 1 L of 50 mM Tris-HCl buffer (pH 7.5) with saturating amounts (10 mM) of the metal ion from the metal-EDTA complex to be studied (15). The final dialysis buffer was used to prepare all EppA solutions for fluorescence studies.

For titration experiments, microliter aliquots of the metal-EDTA complex were added to 2 ml of EppA solution (35). The protein concentrations were 0.26 μM for $CaEDTA^{2-}$ experiments, 0.65 μM for $MgEDTA^{2-}$ and $HEDTA^{3-}$ experiments, and 0.79 μM for $ZnEDTA^{2-}$ and $CuEDTA^{2-}$ experiments. The fluorescence intensity was measured after the addition of various amounts of the metal-EDTA (0.1 μM to 5 μM) to the EppA solution with an integration time of 5 seconds (47). A control cuvette containing protein sample but receiving only buffer allowed for the correction of fluorescence emission due to dilution. The fluorescence changes of EppA at 340 nm after incremental addition of metal-EDTA was used to determine the dissociation constant. The concentration of EppA-CaEDTA complex was estimated by the following equation:

$$[\text{EppA-CaEDTA}] = [\text{EppA}] \times \{(I_0 - I_c)/(I_0 - I_f)\} \qquad \text{Eq. 1}$$

In the equation, [EppA] represents the initial concentration of EppA, I_0 is the fluorescence intensity of EppA at the initial titration point, I_c is the fluorescence intensity of EppA at a specific titration point, and I_f is the fluorescence intensity at saturating concentrations of CaEDTA. The K_d was determined from a plot of [EppA-CaEDTA] (y-axis) vs. [Total EDTA] (x-axis) fitted with equation 2, using Grafit 5.0 (28). *Cap* was the binding capacity of EppA.

$$y = \frac{-(K_d + x + Cap) + \sqrt{(Cap + x + K_d)^2 - 4xCap}}{2} \qquad \text{Eq. 2}$$

Isothermal titration calorimetry. Experiments were done by using a Microcal ITC instrument (Microcal, North Hampton, MA). In order for the machine to properly measure the exothermic and endothermic heat, the jacket surrounding the sample and reference cells was kept at 25°C (46). Purified EppA was dialyzed in 20 mM 3-(N-morpholino) propane sulfonic acid (MOPS) buffer and 10 mM $MgCl_2$ for 4 changes of the buffer to ensure that equilibrium was obtained. The final dialysis buffer was used to dilute EDTA to the proper concentration so that heat of dilution would be minimized. The heat of dilution was measured by injecting MgEDTA into the dialysis buffer to allow for background subtraction when fitting the data (48). For the experiments, 3 ml of 7.4 μM EppA was titrated with repeated injection of 1 μl of 300 μM MgEDTA prepared in the same buffer. The injection data was fit to a single site model using a least squares algorithm that is provided by the instrument software (48). The stoichiometry (N), association constant (K_a), enthalpy (ΔH), and entropy (ΔS) were also calculated from the fit data (48). The dissociation constant (K_d) is the inverse of the association constant (48).

Aqueous Speciation of EDTA. The aqueous speciation of EDTA was calculated using the chemical equilibrium modeling system MINEQL+ v. 3.01 (http://www.mineql.com/). Calculations were based on the experimental concentrations of cations, anions, pH, buffers, and EDTA in a specific assay solution (55). The dominant species discussed for each experiment represented the major species among the overall species distribution (31).

RESULTS

Sequence analysis of the ABC transporter genes. The genes (*eppABCD*) immediately upstream of *emoA* encode a hypothetical ABC-type transporter (3), exhibiting similarities to other bacterial solute binding ABC transporters (19). The first gene in the transport operon, *eppA*, encodes for a 593-amino acid protein that contains a cleavable signal sequence (1-26 amino acid residues), indicative of a periplasmic protein. EppA contains a conserved domain belonging to the family 5 bacterial extracellular solute-binding proteins (amino acids 106-456) (CDD 6088, NCBI Conserved Domain Database) (1), and is most similar to proteins of the 3.A.1.5 peptide/opine/nickel uptake transporter (PepT) family in the Transport Commission Database (TC-DB) (http://tcdb.ucsd.edu/tcdb/background.php) (1, 42). EppA shares 27% identity and 44% similarity with the oligopeptide binding protein OppA from *Mycobacterium tuberculosis* (1).

The next gene, *eppB*, encodes for a putative permease protein with 315 amino acid residues. EppB shares the highest identity and homology with permease proteins that are responsible for transporting oligopeptides. Immediately downstream of *eppB* is *eppC*, which encodes for a 308-amino acid protein that contains the conserved EAA loop (residues 201-220) between two transmembrane helices (1, 19). Both EppB and EppC contain conserved domains that share the highest homology with the permease components of the ABC-type dipeptide/oligopeptide/nickel transport systems (CDD 10891) (1), and each has a six predicted membrane-spanning α-helices, as predicted by COFAS (Chou-Fasman secondary structure prediction) and GREASE (a Kyte-Doolittle

hydrophobicity plot) (8, 19, 25), consistent with other integral membrane proteins of ABC transporters (6, 16).

Downstream of *eppC* is *eppD*, which encodes an ATP-binding protein that is similar with many such proteins from different organisms. This protein is responsible for binding ATP and hydrolysis, providing energy for ligand transport across the membrane. The ATP-binding protein is tightly associated with the membrane transporter proteins on the periphery of the cytoplasmic membrane within the cytoplasm (37). EppD is highly hydrophilic by sequence analysis, which is a typical property of this class of proteins (37). EppD contains both the Walker A (residues 355-363) and Walker B (residues 190-197) motifs which are characteristic of numerous nucleotide binding proteins (39) and an amino acid linker sequence which is a conserved signature of the ATP-binding domains concerned with ABC-type transporters (6, 19, 29, 44).

Further sequence analysis shows that the transporter genes are likely organized in a single operon with *emoA* and *emoB* genes, coding for EDTA monooxygenase and NADH:FMN oxidoreductase, as the stop codon for *eppD* overlaps with the start codon of *emoA* (3). Since *emoA* and *emoB* are inducible by growing on EDTA and are transcribed on the same mRNA molecules (3), the expression of the transporter genes together with *emoA* and *emoB*, when growing on EDTA, would be indicative of a transporter system involved in EDTA uptake.

Whole cell growth with different metal-EDTA species. The K_d values (Table 2) suggest that BNC1 cells can transport $MgEDTA^{2-}$ and $CaEDTA^{2-}$ into the cells for consumption and BNC1 may use $ZnEDTA^{2-}$ but should not use $CuEDTA^{2-}$. This prediction was verified by whole cells studies. When metal-EDTA was added into the

growth medium, it respeciated depending on the concentration of EDTA and metals, pH, and stability constants in the database: $NaEDTA^{2-}$ respeciated to $CaEDTA^{2-}$ (99%) and $MgEDTA^{2-}$ (1%); $ZnEDTA^{2-}$ yielded $ZnEDTA^{2-}$ (94%) and $CaEDTA^{2-}$ (6%); $CuEDTA^{2-}$ remained as itself (~99%). BNC1 grew well with added $NaEDTA^{2-}$ (which respeciates to $CaEDTA^{2-}$). Slower growth and complete lack of growth were observed with added $ZnEDTA^{2-}$ and $CuEDTA^{2-}$, respectively (Fig. 1).

EDTA uptake was induced in EDTA-grown cells. $CaEDTA^{2-}$ was selected for the assay since it represented 95% of the added $NaEDTA^{2-}$ in the EDTA medium, according to aqueous speciation analysis. EDTA-grown cells transported $CaEDTA^{2-}$ at a faster rate than LB-grown cells (Fig. 2), indicating that BNC1 has an EDTA uptake system that is inducible by growing on EDTA.

EDTA transport and metabolism is an EDTA inducible system. The correlation between transport and metabolism of different metal-EDTA species has been proposed (22), but the inducibility of the system by EDTA has not been studied. To further understand specificity of transport, the degradation of different metal-EDTA species by resting cells grown in either EDTA medium or $MMNH_3$ medium were tested. Ammonium production is directly correlated to EDTA metabolism (15). When BNC1 cell suspensions were incubated with $CaEDTA^{2-}$, the EDTA-grown cells produced more ammonium than the $MMNH_3$ grown cells did (Fig. 3A), suggesting the EDTA degradation genes are inducible by growing on EDTA. The ability of EDTA-grown cells to degrade different metal-EDTA species was further tested. The EDTA-grown cells degraded EDTA and produced approximately 310 μM ammonium from both 1mM $MgEDTA^{2-}$ and $CaEDTA^{2-}$, and produced about 180 μM ammonium from 1 mM

$ZnEDTA^{2-}$, but only produced a negligible amount of ammonium from $CuEDTA^{2-}$ (Fig. 3B). Since EmoA oxidizes $CuEDTA^{2-}$ (3), the lack of $CuEDTA^{2-}$ degradation by the EDTA grown cells must be due to the failure of uptake for this stable EDTA species.

RT-PCR was used to analyze the co-expression of the transporter genes (*eppABCD*) and the first gene in EDTA metabolism (*emoA*) (Fig 4). Primers were designed to span the entire hypothetical transport gene cluster and *emoA*. RT-PCR analysis of the total RNA extracted from $MMNH_3$ grown cells and EDTA grown cells showed that the gene cluster was expressed in the $MMNH_3$ grown cells at a minimal level, but expressed in the EDTA grown cells at a significantly higher level (Fig. 4). A primer located upstream of *eppA* (OoxA1, Fig. 4) and the primer RT-2 did not produce any detectable products (Fig. 4). Thus, *eppA* is the first gene of the gene cluster, including both the transporter and metabolism genes. Because the transporter genes and EDTA-metabolizing genes are co-transcribed, the transporter is responsible for EDTA uptake.

Overproduction and purification of the periplasmic binding protein, EppA. The DNA fragment that codes for the leaderless mature form of EppA (amino acid residues 27 to 567) was cloned into expression vector pET30-LIC. Overexpression of the cloned gene produced highly soluble recombinant EppA with an N-terminal His-tag (EppA-His) (Fig. 5, lane 2). When the cells from a 500-ml culture were disrupted, 12.5 mg of protein was obtained in the extract. Approximately 2 mg of EppA was obtained after the EconoQ and Ni^{2+}-NTA agarose columns (Fig. 5, lane 3 and 4). The pure EppA was stored at –80ºC, and no precipitation was observable in the solution after a month.

Binding of metal-EDTA complexes by EppA. Gel mobility shift, spectrophotometric, spectrofluorometric, and isothermal titration calorimetry assays were used to provide evidence that EppA binds different metal-EDTA complexes. The EDTA dependent gel-mobility shift of EppA was examined for $HEDTA^{3-}$, $MgEDTA^{2-}$, and $CaEDTA^{2-}$. As shown in Fig 6, EppA incubated with metal-EDTA species runs slightly behind unbound EppA. The lack of a large difference in the running patterns of bound EppA versus unbound EppA may be due to the small conformational changes that occur when EppA binds metal-EDTA, therefore minimally affecting the migration pattern (18). Molecular modeling of EppA (data not shown) has also provided evidence that the binding pocket is relatively small compared to other periplasmic binding proteins (12), validating the lack of a major difference in the running patterns of metal-EDTA bound and unbound EppA. Therefore, since the mobility shift between the bound and unbound EppA is slight, different approaches were taken to provide evidence that EppA binds metal-EDTA species.

Spectrophotometric and spectrofluorometric assays were used to provide evidence that EppA binds different metal-EDTA complexes. Fluorescence quenching is a common method used to study ligand binding by proteins; the intrinsic fluorescence of a protein, due to aromatic amino acid residues, is quenched upon ligand binding because the microenvironment of certain aromatic amino acid residues is modified (32). The technique was applied to study EDTA binding by EppA. Unbound EppA has an emission spectrum peak around 324 nm when excited at 280 nm. The emission intensity was reduced after the addition of 100 μM $CaEDTA^{2-}$, which was expected to saturate EppA (Fig. 7). No blue or red shift was observed in the emission peak. No fluorescence

changes were observed with controls, in which the same volume of the Tris-HCl buffer was added instead of the ligand (metal-EDTA) to the sample solution, or $CaEDTA^{2-}$ was added to the buffer with EmoB (3). The fluorescence changes of EppA at 340 nm after incremental addition of $CaEDTA^{2-}$ were fitted by using Grafit 5.0 (Fig. 8) (28), to obtain the dissociation constant (K_d) of EppA-$CaEDTA^{2-}$ complex (Table 2). The K_d values also were determined for EppA binding of $MgEDTA^{2-}$, $ZnEDTA^{2-}$, and $HEDTA^{3-}$ (Table 2). The binding of EppA to $HEDTA^{3-}$ was a surprise, as it should have a much different structure than any of the metal-EDTA complexes. Further investigation found that the buffer system was not completely Ca^{2+} free: the Tris-HCl reagent contains 1 ppm calcium, corresponding to approximate 0.15 μM in 50 mM Tris buffer. Thus, EppA may have bound $CaEDTA^{2-}$ in the $HEDTA^{3-}$ sample. The $CuEDTA^{2-}$ complex absorbs in the 340 nm region, so the spectrum was analyzed at 380 nm. No apparent changes were observed; therefore we conclude that EppA does not bind $CuEDTA^{2-}$.

The change in UV absorption spectrum of EppA upon binding different metal-EDTA species also were used to show EppA binding (Fig. 9). There was a slight increase in the absorption spectrum at 280 nm when an excess of $CaEDTA^{2-}$ was added to EppA (Fig. 9A) (18). Differential spectrum of specific metal-EDTA species (Fig. 9B) showed that $CaEDTA^{2-}$ and $MgEDTA^{2-}$ cause a hyperchromatic shift compared to $ZnEDTA^{2-}$ and $CuEDTA^{2-}$. These absorption changes are most likely due to orientation changes of specific amino acids caused by direct ligand binding (54).

Finally, isothermal titration calorimetry was used to corroborate the finding that EppA bound metal-EDTA complexes because isothermal titration calorimetry is an established technique for substrate binding (39). Since EppA was shown to bind

$MgEDTA^{2-}$, the complex was selected for further analysis. A known concentration of EppA was titrated with the injection of small aliquots of $MgEDTA^{2-}$ (Fig. 10). The initial injection generated the largest amount of heat associated with the binding (ΔH). As more $MgEDTA^{2-}$ was added, there was a reduced amount of complex formation and smaller ΔH in each subsequent injection. Upon saturation, ΔH becomes zero. The data were fitted with the Microcal data-fitting program to obtain the K_d. The calculated K_d from ITC was approximately 1 μM. This value was comparable to the K_d value determined with the fluorescence quenching method (Table 2).

DISCUSSION

The location of the ABC-type transporter genes immediately next to the EDTA metabolic genes suggests the potential role of the transporter in EDTA uptake. We present five lines of experimental evidence to support the hypothesis that *eppABCD* encodes for the ABC-type transporter responsible for EDTA uptake in EDTA-degrading bacterium BNC1. First, whole cell growth (Fig. 1), uptake (Fig. 2) and degradation (Fig. 3) studies demonstrate that $CaEDTA^{2-}$ uptake is facilitated by a specific transporter system that is induced in presence of EDTA. Second, sequence analysis of the transporter genes indicates that each component exhibits similartiy to other solute transporter systems and the transporter genes and EDTA-metabolizing genes are likely organized in a single operon. Third, RT-PCR expression analysis of the EDTA gene cluster demonstrates that the transporter genes are co-transcribed with *emoA* on the same mRNA molecules when the cells are grown on EDTA (Fig. 3). Fourth, EppA, the periplasmic binding protein of the transporter system, can selectively bind metal-EDTA complexes (Table 2). Last, the binding selectivity for various metal-EDTA complexes by EppA correlates with the ability of BNC1 to grow on and degrade these complexes (Table 2, Fig. 1 and Fig. 3, respectively). The lack of affinity of EppA for $CuEDTA^{2-}$ apparently accounts for its lack of uptake and degradation by BNC1 cells, because EDTA monooxygenase (EmoA), a cytoplasmic protein, uses $CuEDTA^{2-}$ as a substrate *in vitro* (11, 22). Taken together, we conclude that the ABC-type transporter is responsible for EDTA uptake into BNC1 cells. Thus, the hydrophilic metal-EDTA complexes, smaller than 500 Daltons, should diffuse freely through porins in the outer membrane of gram negative bacteria (11, 22). In the periplasm, EppA binds selected metal-EDTA

complexes, and delivers them to the transporter proteins (EppBCD) on the cytoplasmic membrane for uptake.

Metabolism of metal-EDTA species by bacteria BNC1 and DSM 9103 has been shown to depend on the thermodynamic stability of the metal-EDTA complex (22, 37). Complexes, that have been studied in relation to metabolism by BNC1, are divided into three groups: 1) degradable species with thermodynamic stability constants (*K*) (31) of $10^{13.81}$ or less (Ba-, Mg-, Ca-, and Mn-$EDTA^{2-}$); 2) $ZnEDTA^{2-}$ with a *K* of $10^{16.44}$, but degradable; and 3) non-degradable species that have thermodynamic stability constants above $10^{16.26}$ (Cd-, Pb-, Ni-, Cu-$EDTA^{2-}$, and Fe(III)-$EDTA^{-}$). In this study, specific metals from each group were chosen for degradation studies and EppA-binding assays. The high affinities of EppA for $CaEDTA^{2-}$ and $MgEDTA^{2-}$ (Table 2) are consistent with the degradation studies (Fig. 3). The K_d of EppA-$ZnEDTA^{2-}$ complex is 28.6 μM (Table 2), and BNC1 degrades $ZnEDTA^{2-}$ more slowly than $CaEDTA^{2-}$ and $MgEDTA^{2-}$ (Fig. 3). EppA does not bind $CuEDTA^{2-}$ and the cells do not degrade it (Fig. 3). The data demonstrate that $CaEDTA^{2-}$ and $MgEDTA^{2-}$ complexes are preferentially transported into the cell by the ABC transporter system. It also is clear that lack of transport and thus degradability of $CuEDTA^{2-}$ is due to the inefficient binding by EppA (Fig.3). However, it is uncertain whether $ZnEDTA^{2-}$ is directly transported into the cell. Its K_d value indicates that it can be transported by the ABC transporter system, but it is degraded more slowly than $CaEDTA^{2-}$ and $MgEDTA^{2-}$ (Table 2 and Fig. 3). The decreased amount of degradation may be due to either the lower affinity of EppA for ZnEDTA, or the limited respeciation of $ZnEDTA^{2-}$ to $CaEDTA^{2-}$ and $MgEDTA^{2-}$ in the growth medium. It also is possible that $CaEDTA^{2-}$, $MgEDTA^{2-}$, and $ZnEDTA^{2-}$ may be transported

simultaneously. Nonetheless, our data suggest that non-degradable metal-EDTA complexes are likely not transported into bacterium BNC1 cells for metabolism. Further, since EDTA monooxygenase (EmoA), a cytoplasmic protein, oxidizes $CuEDTA^{2-}$ (11, 22), but BNC1 whole cells fail to degrade $CuEDTA^{2-}$ (Fig. 1B), the lack of degradation must be due to the inability to bind and transport the $CuEDTA^{2-}$ complex.

The structure differences of the metal-EDTA complexes may determine whether they are bound to EppA or not. EDTA is a sexdentate ligand, but its coordination with metal ions is constrained by the ion sizes so that large metals are accessible to other ligands (2). The structure of $Na_2[Mg(H_2O)Y]5H_2O$ (where Y represents EDTA) is 7-coordinate with a monocapped trigonal prism stereochemistry (2) and the structure of $[Ca(H_2O)_3Y]^{2-}$ is 9-coordinate (2). The structure of $[Cu(H_2O)YH_2]$ is six coordinate with a pentadentate EDTA, meaning that one acetate is unattached and a water molecule completes the octahedron (56). This is also the case for $NiEDTA^{2-}$ and $CoEDTA^{2-}$ (56). Thus, EDTA is sexdentate in $MgEDTA^{2-}$ and $CaEDTA^{2-}$ (2), whereas, EDTA is pentadentate in $CuEDTA^{2-}$, $NiEDTA^{2-}$, and $CoEDTA^{2-}$ with a free acetate group, in which H_2O and possibly other molecules complete the coordination (57). However, structural determination of EppA with a bound ligand is required to give a definitive answer for the binding preference of EppA.

When Na_2EDTA^{2-} was added directly to a solution containing the EppA solution in the absence of added divalent cations, it dissociated mainly to $HEDTA^{3-}$ (~90%), calculated by the aqueous speciation analysis. However, the Tris buffer contained trace Ca^{2+} (ca. 0.15 μM), resulting in approximately 3.1% ($CaEDTA^{2-}$) of the total EDTA species (Table 2). We believe that EppA binds $CaEDTA^{2-}$ instead of $HEDTA^{3-}$, as the

direct binding of $HEDTA^{3-}$ is unlikely because of the structural difference between $HEDTA^{3-}$ and $CaEDTA^{2-}$ (2). Accordingly, $CaEDTA^{2-}$ and $MgEDTA^{2-}$, but not $HEDTA^{3-}$, are likely transported into the cell for metabolism. Soils generally contain large quantities of calcium in rocks and minerals, and Ca^{2+} is released by weathering (20). The environmental saturating concentration of Ca^{2+}, relative to EDTA levels, also favors the formation of $CaEDTA^{2-}$, instead of $HEDTA^{3-}$. In addition, the microenvironments that exist at the cell surface and in the periplasm potentially influence the speciation of the metal-EDTA species to favor $CaEDTA^{2-}$ and $MgEDTA^{2-}$ uptake. Ca^{2+} and Mg^{2+} are the main metal ions in the cell wall and outer membrane of gram negative bacteria, as they are required to reduce the charge repulsion between the highly anionic lipopolysaccharides (LPS), forming LPS-LPS and LPS-membrane protein salt bridges (10, 17, 45). Within the periplasm, the amount of Ca^{2+} is slightly higher than Mg^{2+} (10, 17, 45). Ca^{2+} is important for this region of the cell, especially for the cell wall, due to its ability to bridge carboxylic groups better than any other cations (17). The relative abundance of Ca^{2+} and Mg^{2+} at the cell surface and in the periplasm may facilitate the formation of $CaEDTA^{2-}$ and $MgEDTA^{2-}$ from unstable metal-EDTA complexes, explaining why such complexes are metabolized by BNC1 (22). However, the metal-EDTA complexes with stability constants higher than $10^{16.26}$ are unlikely to produce significant amounts of $MgEDTA^{2-}$ or $CaEDTA^{2-}$, which have a much smaller stability constants ($10^{6.4}$ and $10^{8.4}$, respectively) (22). This explains why complexes with high stability constants, with the exception of $ZnEDTA^{2-}$, are not degradable by BNC1. As discussed above, $ZnEDTA^{2-}$ has the potential to be directly transported by EppA into BNC1 for consumption. In addition, the dissociation kinetics of metal-EDTA complexes

may also control whether respeciation with Mg^{2+} or Ca^{2+} will occur at a reasonable rate. Since EDTA monooxygenase has a substrate range that includes substrates not metabolized by whole cells (for example, $CuEDTA^{2-}$) (3), the ABC transporter system must determine which metal-EDTA complexes are metabolized by BNC1. Thus, the reason that the stable metal-EDTA complexes are not metabolized by BNC1 is due to the lack of transport. At least for BNC1 and microorganisms using similar transporter system for EDTA uptake, the recalcitrance of EDTA in the environment is due to the presence of metal ions that form stable, resistant metal-EDTA complexes.

Bacterial degradation of other environmentally important chelating agents, i.e. NTA and citrate, has been studied (14, 43). Both of these chelating agents are speculated to enhance the mobility of metal ions in mixed waste environments (14, 56). The degradation rates of NTA by *Aminobacter aminovorans* (formerly *Chelobacter heintzii*) depends on the biologically available rate controlling form, $CaNTA^{-}$ (51). The hydrophilic nature of NTA implies that it is transported across the cell membrane by a specific transporter; however, a specific NTA transporter has not been discovered from the bacterium. Citrate degradation has been studied extensively in many different organisms. *Pseudomonas flourescens* metabolizes metal-citrate complexes depending on the specific structure of the complex, e.g. the complexes with a free hydroxyl group (i.e. Ca^{2+}-, Fe^{3+}- and Ni^{2+}-citrate) are readily degraded (14). It is uncertain whether the degradation preference is because of the lack of uptake or metabolism by the microorganism (14). However, citrate transport is affected by the bound metal in several microorganisms (24). *Bacillus subtilis* has two homologous secondary citrate transporters specific for different metals: CitM transports metal-citrate complexes of Mg^{2+}, Ni^{2+}, Co^{2+},

Mn^{2+}, and Zn^{2+}, and CitH uptakes Ca^{2+}, Sr^{2+} and Ba^{2+}-citrate complexes (24). It is apparent that metals bound by the chelating agents affect the biodegradation of the chelators. For EDTA degradation by bacterium BNC1, it is the uptake system that is more selective, determining which metal-EDTA complexes will be transported into the cell for metabolism.

ACKNOWLEGEMENTS

This research was funded by the Natural and Accelerated Bioremediation Research (NABIR) program, Biological and Environmental Research (BER), U.S. Department of Energy (grant #DE-FG03-01ER63081). JH was also supported by the National Science Foundation (NSF) Integrative Graduate Education and Research Training (IGERT) program at Washington State University (grant DGE-9972817). We thank Dr. Lisa Gloss for the use of the spectrofluorometer and suggestions, Andy Plymale for his work with whole cell uptake experiments, Dr. Gerhart Munski for helping with microcalorimetry, and Dr. Harvey Bolton Jr. for his suggestions.

REFERENCES

1. **Altschul, S., T. Madden, S. Schaffer, J. Zhang, Z. Zhang, W. Miller, and D. Lipman.** 1997. Gapped BLAST and PSI-BLAST: a new generation of protein database search programs. Nucleic Acids Res. **25:**3389-3402.
2. **Bell, C.** 1977. Principles and applications of metal chelation. Oxford University Press, Oxford.
3. **Bohuslavek, J., J. Payne, Y. Liu, H. Bolton, and L. Xun.** 2001. Cloning, sequencing, and characterization of a gene cluster involved in EDTA degradation from the bacterium BNC1. Appl. Environ. Microbiol. **67:**688-695.
4. **Bolton, H., Jr., S. W. Li, D. J. Workman, and D. C. Girvin.** 1993. Biodegradation of synthetic chelates in subsurface sediments from the southeast coastal plain. J. Enviorn. Qual. **22:**125-132.
5. **Bonicke, R., and B. Lisboa.** 1959. Uber das Vorkommen von Acylamidasen in Mycobacterien: I. Mitteilung: Die enzymatische Desamidierung aromatischer und aliphatischer Caronsaureamide. Zbl. Bakt. I.ABt Orig. **175:**403-421.
6. **Boos, W., and J. M. Lucht.** 1996. Periplasmic binding protein-dependent ABC transporters, p. 1175-1209. *In* R. Curtis III, E. Ingraham, E. C. C. Lin, K. B. Low, B. Magasanik, W. S. Rezinikoff, M. Riley, M. Schaechter, and H. Umbarger (ed.), Escherichia coli and Salmonella: cellular and molecular biology. American Society of Microbiology, Washington, D. C.
7. **Bucheli-Witschel, M., and T. Egli.** 2001. Environmental fate and microbial degradation of aminopolycarboxylic acids. FEMS Microbiol. Rev. **25:**69-106.

8. **Chou, P., and G. Fasman.** 1978. Prediction of secondary structure of proteins from their amino acid sequence. Adv. Enzymol. Relat. Areas Mol. Biol. **47:**45-148.

9. **Cleveland, J., and T. Rees.** 1981. Characterization of plutonium in Maxey Flats radioactive trench leachates. Science **212:**1506-1509.

10. **Coughlin, R., S. Tonsager, and E. McGroarty.** 1983. Quantification of metal cations bound to membranes and extracted lipopolysaccharide of *Escherichia coli*. Biochemistry **22:**2002-2007.

11. **Decad, G., and H. Nikaido.** 1976. Outer membrane of gram-negative bacteria. XII. Molecular-sieving function of cell wall. J. Bacteriol. **128:**325-336.

12. **Dunker, K.** 2001. Personal communication.

13. **Fiedler, G., M. Pajatsh, E. Kremmer, and A. Bock.** 1996. Genetics of a novel starch utilization pathway in *Klebsiella oxytoca*. J Mol Biol **256**.

14. **Francis, A., C. Dodge, and J. Gilow.** 1992. Biodegradation of metal citrate complexes and implications for toxic-metal mobility. Nature **356:**140-142.

15. **Henneken, L., B. Nortemann, and D. Hempel.** 1995. Influence of physiological conditions on EDTA degradation. Appl. Microbiol. Biotechnol. **44:**190-197.

16. **Higgins, C.** 1992. ABC transporters: from microorganisms to man. Annu. Rev. Cell Biol **8:**67-113.

17. **Hughes, M. N., and R. K. Poole.** 1989. Metals and Micro-organisms. Chapman and Hall, New York.

18. **Imperial, J., M. Hadi, and N. Amy.** 1998. Molybdate binding by ModA, the periplasmic component of the *Escherichia coli mod* molybdate transport system. Biochim. Biophys. Acta **1370:**337-346.

19. **Jensen, J., N. Peters, and T. Bhuvaneswari.** 2002. Redundancy in periplasmic binding protein-dependent transport systems for trehalose, sucrose, and maltose in *Sinorhizobium meliloti*. J. Bacteriol. **184:**2978-2986.

20. **Johnson, D. W., J. Turner, and J. M. Kelly.** 1982. The effects of acid rain on forest nutrient status. Water Resour. **18:**449-461.

21. **Karahalios, P., P. Mamos, D. Vynios, D. Papaioannou, and D. Kalpacis.** 1998. The effect of acylated polyamine derivatives on polyamine uptake mechanism, cell growth, and polyamine pools in Escherichia coli, and the pursuit of structure/activity relationships. Eur. J. Biochem. **251:**998-1004.

22. **Kluner, T., D. Hempel, and B. Nortemann.** 1998. Metabolism of EDTA and its metal chelates by whole cells and cell-free extracts of strain BNC1. Appl. Microbiol. Biotechnol. **49:**194-201.

23. **Krallmann-Wenzel, U.** 1985. An improved method of ammonia determination, applicable to amidases and other ammonia-producing enzyme systems of *Mycobacteria*. Am. Rev. Respir. Dis. **131:**432-434.

24. **Krom, B., B. Warner, W. Konings, and J. Lolkema.** 2000. Complementary metal ion specificity of the Me-Citrate transporters CitM and CitH of *Bacillus subtilis*. J. Bacteriol. **182:**6374-6381.

25. **Kyte, J., and R. F. Doolittle.** 1982. A simple method for displaying the hydropathic character of a protein. J. Mol. Biol. **157:**105-132.

26. **Laemmli, U. K.** 1970. Cleavage of structural proteins during the assembly of the head of bacteriophage T4. Nature (London) **227:**680-685.

27. **Lauff, J., D. Steele, L. Coogan, and J. Breitfeller.** 1990. Degradation of the ferric chelate of EDTA by a pure culture of an *Agrobacterium* sp. Appl. Environ. Microbiol. **56:**3346-3353.

28. **Leatherbarrow, R. J.** 2001. Grafit, 5.0.1 ed. Erithicus, Software, Ltd., Staines, England.

29. **Linton, K., and C. Higgins.** 1998. The Escherichia coli ATP-binding cassette (ABC) proteins. Mol Micrbiol **28:**5-13.

30. **Liu, Y., T. Louie, J. Payne, J. Bohuslavek, H. Bolton, and L. Xun.** 2001. Identification, purification, and characterization of iminodiacetate oxidase from the EDTA-degrading bacterium BNC1. Appl. Environ. Microbiol. **67:**696-701.

31. **Martell, A., and R. Smith.** 1974. Critical Stability Constants, vol. 1. Plenum Press, New York.

32. **Martineau, P., S. Szmelcman, J. Spurlino, F. Quiocho, and M. Hofnung.** 1990. Genetic approach to the role of tryptophan residues in the activities and fluorescence of a bacterial periplasmic maltose-binding protein. J. Mol. Biol. **214:**337-352.

33. **Means, J., and D. Crerar.** 1978. Migration of radioactive wastes: Radionuclide mobilization by complexing agents. Science **200:**1477-1486.

34. **Means, J., T. Kucak, and D. Crerar.** 1980. Relative degradation rates of NTA, EDTA, and DTPA and environmental implications. Environ. Pollut. (Series B) **1:**45-60.

35. **Miller, D., J. Olson, J. Pflugrath, and F. Quiocho.** 1983. Rates of ligand binding to periplasmic proteins involved in bacterial transport and chemotaxis. J. Bio. Chem. **258:**13665-13672.

36. **Mukhopadhyay, S., V. Kapatral, W. Xu, and A. Chakrabarty.** 1999. Characterization of a Hank's Type serine/threoine kinase and serine/threonine phosphoprotein phosphatase in *Pseudomonas aeruginosa*. J. Bacteriol. **181:**6615-6622.

37. **Nortemann, B.** 1999. Biodegradation of EDTA. Appl. Microbiol. Biotechnol. **51:**751-759.

38. **Nortemann, B.** 1992. Total degradation of EDTA by mixed cultures and a bacterial isolate. Appl. Environ. Microbiol. **58:**671-676.

39. **O'Brien, R., B. Chowdhry, and J. Ladbury.** 2001. Isothermal titration calorimetry of biomolecules. *In* S. Harding and B. Chowdhry (ed.), Protein-ligand interactions: hydrodynamics and calorimetry. Oxford University Press, New York.

40. **Payne, J., H. Bolton, J. Campbell, and L. Xun.** 1998. Purification and characterization of EDTA monooxygenase from the EDTA-degrading bacterium BNC1. J. Bacteriol. **180:**3823-3827.

41. **Rech, S., C. Wolin, and P. Gunsalus.** 1996. Properties of the periplasmic ModA molybdate-binding protein of *Escherichia coli*. J. Bio. Chem. **271:**2557-2562.

42. **Saier, M.** 2000. A functional-phylogenetic classification system for transmembrane solute transporters. Microbiol. Mol. Biol. Rev. **64:**354-411.

43. **Satroutdinov, A., E. Dedyukhina, T. Chistyakova, M. Witschel, I. Minkevich, V. Eroshin, and T. Egli.** 2000. Degradation of metal-EDTA complexes by resting cells of the bacterial strain DSM 9103. Environ. Sci. Tech. **34:**1715-1720.

44. **Saurin, W., and E. Dassa.** 1994. Sequence relationships between integral inner membrane proteins of binding protein-dependent transport system: evolution by recurrent gene duplications. Protein Sci. **3:**325-344.

45. **Schindler, M., and M. Osborn.** 1979. Interaction of divalent cations and Polymyxin B with lipopolysaccharide. Biochemistry **18:**4425-4430.

46. **Sleigh, S., A. Wilkinson, J. Ladbury, and J. Tame.** 1999. Cyrtallographic and calorimetric analysis of peptide binding to OppA protein. J. Mol. Biol. **291:**393-415.

47. **Sprencel, C., Z. Cao, Z. Qi, D. Scott, M. Montague, N. Ivanoff, J. Xu, K. Raymond, S. Newton, and P. Klebba.** 2000. Binding of ferric enterobactin by the *Escherichia coli* periplasmic binding protein FepA. J. Bacteriol. **182:**5359-5364.

48. **Stauffer, M., J. Young, and J. Evans.** 2001. Shikimate-3-phosphate binds to the isolated N-terminal domain of 5-enolpyruvylshikimate-3-phosphate synthase. Biochemistry **40:**3951-3957.

49. **Tiedje, J. M.** 1977. Influence of environmental parameters on EDTA biodegradation in soils and sediments. J. Environ. Qual. **6:**21-26.

50. **Toste, A., B. Osborn, K. Polach, and T. Lechner-Fish.** 1995. Organic analyses of an actual and simulated mixed waste: Hanford's organic complexant revisited. J. Radioanal. Nucl. Chem. **194:**25-34.

51. **Vanbriesen, J., Rittmann, B., Xun, L., Girvin, D., H. Bolton.** 2000. The rate-controlling substrate for biodegradation by *Chelatobacter heintzii*. Environ. Sci. Technol. **34**, 3346-3353

52. **Vandecasteele, S., W. Peetermans, R. Merckx, and J. Van Eldere.** 2001. Quantification of expression of *Staphylococcus epidermidis* housekeeping genes with Taqman quantitative PCR during in vitro growth and under different conditions. J. Bacteriol. **183:**7094-7101.

53. **Witschel, M., S. Nagel, and T. Egli.** 1997. Identification and characterization of the two-enzyme system catalyzing the oxidation of EDTA in the EDTA-degrading bacterial strain DSM 9103. J. Bacteriol. **179:**6937-6943.

54. **Wolf, A., K. Lee, J. Kirsch, and G. Ames.** 1996. Ligand-dependent conformational plasticity of the periplasmic histidine-binding protein HisJ. J. Biol. Chem. **271:**21243-21250.

55. **Xun, L., R. Reeder, A. Plymale, D. Girvin, and H. Bolton.** 1996. Degradation of metal-nitrilotriacetate complexes by nitrilotriacetate monooxygenase. Environ. Sci. Technol. **30:**1752-1755.

56. **Xun, L., R. B. Reeder, A. E. Plymale, D. C. Girvin, and H. Bolton, Jr.** 1996. Degradation of metal-nitrilotriacetate (NTA) complexes by NTA monooxygenase. Environmental Science & Technology. 30:1753-1755.

57. **Zubkowski, J., D. Perry, E. Valente, and S. Lott.** 1995. A seven coordinate Co-EDTA complex. Crystal and molecular structure of aquo(ethylenediaminetriacetic acid)cobalt(III) dihydrate. Inorg. Chem. **34:**6409-6411.

Table 1. Primers used in this study.

Primer	Sequence	Notes
MS-6	5'-GACGACGACAAGATGGACAATTTGGTCACCGGGGACTTG-3'	Forward primer of *eppA* gene
MS-7	5'-GAGGAGAAGCCCGGTTGATGACGACGAACATGAGAAAGC-3'	Reverse primer of *eppA* gene
RT-1	5'-ATGAATCCGTCCGCCAACTGGTAT-3'	Cotranscription of *eppA* and *emoA*
RT-8	5'-GCTCATAGCGATTGTCATGTGTGG-3'	Cotranscription of *eppA* and *emoA*
OX-1	5'-CTTCTTCACAGCGGCACACG-3'	Negative control primer 1
RT-2	5'-GCCACATCCAGTATCGGTCGAGAA-3'	Negative control primer 2

Table 2. Determined Dissociation Constants for EppA

Metal-EDTA species[1]	K_d (μM)
$CaEDTA^{2-}$	0.43 ± 0.07
$MgEDTA^{2-}$	0.58 ± 0.08
$HEDTA^{3-}$	1.3 ± 0.3
$ZnEDTA^{2-}$	28.6 ± 4.9

[1]Experiments were done in 50 mM Tris-HCl buffer (pH 7.5) with 1 mM of the corresponding metal ion at room temperature. Aqueous speciation showed the dominant metal-EDTA species were approximately 99% $CaEDTA^{2-}$, 98.9% $MgEDTA^{2-}$, 90% $HEDTA^{3-}$(with 3.1% $CaEDTA^{2-}$ due to trace amounts of Ca^{2+} in the buffer), and 99% $ZnEDTA^{2-}$ respectively.

Figure 1. Whole cell growth curves of BNC1 with different metal-EDTA complexes (50 μM): Ca/MgEDTA^{2-} (squares), ZnEDTA^{2-} (circles), and CuEDTA^{2-} (diamonds).

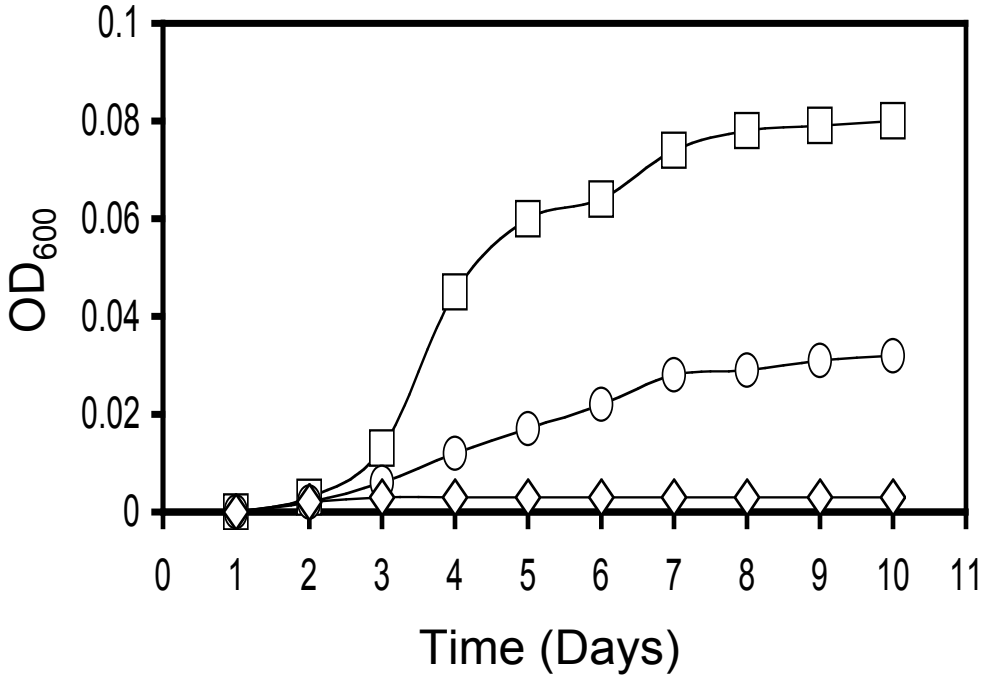
0.1
0.08
0.06
0.04
0.02
0
OD600
0 1 2 3 4 5 6 7 8 9 10 11
Time (Days)

Figure 2. Uptake of ^{14}C-EDTA in the presence of saturating amounts of Ca^{2+} (1 mM). EDTA grown cells (solid line) transported EDTA at a faster rate than the LB grown cells (dotted line).

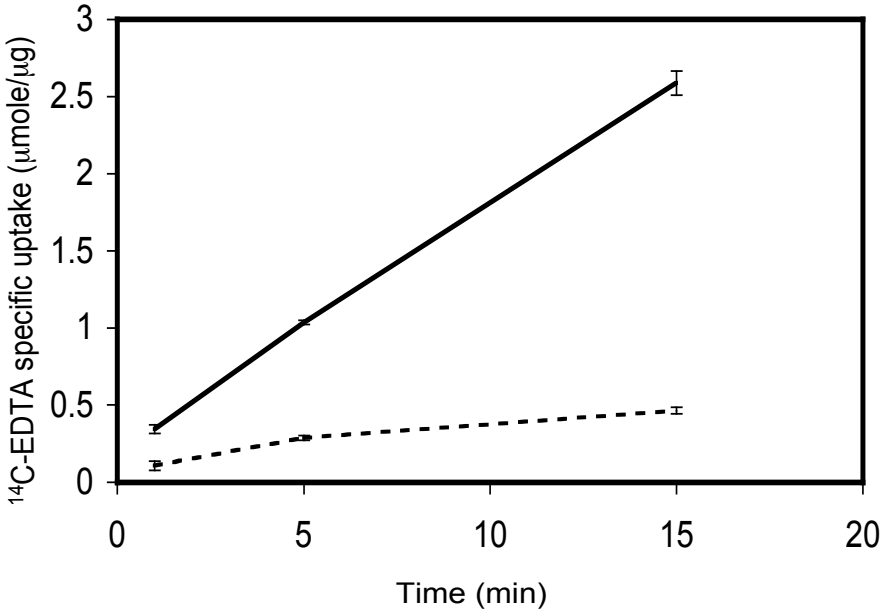
3
2.5
2
1.5
1
0.5
0
^{14}C-EDTA specific uptake (μmole/μg)
0
5
10
15
20
Time (min)

Figure 3. Degradation of EDTA by BNC1 cell suspensions. EDTA grown cells or $MMNH_3$ grown cells were suspended in PIPES buffer at turbidity of 0.5. Metal-EDTA (1 mM) was added to start EDTA degradation, which was monitored by ammonium production. (A) Comparison of $CaEDTA^{2-}$ degradation by EDTA grown cells (solid line) and $MMNH_3$ grown cells (dashed line). Data points are averages of three samples with error bars (standard deviation). (B) Ammonium production by EDTA grown cells incubated with (◆) $CaEDTA^{2-}$, (○) $MgEDTA^{2-}$, (X) $ZnEDTA^{2-}$, and (□) $CuEDTA^{2-}$. Data points are averages of three samples and standard deviations are similar to Fig. 1A. Dominant metal-EDTA species are practically the same as reported in Table 2. (C) Ammonium production by cell suspensions without metal-EDTA.

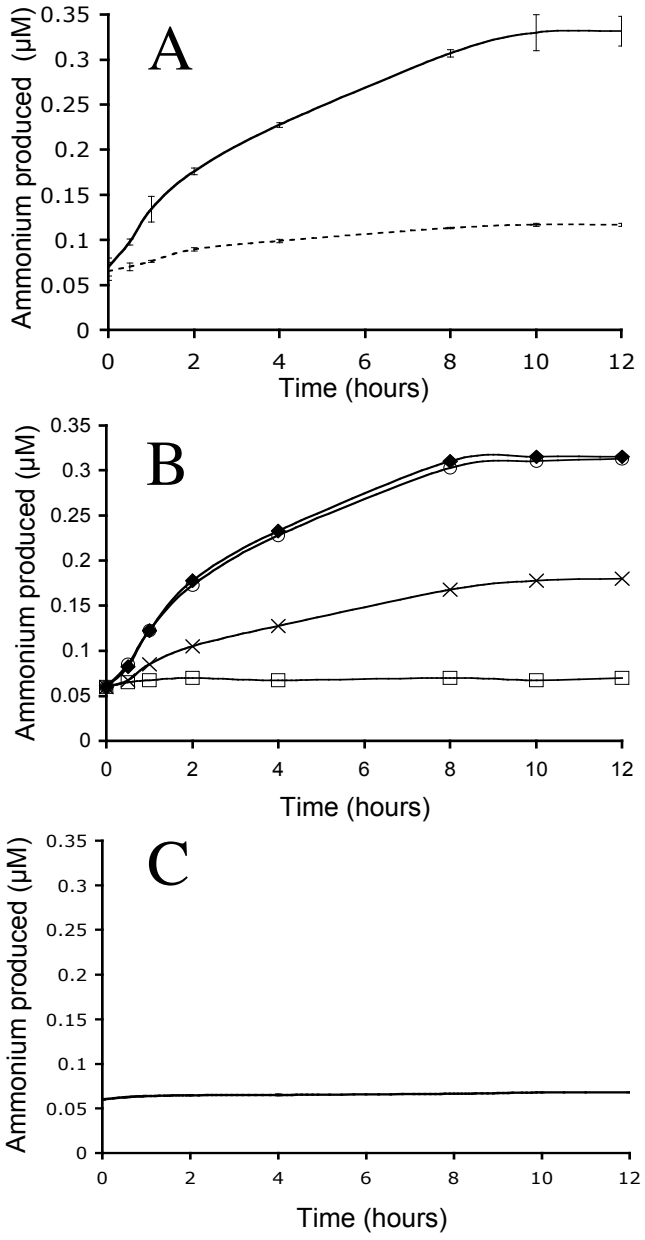
A
Ammonium produced (µM)
0.35
0.3
0.25
0.2
0.15
0.1
0.05
0
0
2
4
6
8
10
12
Time (hours)
B
Ammonium produced (µM)
0.35
0.3
0.25
0.2
0.15
0.1
0.05
0
0
2
4
6
8
10
12
Time (hours)
C
Ammonium produced (µM)
0.35
0.3
0.25
0.2
0.15
0.1
0.05
0
0
2
4
6
8
10
12
Time (hours)

Figure 4. RT-PCR analysis of the co-transcription of *eppABCD* and *emoA* in BNC1. Lane 1, DNA kb ladder; lane 2, total RNA of EDTA grown cells with primers RT-1 and RT-8 (Table 1); lane 3, $MMNH_3$ grown BNC1 cells with primers RT-1 and RT-8; lane 4, EDTA grown BNC1 cells with primers OX-1 and RT-2 (negative control).

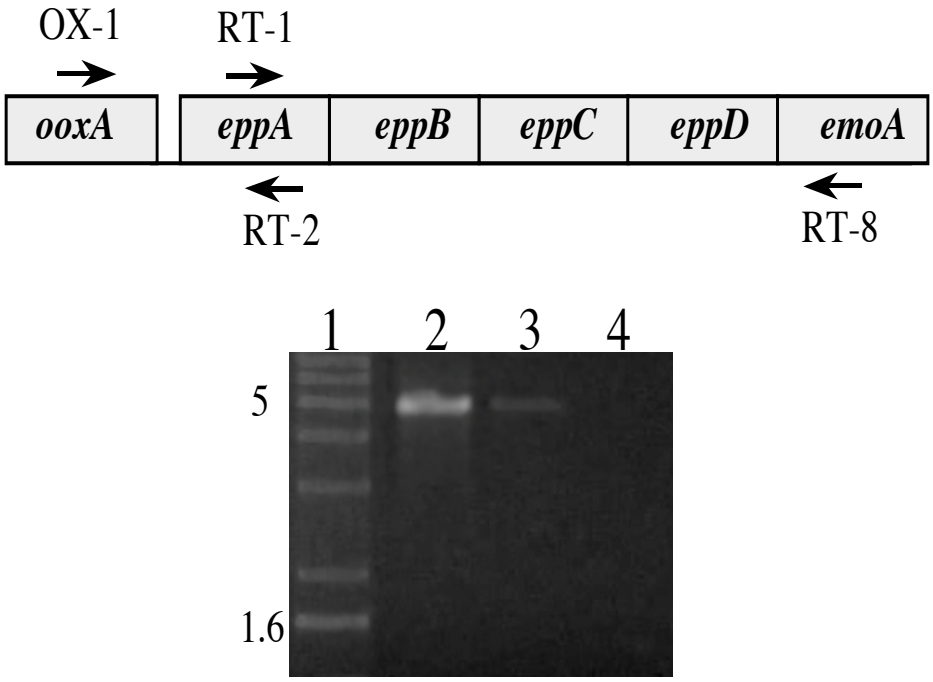
OX-1
RT-1
ooxA
eppA
eppB
eppC
eppD
emoA
RT-2
RT-8
1
2
3
4
5
1.6

Figure 5. SDS-PAGE analysis of EppA purification. Lanes 1, low-range molecular mass standard (Bio-Rad); 2, crude extract (10 μg of protein); 3, protein (7 μg) sample after Econo-Q column; 4, protein (1 μg) sample after Ni^{2+}-NTA-agarose column.

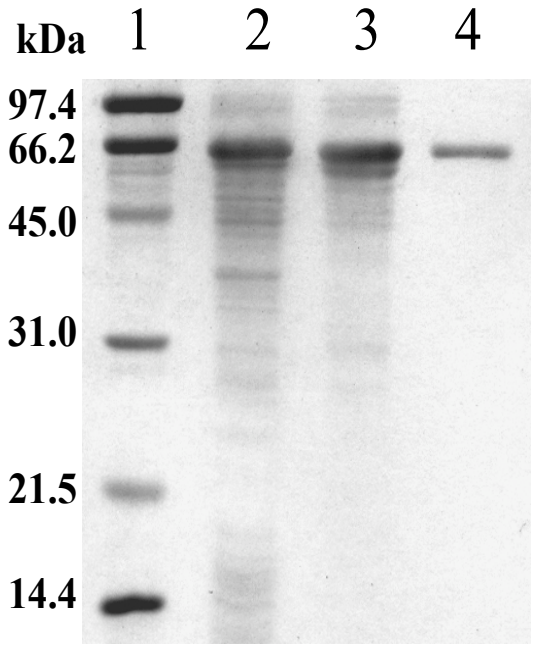
kDa
1
2
3
4
97.4
66.2
45.0
31.0
21.5
14.4

Figure 6. Gel mobility shift analysis of EppA binding different EDTA complexes. 10 μg of EppA was incubated with 1 mM of each EDTA complex for 20 minutes in Tris-HCl buffer. Samples were seperated on a 7% non-denaturing polyacrylamide gel for 50 minutes at 250 V.

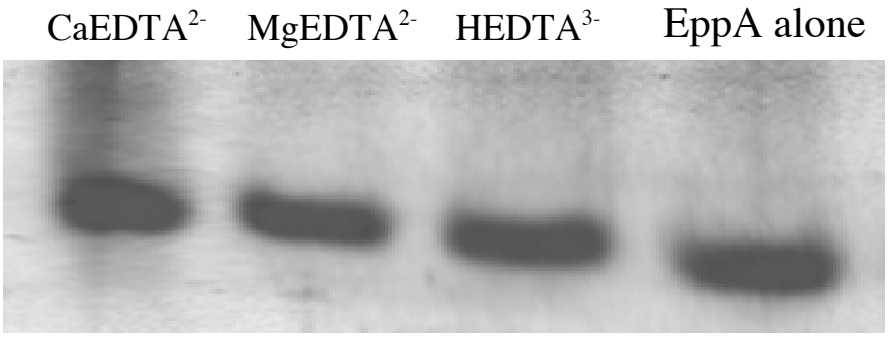
CaEDTA2-
MgEDTA2-
HEDTA3-
EppA alone

Figure 7. Fluorescence quenching of EppA induced through binding of $CaEDTA^{2-}$. The fluorescence spectrum of 1 μM EppA in 50 mM Tris buffer (pH 7.5) (solid line) was quenched by the addition of 1 mM $CaEDTA^{2-}$ (dotted line). The excitation was at 280 nm.

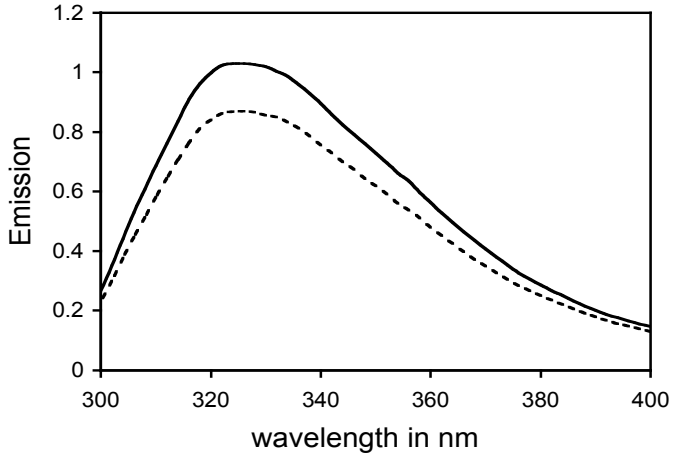
1.2
1
0.8
0.6
0.4
0.2
0
Emission
300
320
340
360
380
400
wavelength in nm

Figure 8. Titration of EppA fluorescence with $CaEDTA^{2-}$. The fluorescence of 0.26 μM EppA in 50 mM Tris buffer was gradually quenched by adding incremental amounts of 1 mM Ca^{2+} $CaEDTA^{2-}$. The data were used to calculate the dissociation constant of the EppA-$CaEDTA^{2-}$ complex.

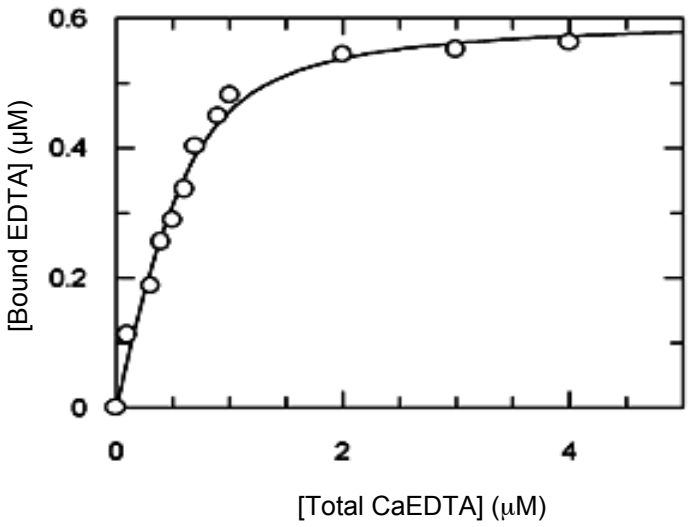
0.6
0.4
0.2
0
0
2
4
[Bound EDTA] (μM)
[Total CaEDTA] (μM)

Figure 9. Changes in the intrinsic UV absorption spectra of EppA upon EDTA binding. All experiments were conducted in 50 mM Tris-HCl (pH 7.5) with 10 μM EppA. (A) The raw spectra of EppA with (+$CaEDTA^{2-}$) and without (-$CaEDTA^{2-}$) 20 μM $CaEDTA^{2-}$. (B) Differential spectra of EppA with (a) $CaEDTA^{2-}$, (b) $MgEDTA^{2-}$, (c) $ZnEDTA^{2-}$, and (d) $CuEDTA^{2-}$ (20 μM), obtained by subtracting the spectrum of EppA from that of EppA with ligand.

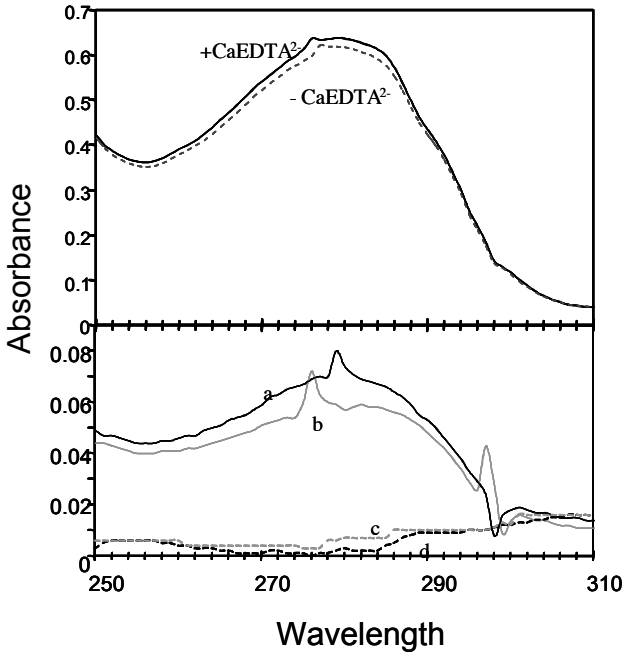
+CaEDTA2-
- CaEDTA2-
Absorbance
0.7
0.6
0.5
0.4
0.3
0.2
0.1
0
0.08
0.06
0.04
0.02
0
a
b
c
d
250
270
290
310
Wavelength

Figure 10. Raw experimental data (top) for binding of MgEDTA by EppA. Fitted model (bottom) to the integrated heats for each injection.

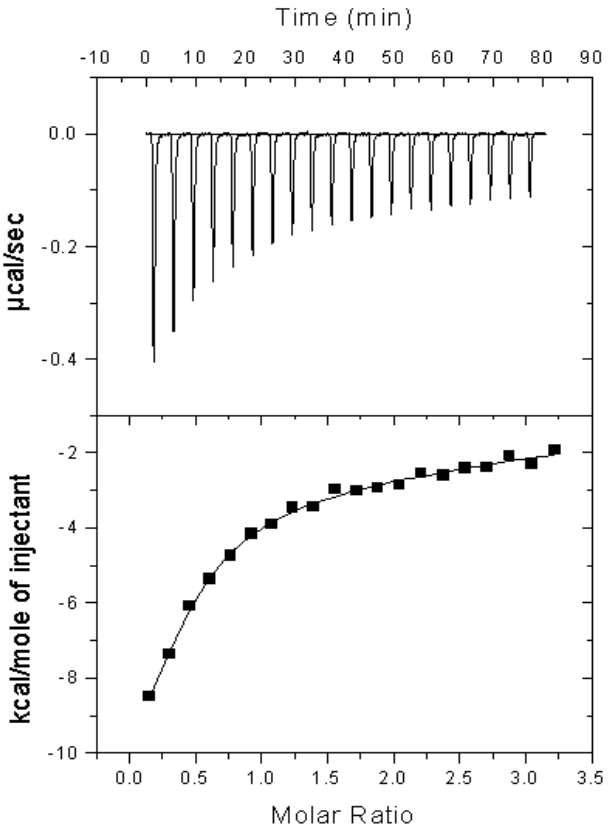
Time (min)
-10 0 10 20 30 40 50 60 70 80 90
0.0
-0.2
-0.4
µcal/sec
-2
-4
-6
-8
-10
kcal/mole of injectant
0.0 0.5 1.0 1.5 2.0 2.5 3.0 3.5
Molar Ratio

CHAPTER THREE

Characterization of Periplasmic EDTA-Binding Protein EppA in NTA Uptake into Bacterium BNC1

ABSTRACT

Nitrilotriacetate (NTA) is a common metal chelating agent that has been co-disposed with radionuclides. NTA increases the solubility and mobility of radionuclides in groundwater, and degradation microorganisms should eliminate the enhanced mobility. Bacterium BNC1 degrades both EDTA and NTA with the same metabolic enzymes. Further study supports the hypothesis that the EDTA transporter also is responsible for NTA transport into BNC1 cells. The transporter genes *eppABCD* and the metabolic gene *emoA* were found to be transcribed on the same mRNA and regulated as an operon in response to NTA in the medium. The periplasmic binding protein, EppA, of the transporter displayed drastic difference in binding specificity to selected metal-NTA complexes. The dissociation constants (K_d) for EppA binding of $MgNTA^-$, $CaNTA^-$, $ZnNTA^-$, and $CuNTA^-$ were 0.14, 0.32, 26, and 137 μM, respectively. The K_d values suggest that the transporter cannot efficiently uptake $CuNTA^-$, which was confirmed by whole cells studies. BNC1 metabolized $CaNTA^-$, $MgNTA^-$, and $ZnNTA^-$, but not $CuNTA^-$. Thus, the transporter is responsible for both NTA and EDTA uptake, and the binding selectivity of EppA confers the specificity for metal-NTA complexes that can be degraded by BNC1 cells.

INTRODUCTION

At the Department of Energy's Hanford site in Washington State the mixed waste consists of heavy metals, radionuclides and organic chelating agents (33). The exact composition of this waste is unknown (6), but the major organic chelator species present are assumed to be ethylenediaminetetraacetate (EDTA), nitrilotriacetate (NTA), and citric acid (33). The co-disposal of chelating agents and radionuclides has lead to the contamination of groundwater with radionuclides (for example, Pu) due to their enhanced mobility once bound to the chelating agents (8, 23). Microbial degradation of these chelating agents should decrease radionuclide mobility.

Several microbial species that can metabolize NTA and/or EDTA have been studied. The best-characterized organisms are *Chelatococcus asaccharovorans* strains TE1 and TE2 (1) and *Chelatobacter heintzii* strains TE4, 29600, 27109, and TE11 (1). Both *C. asaccharovorans* (34, 35) and *C. heintzii* (43) use an $FMNH_2$-dependent NTA monooxygenase for the first catabolic step, producing iminodiacetate (IDA), which is then catalyzed by an IDA dehydrogenase. Although the NTA metabolic pathway is understood for both systems, a specific NTA transporter has not been reported.

Pure bacterial isolates that can degrade EDTA include *Agrobacterium radiobacter* (18), DSM 9103 (42) and BNC1 (27). *A. radiobacter* degrades Fe(III)EDTA and can also metabolize Fe(III)-1,3-propylenediaminetetraacetate (Fe(III)PDTA) (18), but the metabolic pathway has not been characterized (18). DSM 9103 (41) and BNC1 (3) both use an $FMNH_2$ dependent EDTA monooxygenase (cA' and EmoA, respectively) to catalyze the first two EDTA metabolic steps. In BNC1 the iminodiacetate oxidase of (IdaA) catalyzes the last two steps of EDTA degradation (20). Besides EDTA, both

strains can use NTA as a sole carbon and nitrogen source (27, 42). In BNC1, EmoA oxidizes NTA to iminodiacetate (IDA), and IdaA catalyzes IDA to glycine (28).

Although the metabolic pathways for EDTA and NTA have been studied extensively, transport of EDTA and NTA into the cell is not well understood. The transport of EDTA into DSM 9103 was reported to depend on an active transport process, but a specific transporter was not reported (40). BNC1 is the only organism in which a specific EDTA transporter has been identified (Chapter 2). Further understanding of the BNC1 EDTA transporter (EppABCD) has allowed us to propose that this transporter also is responsible for NTA uptake into the cell. EppABCD is an ABC-type transporter, located immediately upstream of the EDTA and NTA metabolic genes *emoA*, *emoB*, and *idaA* (3). EppA, the periplasmic binding protein of the transporter, binds different metal-EDTA species; EppB and EppC are permease proteins in which the metal-EDTA complex will be transported into the cytoplasm; and EppD is the ATPase of the system (Fig. 2 from Chapter 1) (5, 12). The transporter is inducible by EDTA, and EppA binds different metal-EDTA species preferentially (Chapter 2). We report here that this transporter also is responsible for NTA uptake. Thus, BNC1 uses the same transporter and metabolic enzymes for both EDTA and NTA degradation.

MATERIALS AND METHODS

Bacterial strains and plasmids. The NTA-degrading bacterium BNC1 was kindly provided by Bernd Nörtemann (Technical University of Braunshweig, Braunshweig, Germany). BNC1 was cultured with disodium NTA (0.3 g/liter) in a mineral salts medium (MMNTA) (27). BNC1 also was grown in mineral salts media (27) supplemented with NH_3Cl (10 mM) ($MMNH_3$) or Luria-Bertani (LB) medium. *Escherichia coli* strain BL21(DE3) (Novagen, Madison, WI) was grown in LB medium.

Chemicals. Reagents used were of the highest purity available and were purchased from Sigma Co. (St. Louis, MO), Aldrich Chemical Co. (Milwaukee, WI), or Fisher Scientific Co. (Pittsburgh, PA). All PCR reactins were preformed with *Taq* DNA polymerase (Invitrogen, Carlsbad CA) and primers were purchased from Gibco BRL (Gaithersburg, MD). Restriction endonucleases and DNA-modifying enzymes were purchased from Gibco BRL or New England Biolabs (Beverly, MA).

Whole cell growth on different metal-NTA species. Whole cell growth studies were conducted in NTA growth medium specific for the metal to be tested. The mineral salts growth medium (27) containing 1.5 mM $MgCl_2$, and 1.5 mM $CaCl_2$, was supplemented with 0.2% (v/v) glycerol and different amounts of $NaNTA^-$, $ZnNTA^-$, or $CuNTA^-$ as the nitrogen source. Sterile media were inoculated with 0.1% of NTA-grown cells from a late log phase culture. The cultures were grown at 30°C with shaking at 200 rpm. The optical density was analyzed at 600 nm, OD_{600nm}.

Degradation of NTA by BNC1 cell suspensions. BNC1 cells were grown in MMNTA and $MMNH_3$ media to late exponential phase. Cells were harvested, washed with 20 mM PIPES buffer (pH 7.5), and resuspended in the same buffer. Experimental

reactions were started by adding 1 mM of the respective metal-NTA complex to the cell suspension. Controls experiments consisted of the cell suspensions with no metal-NTA complex added and 1 mM metal-NTA complex in the PIPES buffer. The metal-NTA ratios were 10:1 for Mg^{2+} and Ca^{2+}, and 1:1 for Zn^{2+} and Cu^{2+}. Additional controls were prepared with BNC1 in the $MMNH_3$ medium with 1 mM of Zn^{2+} or Cu^{2+} to test for their toxicity.

Ammonium concentration was determined using the Krallmann-Wenzel method (17). At specific time points, 0.5-ml samples were removed and centrifuged, and 0.25 ml of the supernatant solution were used for experimental procedures. Added to the sample supernatant was 10 μl of catalyst solution (3 volumes of 2 mM $MnSO_4$ freshly mixed with 1 volume of acetone), 0.5 ml of phenol reagent, and 0.25 ml of 1.5 % hypochlorite solution (4). The sample mixture was incubated for 6 minutes, and the OD_{636nm} was recorded. This reading was used to determine the concentration by comparison to a calibration curve (1 μM to 5 mM NH_3).

Reverse transcription (RT)-PCR. Total mRNA was isolated from BNC1 cells grown to mid-log phase in MMNTA or $MMNH_3$ medium, according to a published method (37). The isolated RNA was treated with RNase-free DNase (GibcoBRL), and further purified with the RNeasy Midi Kit (Qiagen, San Diego, Calif.). RNA samples were screened for DNA contamination by PCR analysis. Samples that yielded no signal contained no DNA and were used for RT-PCR analysis.

RT-PCR reactions were carried out using the OneStep RT-PCR kit (Gibco BRL) in a 100-μl reaction with 2 ng of RNA, and the products were analyzed on 0.7% agarose

gel. Reactions were performed using various combinations of sequence-specific primers (Table 1) (3, 25).

Overexpression and purification of EppA. EppA was purified according to the procedure reported in Chapter 2.

Gel Mobility Shift Assay. Ligand-dependent gel mobility shift assays were performed as described by Rech et al. (29). Approximately 10 μg of EppA was incubated with 1 mM of the respective metal-NTA species in 20 mM Tris-HCL (pH 7.5) for 20 minutes on ice. Samples were loaded on a 7% polyacrylamide gel. Electrophoresis was performed at 250 V at 4° C for 50 minutes. The gel was stained with GelCode Blue Stain reagent (Pierce, Rockford IL) and analyzed visually.

Difference in UV absorption spectra. The changes in the intrinsic UV absorption of EppA were studied using a Pharmacia Biotech Ultrospec 4000 UV/visible spectrophotometer. Experiments were conducted at room temperature in 25 mM Tris-HCl pH 7.5. The absorption spectra of EppA (10 μM) in the presence and absence of metal-NTA (20 μM) were recorded (14, 43).

Measurement of the dissociation constant. Fluorescence spectroscopy measurements were performed as described in Chapter 2. Prior to fluorescence measurements, the protein sample was dialyzed for three hours at 4° C against 1 L of 50 mM Tris-HCl buffer (pH 7.5) with saturating amounts (10 mM) of the metal ion from the metal-NTA complex to be studied (11). The final dialysis buffer was used to prepare all EppA solutions for fluorescence studies.

For titration experiments, microliter aliquots of the metal-NTA complex were added to 2 ml of EppA solution (24). The protein concentrations were fixed at 0.65 μM

for all metal-NTA experiments. The fluorescence intensity was measured after the addition of various amounts of the metal-NTA (0.1 μM to 5 μM) to the EppA solution with an integration time of 5 seconds (31). A control cuvette containing EppA but receiving only buffer allowed for the correction of fluorescence emission due to dilution. Changes in fluorescence of EppA at 340 nm after incremental addition of metal-NTA was used to determine the dissociation constant. For $CuNTA^-$, the fluorescence was measured at 380 nm due to absorbance of $CuNTA^-$ at 340 nm. The concentration of EppA-MgNTA complex was estimated by the following equation:

$$[\text{EppA-MgNTA}] = [\text{EppA}] \times \{(I_0 - I_c)/(I_0 - I_f)\} \qquad \text{Eq. 1}$$

In the equation, [EppA] represents the initial concentration of EppA, I_0 is the fluorescence intensity of EppA at the initial titration point, I_c is the fluorescence intensity of EppA at a specific titration point, and I_f is the fluorescence intensity at saturating concentrations of MgNTA. The K_d was determined from a plot of [EppA-MgNTA] (y-axis) vs. [Total NTA] (x-axis) fitted with equation 2, using Grafit 5.0 (19). *Cap* was the binding capacity of EppA.

$$y = \frac{-(K_d + x + Cap) + \sqrt{(Cap + x + K_d)^2 - 4xCap}}{2} \qquad \text{Eq. 2}$$

Aqueous Speciation of NTA. The aqueous speciation of NTA was calculated as described in Chapter 2.

RESULTS

Whole cell growth with different metal-NTA species. BNC1 grows preferentially on $MgNTA^-$ or $CaNTA^-$ (speciation was 89.9% $CaNTA^-$ and 9.2% $MgNTA^-$ in the medium) (Fig. 1). Slower growth was observed with $ZnNTA^-$ as the added nitrogen source (speciation was 95.5% $ZnNTA^-$ and 4.1% $CaNTA^-$ in the medium) (Fig. 1). When the cells were grown with $CuNTA^-$ (speciation was 89.8% $CuNTA^-$, 5.7% $Cu(OH)NTA^-$, and 4% $CaNTA^-$ in the medium), minimal growth was observed (Fig. 1).

Whole cell degradation of NTA is an inducible system. We reported previously that EDTA transport and metabolism is inducible in BNC1 (Chapter 2), and cells grown on EDTA degraded EDTA faster than cells grown on NH_3 (Chapter 2). Similar results were identified with NTA degradation (Fig 2). Cells grown on NTA metabolized $MgNTA^-$ faster than cells grown on NH_3 (Fig 2A). NTA grown cells also were tested for their ability to degrade different metal-NTA species. Such cells degraded NTA and produced approximately 125 μM ammonium from 1 mM $MgNTA^-$ or $CaNTA^-$, and produced about 92 μM ammonium from 1 mM $ZnNTA^-$, and produced 71 μM ammonium from 1 mM $CuNTA^-$ (Fig 2B).

RT-PCR analysis. RT-PCR was used to analyze the co-expression of the transporter genes (*eppABCD*) and the first gene in NTA metabolism (*emoA*) (Fig 3), as described in Chapter 2 for studying the EDTA system. Primers deigned to span the entire hypothetical transporter gene cluster and *emoA* were used for analysis. RT-PCR analysis of the total RNA extracted from cells grown on NH_3 or NTA showed that the gene cluster was expressed in the cells grown on $MMNH_3$ at a minimal level, but was expressed at a significantly higher level in the cells grown in the presence of NTA (Fig. 3). A negative

control using the primers OoxA1 (complimentary to sequences upstream of *eppA*) and RT-2, yielded no detectable product (Fig. 3). Thus, the transporter genes are co-transcribed with *emoA* and the expression is enhanced when BNC1 grows on NTA. The co-transcription of the transport genes with the NTA/EDTA-metabolizing genes suggests that this transport system is responsible for both NTA and EDTA transport.

Binding of metal-NTA complexes by EppA. The NTA-dependent gel-mobility shift of EppA was examined for $HNTA^{2-}$, $MgNTA^{-}$, and $CaNTA^{-}$. As shown in Fig 4, EppA incubated with metal-NTA species ran slightly behind unbound EppA. The lack of a large difference in the running patterns of bound EppA versus unbound EppA may be due to the small conformational changes that occur when EppA binds metal-NTA (14). Molecular modeling of EppA (data not shown) has also provided evidence that the binding pocket is relatively smaller than in other periplasmic binding proteins (10), consistent with the lack of a major difference in the running patterns of metal-NTA bound and unbound EppA. Therefore, other approaches were taken to provide evidence that EppA binds metal-NTA species.

The spectrophotometric and spectrofluorometric assays described in Chapter 2 also were used to study EppA binding different metal-NTA complexes. Fluorescence quenching is a common method used to study ligand binding by proteins; the intrinsic fluorescence of a protein, due to aromatic amino acid residues, is quenched upon ligand binding because the microenvironment of certain aromatic amino acid residues is modified (22). Fluorescence analysis of EppA revelaed that it had an emission spectrum peak around 325 nm when excited at 280 nm, and the emission intensity was reduced after the addition of 100 μM $MgNTA^{-}$, which was expected to saturate EppA (Fig. 5).

No blue or red shift was observed in the emission peak. No fluorescence changes were observed with controls, in which either Tris-HCl buffer was added instead of the ligand (metal-NTA) to the sample solution, or when $MgNTA^-$ was added to Tris-HCl buffer containing EmoB (3). The fluorescence changes of EppA at 325 nm after incremental addition of $MgNTA^-$ were fitted by using Grafit 5.0 (Fig. 6) (19), to obtain the dissociation constant (K_d) of the EppA-$MgNTA^-$ complex (Table 2). The K_d values also were determined for EppA binding of $CaNTA^-$, $ZnNTA^-$, $HNTA^{2-}$, and CuNTA (Table 2).

The change in UV absorption spectrum also were used to detect binding of EppA with different metal-NTA complexes (Fig. 7). There was a slight increase in the spectrum at 280 nm when an excess of $MgNTA^-$ was added to EppA (Fig. 7A) (14). Differential spectra of specific metal-NTA species (Fig. 7B) showed that $MgNTA^-$ and $CaNTA^-$ cause a hyperchromatic shift compared to $ZnNTA^-$ and $CuNTA^-$. These absorption changes are most likely due to orientation changes of specific amino acids resulting from ligand binding (43).

DISCUSSION

BNC1 possesses the ability to metabolize multiple aminopolycarboxylic acids, making it an ideal organism for understanding the transport and metabolism of EDTA and NTA at the molecular level. Since BNC1 uses the same metabolic enzymes for EDTA and NTA degradation, we hypothesized that the same transporter may be responsible for both EDTA and NTA uptake. As I have reported in Chapter 2, BNC1 has a specific EDTA uptake transporter consisting of four proteins, and the periplasmic binding protein, EppA, confers the selectivity for the metal-EDTA complexes transported into the cell. This also was demonstrated for metal-NTA complexes. Presented here are four lines of evidence that the same transporter also is responsible for NTA transport into the cytoplasm of BNC1. First, whole cell growth (Fig. 1) and degradation (Fig. 2) studies demonstrate that $MgNTA^-$ and $CaNTA^-$ uptake is facilitated by a specific transporter system, which is induced in NTA-growing cells. Second, RT-PCR analysis of cells grown in NTA but not NH_3, demonstrated that the transport genes (*eppABCD*) are NTA inducible and co-transcribed with *emoA*, coding for EDTA monooxygenase, on the same mRNA molecule (Fig. 3). Third, EppA, the periplasmic binding protein of the transporter system, can selectively bind metal-NTA complexes (Table 2). Last, the binding selectivity for various metal-NTA complexes by EppA correlates with the ability of BNC1 to grow on and degrade these complexes (Table 2, Fig. 1 and Fig. 3, respectively). Taken together, the results support the hypothesis that EppABCD is a specific transporter for both EDTA and NTA.

EDTA transport into BNC1 is dependent on the thermodynamic stability constants of the metal-EDTA complex (16, 26). To understand if this is the case for

metal-NTA transport, we first grew BNC1 with different metal-NTA complexes. BNC1 grew to the greatest cell density with $CaNTA^-$ and $MgNTA^-$ ($MgNTA^-$ $K= 10^{5.47}$ and $CaNTA^-$ $K= 10^{6.39}$ (21)) as the dominant species in the medium (89.9% $CaNTA^-$ and 9.2% $MgNTA^-$) (Fig. 1). BNC1 did not reach as high of a cell density with $ZnNTA^-$ ($ZnNTA^-$ $K= 10^{10.66}$ (21)) as the sole nitrogen source (95.5% $ZnNTA^-$ and 4.1% $CaNTA^-$) (Fig. 1), and the growth was marginal with $CuNTA^-$ ($CuNTA^-$ $K= 10^{10.24}$ (21)) as the dominant species in the medium (89.8% $CuNTA^-$, 5.7% $Cu(OH)NTA^-$, and 4% $CaNTA^-$) (Fig. 1). Whole cell growth data provide evidence that $MgNTA^-$ and $CaNTA^-$, which have low thermodynamic stability constants, are the preferred substrates of BNC1.

These results were further corroborated with degradation studies and EppA-binding assays. The high affinity of EppA for $MgNTA^-$ and $CaNTA^-$ (Table 2) is consistent with degradation studies (Fig. 2). EppA binds $ZnNTA^-$ with a K_d of 26 μM (Table 2) and BNC1 degrades $ZnNTA^-$ slower than $CaNTA^-$ and $MgNTA^-$ (Fig. 2) Finally, EppA binds $CuNTA^-$ with the lowest affinity (Table 2), and whole cells grown with the complex produced the least amount of ammonium (Fig. 2). These data demonstrate that $MgNTA^-$ and $CaNTA^-$ complexes are the preferred substrates for the transporter. This means that $ZnNTA^-$ and $CuNTA^-$, which have higher stability constants than $MgNTA^-$ and $CaNTA^-$, may respeciate to $MgNTA^-$ and $CaNTA^-$ in order for NTA transport to occur. This speculation is supported by whole cell growth curves, degradation and binding results. Growth on and degradation of $ZnNTA^-$ and $CuNTA^-$ occurs slower than Mg/$CaNTA^-$, and EppA binds $ZnNTA^-$ and $CuNTA^-$ with lower affinities. Whole cell growth experiments contained saturating amounts of Mg^{2+} and Ca^{2+} in both the $ZnNTA^-$ and $CuNTA^-$-growing cultures, yet neither complex supported

growth comparable to Mg/CaNTA$^-$. Conversely, the fact that ZnNTA$^-$ and CuNTA$^-$ both supported a small amount of growth and measurable ammonium demonstrates that both complexes are used by the cells; however, the low efficiency argues for respeciation before uptake of NTA for ZnNTA$^-$ and CuNTA$^-$. Therefore, the slower rates of growth and degradation are likely due to the kinetic barrier of ZnNTA$^-$ and CuNTA$^-$ respeciating to MgNTA$^-$ and CaNTA$^-$. Further, the low affinity of EppA for ZnNTA$^-$ and CuNTA$^-$ complexes also supports this speculation. ZnNTA$^-$ may be a substrate of EppA, but the low affinity for ZnNTA$^-$ indicates that MgNTA$^-$ and CaNTA$^-$ are the preferred substrates. The thermodynamic stability constants are much lower for ZnNTA$^-$ and CuNTA$^-$ than ZnEDTA^{2-} (K=$10^{16.44}$ (21)) and CuEDTA^{2-} (K=$10^{16.26}$ (21)), and comparatively speaking, their respeciation is much more favorable. Thus, stable metal-EDTA complexes are usually recalcitrant in the environment, but the corresponding metal-NTA complexes are not stable enough to prevent respeciation and then degradation by microorganisms.

The specificity of transport is further seen by the EppA dissociation constant of HNTA^{2-}, which is higher than those of MgNTA$^-$ and CaNTA$^-$ (Table 2). For *C. heintzii*, the transported species is CaNTA$^-$ (36). The environmentally saturating concentration of Ca^{2+} and Mg^{2+} will favor the formation of CaNTA$^-$ and MgNTA$^-$. Also, Ca^{2+} and Mg^{2+} are the major metal ions present in the outer membrane and cell wall of bacteria (9, 13, 30). Ca^{2+} and Mg^{2+} help maintain the proper structure of lipopolysaccharide (LPS) (9, 13, 30). The saturating amounts of Ca^{2+} and Mg^{2+} also will influence the respeciation of ZnNTA$^-$ and CuNTA$^-$ to Mg/CaNTA$^-$. Therefore, we speculate that CaNTA$^-$ and MgNTA$^-$ are the transported species for BNC1.

The geometric coordinate structure was proposed to affect the binding of metal-EDTA complexes by EppA in Chapter 2, and this also may be the case also for NTA. NTA acts as a tridentate or tetradentate ligand depending on the metal ion. Ca-$HN^{+}(CH_2COO^{-})_3$-$2H_20$ (or $CaNTA^{-}$) has a pentagonal bipyrimidal configuration (38). The nitrogen atom of NTA does not coordinate with the Ca^{2+} ion, and the Ca-oxygen bonds are not constrained to a fixed length (38). Another structure reported for $CaNTA^{-}$ indicated that only one bond is formed between an NTA group and a particular calcium atom (7, 39). The $CaNTA^{-}$ structure is very similar to those of H_2NTA^{-} and Na_2NTA^{-} structures (32, 38). NaCuNTA-H_2O is tetradentate with a distorted octahedral coordination, and is a much stronger complex than $CaNTA^{-}$ and H_2NTA^{-} (2, 39). The structure of NaCuNTA is very constrained, but when compared to metal-EDTA complexes, $CuNTA^{-}$ and $CaNTA^{-}$ are much more variable in structure, due to different bond lengths formed within each complex (38, 39). For metal-EDTA complexes it was proposed that EDTA is pentadentate when binding larger metal ions (such as Cu^{2+}, Ni^{2+} and Co^{2+}) and a free acetate group may affect the binding of these complexes by EppA. For metal-NTA complexes this does not seem to be the case. For $CaNTA^{-}$ and H_2NTA^{-}, the plasticity of the complex may allow for the proper conformation in the EppA binding pocket. These complexes are less constrained, in comparison to $CuNTA^{-}$ (39), and the ease of forming the proper configuration may be the difference between binding and not binding. Future work to crystallize this protein would determine the specificity of the binding pocket, and how EppA can bind different metal-EDTA and metal-NTA complexes with such high affinity.

Degradation studies (Fig 2) and RT-PCR analysis (Fig. 3) show that the EppA transporter is inducible by NTA. BNC1 whole cells grown on NTA degraded $MgNTA^-$ faster than NH_3 grown cells (Fig. 2B). Inducibility was further demonstrated with RT-PCR analysis of the transporter genes (*eppABCD*) and *emoA*. Primers designed to overlap *eppABCD* and *emoA* produced a stronger RT-PCR signal with NTA grown cells than NH_3 grown cells (Fig. 3), verifying that NTA induces transcription of the transporter genes and *emoA*, as seen previously for EDTA (Chapter 2). Thus, the operon is inducible by both EDTA and NTA.

The transport and metabolic capabilities of BNC1 offers insight into developing a bioremediation system for mixed waste environments. At the U. S. Department of Energy's Hanford site, there are a reported 38 chelator/complexor fragments existing in the mixed waste environments (33). The formation of multiple chelator/complexor fragments is due to radiolytic, thermal, and/or chemical degradation of the parent compounds EDTA, NTA and citric acid (33). Remediation in this environment requires a microorganism that can metabolize multiple chelators and chelator fragments. The ability of BNC1 to degrade both EDTA and NTA makes it a candidate for remediation of this mixed waste environment. Understanding the metabolic capabilities of BNC1 at the molecular level is important for developing a bioremediation system incorporating BNC1. Microbial degradation of the radionuclide-EDTA and radionuclide-NTA species is the long-term goal for this research.

ACKNOWLEGEMENTS

This research was funded by the Natural and Accelerated Bioremediation Research (NABIR) program, Biological and Environmental Research (BER), U.S. Department of Energy (grant #DE-FG03-01ER63081). JH was also supported by the National Science Foundation (NSF) Integrative Graduate Education and Research Training (IGERT) program at Washington State University (grant DGE-9972817). We thank Dr. Lisa Gloss for the use of the spectrofluorometer and suggestions and Dr. Harvey Bolton Jr. for his suggestions.

REFERENCES

1. **Auling, G., H. Busse, T. Egli, T. El-Banna, and E. Stackebrandt.** 1993. Description of the Gram-negative, obligately aerobic, nitrilotriacetate (NTA)-utilizing bacteria *Chelatococcus asaccharovorans*, gen. nov., sp. nov. Syst. Appl. Microbiol. **12:**104-112.

2. **Battagliz, L., A. Corradi, and M. Tani.** 1975. The crystal and molecular structure of potassium monoaquamono(nitrilotriacetato)-cobalt(II) dihydrate, $K[Co(C_6H_6NO_6)(OH_2]\text{-}2H_2O$. Acta Cryst. **19:**1160-1164.

3. **Bohuslavek, J., J. Payne, Y. Liu, H. Bolton, and L. Xun.** 2001. Cloning, sequencing, and characterization of a gene cluster involved in EDTA degradation from the bacterium BNC1. Appl. Environ. Microbiol. **67:**688-695.

4. **Bonicke, R., and B. Lisboa.** 1959. Uber das Vorkommen von Acylamidasen in Mycobacterien: I. Mitteilung: Die enzymatische Desamidierung aromatischer und aliphatischer Caronsaureamide. Zbl. Bakt. I.ABt Orig. **175:**403-421.

5. **Boos, W., and J. M. Lucht.** 1996. Periplasmic binding protein-dependent ABC transporters, p. 1175-1209. *In* R. Curtis III, E. Ingraham, E. C. C. Lin, K. B. Low, B. Magasanik, W. S. Rezinikoff, M. Riley, M. Schaechter, and H. Umbarger (ed.), Escherichia coli and Salmonella: cellular and molecular biology. American Society of Microbiology, Washington, D. C.

6. **Bucheli-Witschel, M., and T. Egli.** 2001. Environmental fate and microbial degradation of aminopolycarboxylic acids. FEMS Microbiol. Rev. **25:**69-106.

7. **Clegg, W., A. Powell, and M. Ware.** 1984. Structure of trisodium bis(nitrilotriacetato)ferrate(III) pentahydrate, $Na_3[Fe\{N(CH_2CO_2)_2]$.$5H_2O$. Acta Cryst. **C40:**1822-1824.

8. **Cleveland, J., and T. Rees.** 1981. Characterization of plutonium in Maxey Flats radioactive trench leachates. Science **212:**1506-1509.

9. **Coughlin, R., S. Tonsager, and E. McGroarty.** 1983. Quantification of metal cations bound to membranes and extracted lipopolysaccharide of *Escherichia coli*. Biochemistry **22:**2002-2007.

10. **Dunker, K.** 2001. Personal communication.

11. **Henneken, L., B. Nortemann, and D. Hempel.** 1995. Influence of physiological conditions on EDTA degradation. Appl. Microbiol. Biotechnol. **44:**190-197.

12. **Higgins, C.** 1992. ABC transporters: from microorganisms to man. Annu. Rev. Cell Biol **8:**67-113.

13. **Hughes, M. N., and R. K. Poole.** 1989. Metals and Micro-organisms. Chapman and Hall, New York.

14. **Imperial, J., M. Hadi, and N. Amy.** 1998. Molybdate binding by ModA, the periplasmic component of the *Escherichia coli mod* molybdate transport system. Biochim. Biophys. Acta **1370:**337-346.

15. **Johnson, D. W., J. Turner, and J. M. Kelly.** 1982. The effects of acid rain on forest nutrient status. Water Resour. **18:**449-461.

16. **Kluner, T., D. Hempel, and B. Nortemann.** 1998. Metabolism of EDTA and its metal chelates by whole cells and cell-free extracts of strain BNC1. Appl. Microbiol. Biotechnol. **49:**194-201.

17. **Krallmann-Wenzel, U.** 1985. An improved method of ammonia determination, applicable to amidases and other ammonia-producing enzyme systems of *Mycobacteria*. Am. Rev. Respir. Dis. **131:**432-434.

18. **Lauff, J., D. Steele, L. Coogan, and J. Breitfeller.** 1990. Degradation of the ferric chelate of EDTA by a pure culture of an *Agrobacterium* sp. Appl. Environ. Microbiol. **56:**3346-3353.

19. **Leatherbarrow, R. J.** 2001. Grafit, 5.0.1 ed. Erithicus, Software, Ltd., Staines, England.

20. **Liu, Y., T. Louie, J. Payne, J. Bohuslavek, H. Bolton, and L. Xun.** 2001. Identification, purification, and characterization of iminodiacetate oxidase from the EDTA-degrading bacterium BNC1. Appl. Environ. Microbiol. **67:**696-701.

21. **Martell, A., and R. Smith.** 1974. Critical Stability Constants, vol. 1. Plenum Press, New York.

22. **Martineau, P., S. Szmelcman, J. Spurlino, F. Quiocho, and M. Hofnung.** 1990. Genetic approach to the role of tryptophan residues in the activities and fluorescence of a bacterial periplasmic maltose-binding protein. J. Mol. Biol. **214:**337-352.

23. **Means, J., and D. Crerar.** 1978. Migration of radioactive wastes: Radionuclide mobilization by complexing agents. Science **200:**1477-1486.

24. **Miller, D., J. Olson, J. Pflugrath, and F. Quiocho.** 1983. Rates of ligand binding to periplasmic proteins involved in bacterial transport and chemotaxis. J. Bio. Chem. **258:**13665-13672.

25. **Mukhopadhyay, S., V. Kapatral, W. Xu, and A. Chakrabarty.** 1999. Characterization of a Hank's Type serine/threoine kinase and serine/threonine phosphoprotein phosphatase in *Pseudomonas aeruginosa*. J. Bacteriol. **181:**6615-6622.

26. **Nortemann, B.** 1999. Biodegradation of EDTA. Appl. Microbiol. Biotechnol. **51:**751-759.

27. **Nortemann, B.** 1992. Total degradation of EDTA by mixed cultures and a bacterial isolate. Appl. Environ. Microbiol. **58:**671-676.

28. **Payne, J., H. Bolton, J. Campbell, and L. Xun.** 1998. Purification and characterization of EDTA monooxygenase from the EDTA-degrading bacterium BNC1. J. Bacteriol. **180:**3823-3827.

29. **Rech, S., C. Wolin, and P. Gunsalus.** 1996. Properties of the periplasmic ModA molybdate-binding protein of *Escherichia coli*. J. Bio. Chem. **271:**2557-2562.

30. **Schindler, M., and M. Osborn.** 1979. Interaction of divalent cations and Polymyxin B with lipopolysaccharide. Biochemistry **18:**4425-4430.

31. **Sprencel, C., Z. Cao, Z. Qi, D. Scott, M. Montague, N. Ivanoff, J. Xu, K. Raymond, S. Newton, and P. Klebba.** 2000. Binding of ferric enterobactin by the *Escherichia coli* periplasmic binding protein FepA. J. Bacteriol. **182:**5359-5364.

32. **Stanford, R.** 1967. The crystal structure of nitrilotriacetic acid. Acta Cryst. **23:**825-833.

33. **Toste, A., B. Osborn, K. Polach, and T. Lechner-Fish.** 1995. Organic analyses of an actual and simulated mixed waste: Hanford's organic complexant revisited. J. Radioanal. Nucl. Chem. **194:**25-34.

34. **Uetz, T., and T. Egli.** 1993. Characterization of an inducible membrane-bound iminodiacetate dehydrogenase from *Chelatobacter heintzii* ATCC 29600. Biodegradation.

35. **Uetz, T., R. Schneider, M. Snozzi, and T. Egli.** 1992. Purification and characterization of a two-component monooxygenase that hydroxylates nitrilotriacetate from '*Chelatobacter*' strain ATCC 29600. J. Bacteriol. **174:**1179-1188.

36. **Vanbriesen, J., Rittmann, B., Xun, L., Girvin, D., H. Bolton.** 2000. The rate-controlling substrate for biodegradation by Chelatobacter heintzii. Environ. Sci. Technol. **34**, 3346-3353

37. **Vandecasteele, S., W. Peetermans, R. Merckx, and J. Van Eldere.** 2001. Quantification of expression of *Staphylococcus epidermidis* housekeeping genes with Taqman quantitative PCR during in vitro growth and under different conditions. J. Bacteriol. **183:**7094-7101.

38. **Whitlow, S.** 1972. The crystal structure of calcium nitrilotriacetate dihydrate. Acta Cryst. **B28:**1914.

39. **Whitlow, S.** 1973. Structure of sodium nitrilotriacetatocopper(II) monohydrate. Inorg. Chem. **12:**2286-2289.

40. **Witschel, M., T. Egli, A. Zehnder, and M. Spycher.** 1999. Transport of EDTA into cells of the EDTA-degrading bacterial strain DSM 9103. Microbiology **145:**973-983.

41. **Witschel, M., S. Nagel, and T. Egli.** 1997. Identification and characterization of the two-enzyme system catalyzing the oxidation of EDTA in the EDTA-degrading bacterial strain DSM 9103. J. Bacteriol. **179:**6937-6943.

42. **Witschel, M., H. Weilenmann, and T. Egli.** 1995. Degredation of EDTA by a bacterial isolate. Poser presented at the 54th annual meeting of the Swiss Society of Microbiology, Lugano.

43. **Wolf, A., K. Lee, J. Kirsch, and G. Ames.** 1996. Ligand-dependent conformational plasticity of the periplasmic histidine-binding protein HisJ. J. Biol. Chem. **271:**21243-21250.

44. **Xu, Y., M. Mortimer, T. Fisher, M. Kahn, F. Brockman, and L. Xun.** 1997. Cloning, sequencing, and analysis of a gene cluster from Chelatobacter heintzii ATCC 29600 encoding nitrilotriacetate monooxygenase and NADH:Flavin mononucleotide oxidoreductase. J. Bacteriol. **179:**1112-1116.

Table 1. Primers used in this study

Primer	Sequence	Notes
MS-6	5'-GACGACGACAAGATGGACAATTTGGTCACCGGGGACTTG-3'	Forward primer of *eppA* gene
MS-7	5'-GAGGAGAAGCCCGGTTGATGACGACGAACATGAGAAAGC-3'	Reverse primer of *eppA* gene
RT-1	5'-ATGAATCCGTCCGCCAACTGGTAT-3'	Cotranscription of *eppA* and *emoA*
RT-8	5'-GCTCATAGCGATTGTCATGTGTGG-3'	Cotranscription of *eppA* and *emoA*
OX-1	5'-CTTCTTCACAGCGGCACACG-3'	Negative control primer 1
RT-2	5'-GCCACATCCAGTATCGGTCGAGAA-3'	Negative control primer 2

Table 2. Determined Dissociation Constants for EppA

Metal-NTA species	K_d **(μM)**
$MgNTA^-$	0.14 ± 0.03
$CaNTA^-$	0.32 ± 0.1
$HNTA^{2-}$	0.53 ± 0.05
$ZnNTA^-$	26 ± 1.2
$CuNTA^-$	137 ± 14.7

Experiments were done in 50 mM Tris-HCl buffer (pH 7.5) with 1 mM of the corresponding metal ion at room temperature. Aqueous speciation showed the dominant metal-EDTA species were approximately 99.6% $MgNTA^-$, 99% $CaNTA^-$, 86.2% $HNTA^{2-}$(with 10% $CaNTA^-$ and 3.6% $MgNTA^-$ due to trace amounts of Ca^{2+} and Mg^{2+} in the buffer), 99% $ZnNTA^-$, and 83.3% $CuNTA^-$ (with 16.6% $Cu(OH)NTA^-$) respectively.

Figure 1. Whole cell growth curves of BNC1 with different metal-EDTA complexes (50 μM), Ca/MgNTA$^-$, ZnNTA$^-$, and CuNTA$^-$, as the sole nitrogen source.

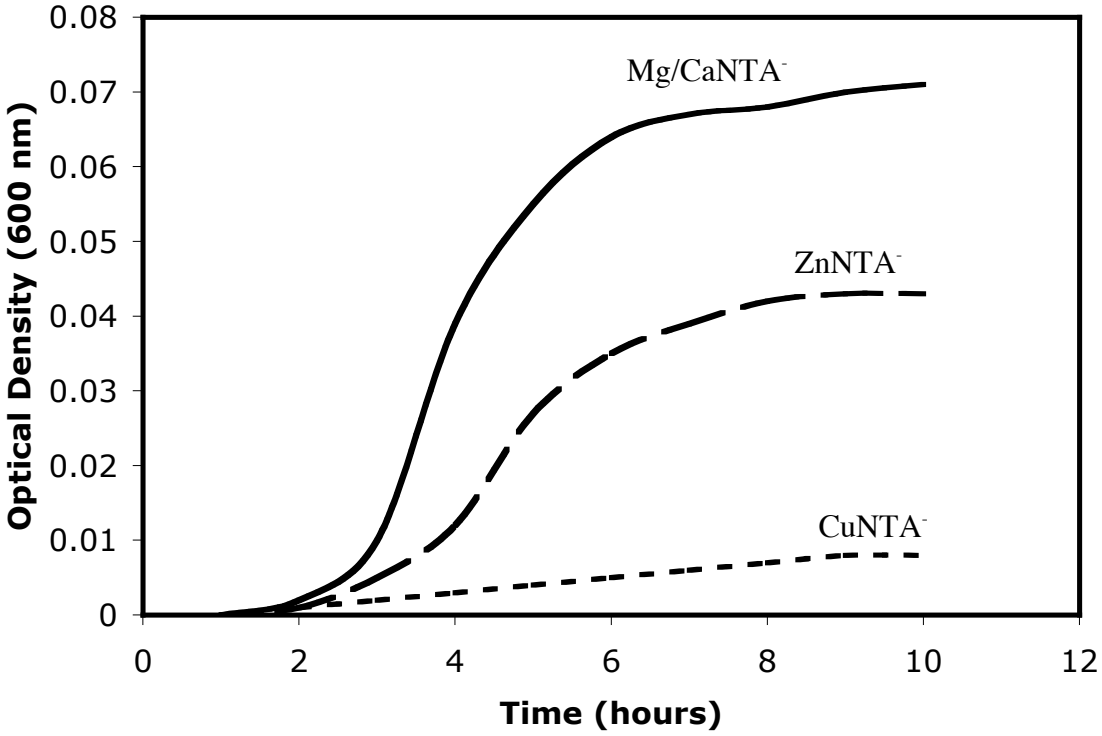
0.08
0.07
0.06
0.05
0.04
0.03
0.02
0.01
0
Optical Density (600 nm)
Mg/CaNTA-
ZnNTA-
CuNTA-
0
2
4
6
8
10
12
Time (hours)

Figure 2. Degradation of NTA by BNC1 cell suspensions. (A) Ammonium produced when $MgNTA^-$ was used as the nitrogen source for NTA grown cells (solid line) and $MMNH_3$ grown cells (dashed line). (B) Ammonium produced when BNC1 is incubated with $MgNTA^-$ (black solid line), $CaNTA^-$ (grey solid line, $ZnNTA^-$ (black dashed line), and $CuNTA^-$ (grey dashed line). (C) Ammonium produced from BNC1 cell suspensions without the addition of metal-NTA.

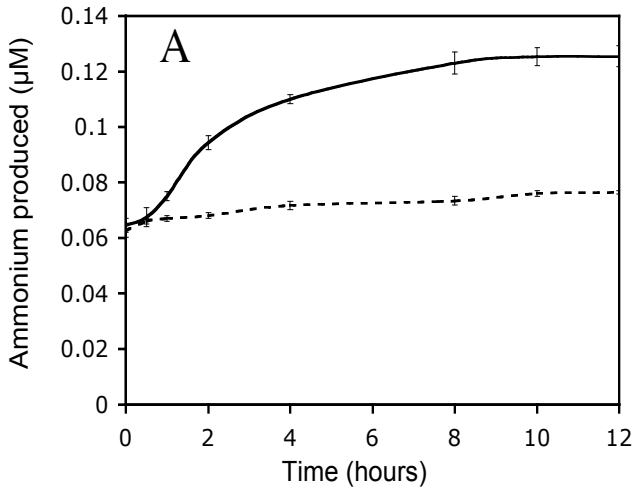
A
Ammonium produced (µM)
0.14
0.12
0.1
0.08
0.06
0.04
0.02
0
0
2
4
6
8
10
12
Time (hours)

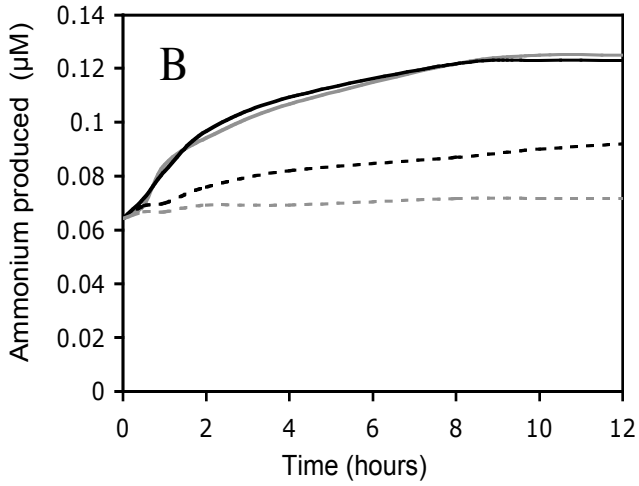
B
Ammonium produced (µM)
0.14
0.12
0.1
0.08
0.06
0.04
0.02
0
0
2
4
6
8
10
12
Time (hours)

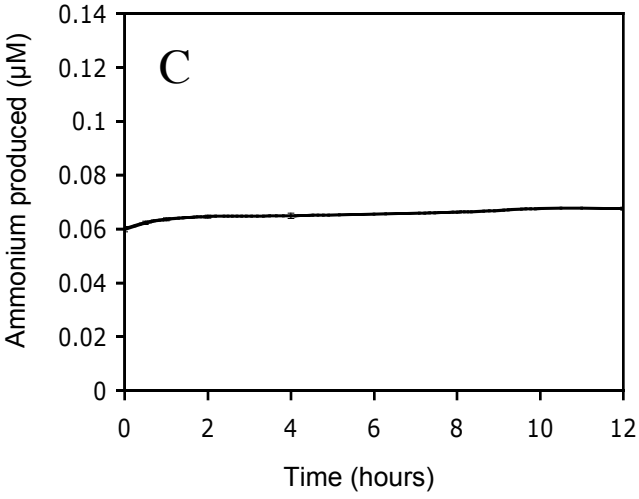
C
Ammonium produced (µM)
0.14
0.12
0.1
0.08
0.06
0.04
0.02
0
0
2
4
6
8
10
12
Time (hours)

Figure. 3. RT-PCR analysis showing the co-transcription of the transport operon (*eppABCD*) with *emoA*. Lane 1, DNA 1 kb ladder. Lane 2, NTA grown BNC1 cells, primers RT-1 and RT-8. Lane 3, $MMNH_3$ grown BNC1 cells, primers RT-1 and RT-8. Lane 4, NTA grown BNC1 cells, primers OX-1 and RT-2 (negative control). Positive controls were also done using genomic DNA (data not shown).

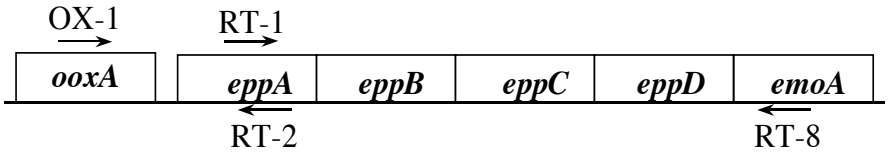
OX-1
RT-1
ooxA
eppA
eppB
eppC
eppD
emoA
RT-2
RT-8

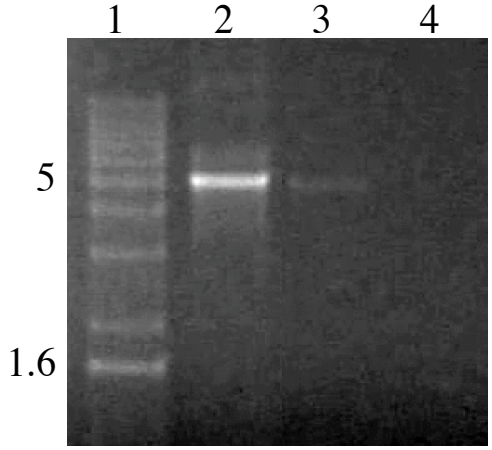
1
2
3
4
5
1.6

Figure 4. Gel mobility shift analysis of EppA binding different NTA complexes. 10 μg of EppA was incubated with 1 mM of each different NTA complex for 20 minutes in Tris-HCl buffer. Samples were ran on a 7% non-denaturing polyacrylamide gel for 50 minutes at 250 V.

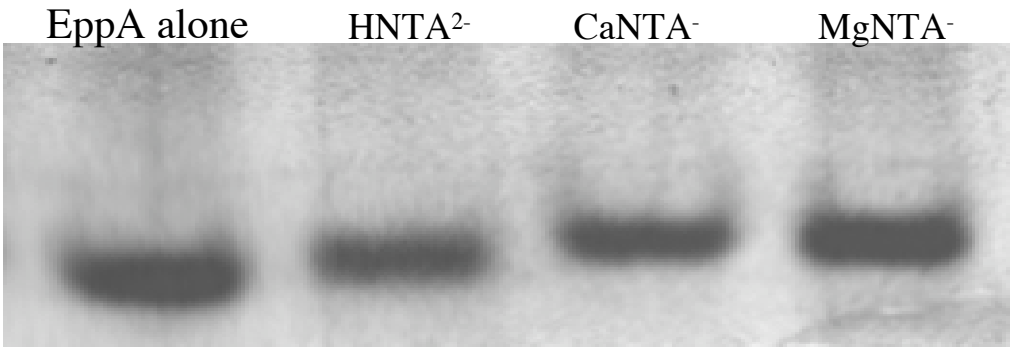
EppA alone
HNTA2-
CaNTA-
MgNTA-

Figure 5. Fluorescence quenching of EppA induced by the binding of $MgNTA^-$. EppA (1 μM) without substrate was excited at 280 nm (solid line). $MgNTA^-$ was added at a saturating amount (10 mM) to the EppA sample, and excited at 280 nm (dotted line).

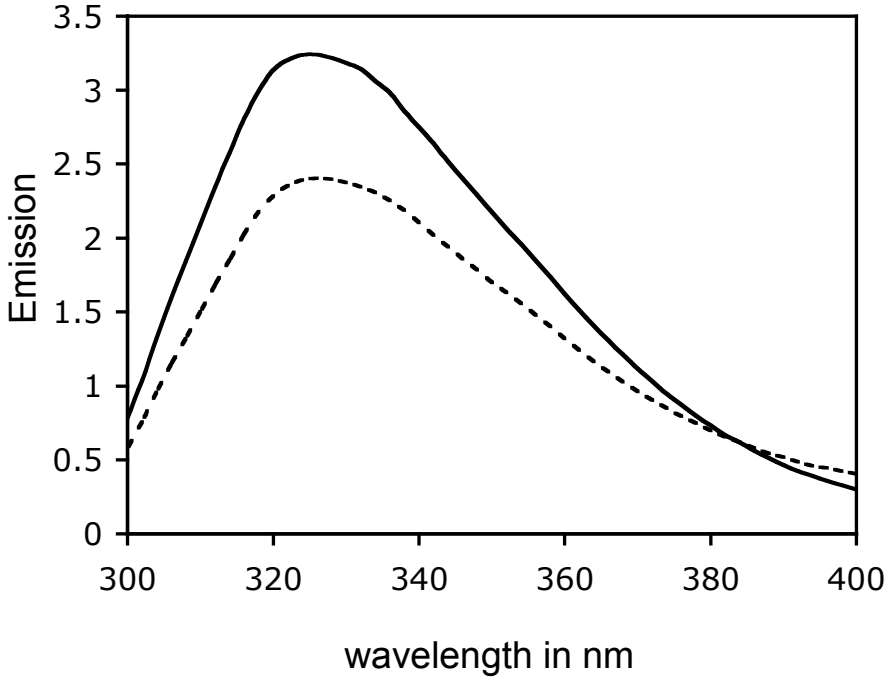
3.5
3
2.5
2
1.5
1
0.5
0
Emission
300
320
340
360
380
400
wavelength in nm

Figure 6. Binding of $MgNTA^{2-}$ to EppA. Fluorescence measurements of EppA using excitation and emission of 280 and 328 respectively in the presence of $MgNTA^{2-}$. EppA fluorescence emissions were quenched when $MgNTA^{2-}$ was added due to binding. The concentration dependence of binding (fractional saturation) was used to estimate the binding constants of EppA for all the metal-NTA complexes.

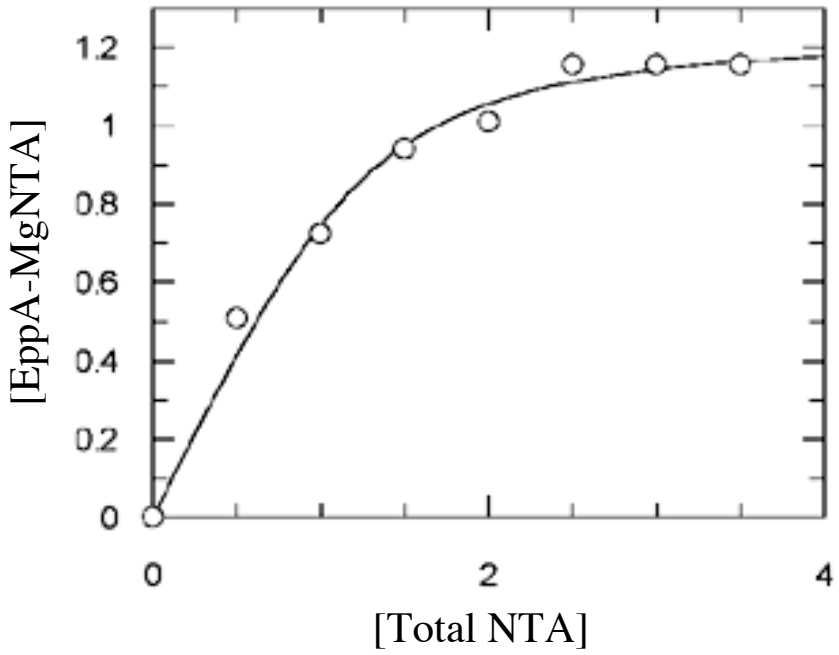
[EppA-MgNTA]
1.2
1
0.8
0.6
0.4
0.2
0
0
2
4
[Total NTA]

Figure 7. Changes in the intrinsic UV absorption spectra of EppA upon NTA binding. All experiments were done in 25 mM Tris-HCl (pH 7.5) with 10 μM EppA. (A) The raw spectra of EppA with (+$MgNTA^-$) and without (-$MgNTA^-$) $MgNTA^-$ (20 μM). (B) Differential spectrum of EppA with (a) $MgNTA^-$, (b) $CaNTA^-$, (c) $ZnNTA^-$, and (d) $CuNTA^-$ (all at 20 μM).

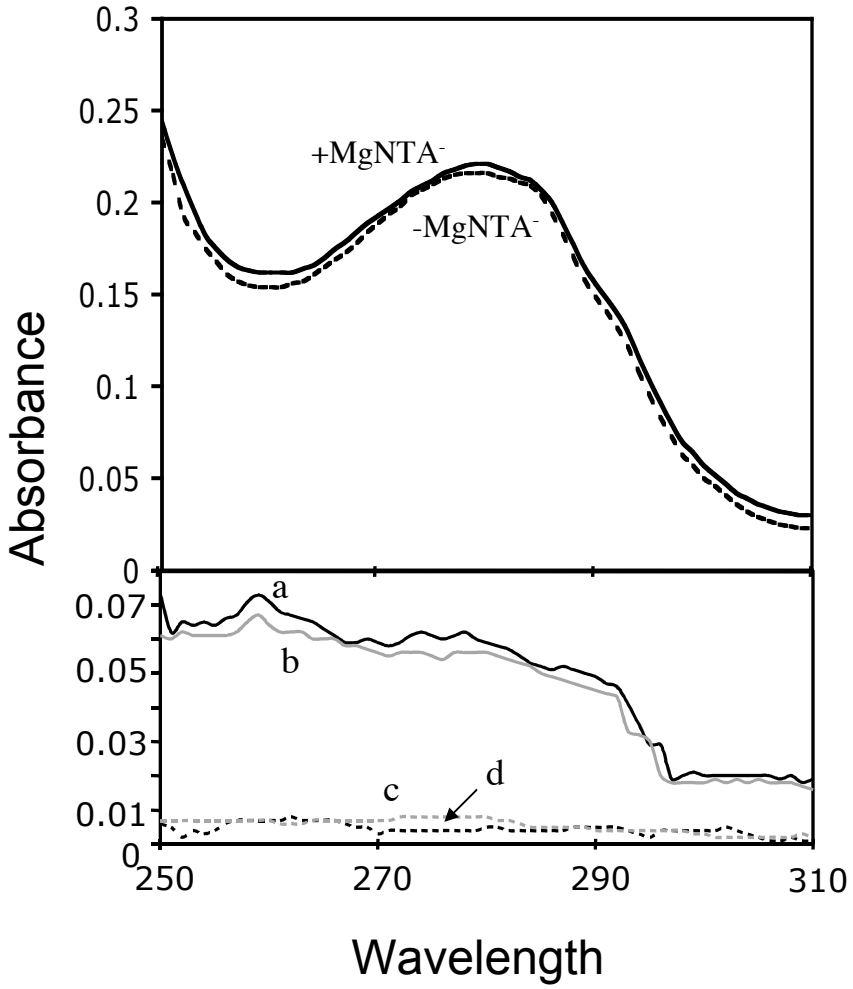
0.3
0.25
0.2
0.15
0.1
0.05
0
Absorbance
+MgNTA-
-MgNTA-
0.07
0.05
0.03
0.01
0
a
b
c
d
250
270
290
310
Wavelength

CHAPTER FOUR

Cloning and Expression of the EDTA/NTA Transport and Metabolic Gene Cluster into *Escherichia coli* W3110

ABSTRACT

Ethylenediaminetetraacetate (EDTA) and nitrilotriacetate (NTA) are common chelating agents that form stable metal-EDTA/NTA complexes. The EDTA and NTA-degrading bacterium BNC1 has a gene cluster containing the EDTA- and NTA-metabolizing genes (*emoA* and *emoB*) immediately downstream of a hypothetical ABC transporter (*eppABCD*). EppABCD, thus far, has been characterized biochemically *in vitro*. Here we report that the genes encoding the transporter and metabolic enzymes for EDTA and NTA degradation are transferable and functional in *Escherichia coli*. W3110(pEDTA) was able to metabolize both EDTA and NTA similar to BNC1, therefore providing evidence that EppABCD is responsible for both EDTA and NTA transport into BNC1. Further, this is the first step to determine if the genes for EDTA and NTA biodegradtion can be transferred to another microorganism to provide new organisms able to degrade these contaminants at mixed waste environment at Department of Energy sites.

INTRODUCTION

Categorizing the mixed radioactive and heavy metal waste across the world is a continuing process. The efforts to do so are sponsored by both private and government institutions due to ecological impacts and disasters such as Chernobyl (10, 21, 24). The cleanup of mixed waste contamination is a daunting task due to the presence of heavy metals, radionuclides and organic pollutants (16, 24). For example, the Department of Energy's Hanford site in Washington State contains radioactive waste from the processing of nuclear fuels and from waste processing procedures co-disposed with high concentrations of the chelating agents EDTA and NTA(11, 24). The presence of EDTA and NTA with radionuclides and heavy metals can increase their solubility and mobility in the groundwater (5, 25).

Microbial degradation of the chelating agents would potentially decrease the mobility of chelated radionuclides and heavy metals in the environment. Bacterial strain BNC1 is able to metabolize both EDTA and NTA; therefore, it is an ideal strain to study in reference to sites contaminated with EDTA and NTA. We have extensively studied the cellular transport and metabolic system responsible for both EDTA and NTA degradation in BNC1 (2, 20, Chapter 2 and Chapter 3). EDTA and NTA are transported into the cell through an ABC-type transporter (EppABCD). EppA is the periplasmic binding protein of the transporter, binding different metal-EDTA/-NTA species before cellular uptake (Chapter 2 and Chapter 3); EppB and EppC are membrane translocating proteins through which the metal-EDTA/-NTA complex will pass into the cytoplasm; and EppD is the ATPase of the system (Fig. 2 from Chapter 1, 4, 7). Cellular uptake of EDTA and NTA is selective, depending on the ion in the metal-EDTA or metal-NTA complex. Only

several metal-EDTA and metal-NTA complexes with low stability constants ($K \leq 10^{13.81}$ for EDTA and $K \leq 10^{6.39}$ for NTA) are bound efficiently by EppA, and allow the chelate to be subsequently transported into the cell. Binding of both the metal-EDTA and metal-NTA species is likely restricted by the geometrical structures of the complexes (Chapter 2 and Chapter 3). Once inside the cytoplasm, EDTA and NTA are metabolized by EmoA and IdaA (15, 20). EmoA (an EDTA monooxygenase) catalyzes the first two steps of EDTA metabolism. EmoA oxidizes EDTA to ethylenediaminetriacetate (ED3A) and then ED3A to ethylenediaminediacetate (EDDA); both reactions occur with the consumption of $FMNH_2$, which is provided by EmoB, an $NADH_2$:FMN oxidoreductase (20). The iminodiacetate oxidase (IdaA) catalyzes the last two steps of EDTA catalysis. IdaA first oxidizes EDDA to ethylenediaminemonoacetate and then to ethylenediamine (ED), with the co-production of glyoxylate and H_2O_2 (15). EmoA also oxidizes NTA to iminodiacetate (IDA) and glyoxylate, and IdaA converts IDA to glycine and glyoxylate (15).

Thus far, characterization of the EDTA and NTA transport and metabolic systems has been biochemical. Therefore we aimed to provide *in vivo* evidence that EppABCD is a specific EDTA and NTA transporter. Here we report that the genes encoding the transporter and metabolic enzymes for EDTA and NTA degradation are transferable and functional in *Escherichia coli*. The results demonstrate that the genes are responsible for EDTA/NTA transport and metabolism *in vivo*. This determines that the genes for EDTA and NTA biodegradation can be transferred to another microorganism to provide new organisms able to degrade these contaminants at mixed waste environments at Department of Energy sites.

MATERIALS AND METHODS

Bacterial strains and plasmids. The EDTA- and NTA-degrading bacterium BNC1 was kindly provided by Bernd Nörtemann (Technical University of Braunshweig, Braunshweig, Germany). BNC1, *E. coli* W3110, and W3110(pEDTA) were grown in a mineral salts medium with 1 mM EDTA (MMEDTA), NTA (MMNTA), NH_4Cl ($MMNH_3$), or ethylenediamine (MMED) as the sole nitrogen source (18). Plasmids used for cloning were pPCR2.1 TOPO (Invitrogen, Carlsbad, CA) and pBBR1MCS-2 (12). When appropriate, ampicillin (100 μg/ml) and kanamycin (50 μg/ml) were added to growth medium.

Chemicals. The reagents used were of the highest purity available and were purchased from Sigma Co. (St. Louis, MO), Aldrich Chemical Co. (Milwaukee, WI), or Fisher Scientific Co. (Pittsburgh, PA). All PCR reactions were preformed with *Taq* DNA polymerase or eLONGase enzyme mix (Gibco BRL, Gaithersburg, MD) and primers were purchased from Gibco BRL. Restriction endonucleases and DNA-modifying enzymes were purchased from Gibco BRL or New England Biolabs (Beverly, MA).

PCR of 16S rDNA gene. Initial generation of the 16S rDNA product from BNC1 was performed with universal primers GB01 (5'-GAGAGTTGATCCTGGCTTCAG-3') and GB02 (5'-AAGGAGGTGATCCCAGCC-3'). The PCR reaction consisted of approximately 10 ng of genomic DNA and 0.2 μM of each primer. The reaction produced approximately a 1.4-kb gene product (Fig 1.). The DNA fragment was gel-purified with a Qiagen gel extraction kit (Qiagen, San Diego, CA) and used in subsequent sequencing reactions. Purified products were sequenced by using the ABI Prism BigDye™ terminator cycle sequencing kit (Applied Biosystems,

Foster City, CA) in a mixture containing 50 ng DNA template, 3.2 pmol (0.25 μL) DNA primer, 4 μL Big Dye mix and 1.75 μL ddH_2O for a final volume of 10 μL. The 16s rDNA cycle sequencing conditions included an initial denaturing at 94°C for 4 min, 30 cycles of denaturing at 96°C for 10 sec, annealing at 50°C for 5 sec, and elongation at 60°C for 4 min. Samples were cleaned by using Performa™ DTR Gel Filtration cartridges (Edge Bio Systems, Gaithersburg, MD) and then analyzed at the WSU Laboratory of Bioanalysis and Biotechnology (LBBI). From the determined sequence, specific primers were designed: JPH2 (5'-CGTGATCCGGTATTGAGAGTCGT-3'), JPH3 (5'-GCTAGCGTTGTTCGGAAT-3'), JPH4 (5'-CCAACATCTCACGACACG-3'), and JPH5 (5'-CAGTGTGGCTGATCATCC-3'). These primers allowed for the step-wise sequencing of the entire PCR product.

Analysis of sequence data. The 16S rDNA sequence of BNC1 was used in a BLASTN Megablast search (1). The ten sequences with the highest identity were aligned pair-wise and the similarities were calculated and converted to a distance matrix with the Jukes-Cantor coefficient in the DNADIST program (PHYLIP version 3.572c) (6, 23). A dendrogram was produced by using the NEIGHBOR program of PHYLIP (6) (Fig. 2), and the treefile produced was opened in TREEVIEW (19), which generated the unrooted phylogenetic tree (Fig 3).

Cloning of EDTA/NTA transport operon. The eppABCD gene cluster was amplified with primers EPPABCD (5'-TACTCAGGAGGTACCTTCGGGTTG-3'), containing a *KpnI* restriction site (underlined) and EPPABCD (5'-GTCCGTTTCTAGAGGGTTAATAG-3'), containing a *XbaI* restriction site (underlined). The long range PCR reaction was carried out with the eLONGase enzyme

(GibcoBRL) and 10 ng of BNC1 genomic DNA. The PCR product was gel-purified and incubated with 1 mM dATP, 2.5 mM $MgCl_2$, and *Taq* DNA polymerase (Invitrogen) for 15 minutes at 72° C to generate poly-A overhangs. 1 μl of this mix was incubated with 1 μl of the pPCR2.1 TOPO vector for 20 minutes at room temperature (creating pTOPO-EppABCD). 1 μl of this reaction mix was used for transformation. Clones containing the pTOPO-EppABCD plasmid were picked and verified by plasmid isolation and PCR. pTOPO-EppABCD was purified and digested with *KpnI* and *XbaI*. This fragment was ligated with pBlueScript previously digested by *KpnI* and *XbaI*, forming pEppABCD, which was transformed into *E. coli* JM109 cells. Clones containing pEppABCD were verified by plasmid isolation and PCR.

Cloning of entire EDTA/NTA transport and metabolic operon. The cloning procedure is outlined in Fig. 4. The entire EDTA/NTA transport and metabolic gene cluster was amplified with the primers EDTA-F (5'-GGGGACAAGTTTGTACAAAAAAGCAGGCTTCTAGAGAGAATCCAGAATGYCTACGTCGCC-3'), containing an *XbaI* restriction site (underlined) and EDTA-R (5'-GGGGACCACTTTGTACAAGAAAGCTGGGGTAATGCATCCTTCTCGCCGTTAATCTCTGC-3') containing a *NsiI* restriction site (underlined). The long range PCR reaction was preformed with the eLONGase enzyme (GibcoBRL) and 10 ng of BNC1 genomic DNA. The PCR product was gel-purified and incubated with 1 mM dATP, 2.5 mM $MgCl_2$, and *Taq* DNA polymerase (Invitrogen) for 15 minutes at 72° C to generate poly-A overhangs. 1 μl of this mix was incubated with 1 μl of the pPCR2.1 TOPO vector for 20 minutes at room temperature (creating pTOPO-EDTA). 1 μl of this

reaction mix was used for transformation. Clones containing the pTOPO-EDTA plasmid were picked and verified by plasmid isolation and PCR.

pTOPO-EDTA was purified and digested with *XbaI* and *NsiI*. This fragment was ligated into pBBR1MCS-2 previously digested by *XbaI* and *NsiI* (Fig. 5), and the product was transformed into *E. coli* JM109 cells. Clones containing pEDTA were verified by plasmid isolation and PCR. This plasmid was then transformed into *E. coli* strain W3110 (generating W3110(pEDTA)), which was used for subsequent studies.

Growth curves of W3110(pEDTA). W3110(pEDTA) was able to grow in MMEDTA and MMNTA media. A 0.1% inoculum of late log phase culture of W3110(pEDTA) grown in the same medium was used for each culture. The optical density was analyzed at 600 nm, OD_{600nm}, on a Pharmacia Biotech Ultrospec 4000 UV/visible spectrophotometer at specific time points to generate growth curves (Fig. 6). Controls included W3110 grown in MMEDTA, MMNTA, MMED, or the medium with out nitrogen source and W3110(pEDTA) in $MMNH_3$ medium.

Degradation of EDTA and NTA by W3110(pEDTA) cell suspensions. The procedure used was based on the Nörtemann method (18). W3110(pEDTA) cells were grown in MMEDTA, MMNTA, and $MMNH_3$ media to late exponential phase. Cells were harvested, washed twice with 20 mM PIPES buffer (pH 7.5), and resuspended the same buffer at a turbidity of 1. Degradation was started by adding 1 mM metal-EDTA or metal-NTA complex. Controls experiments consisted of BNC1 cell suspensions without the addition of metal-EDTA or metal-NTA and the addition of 1 mM of the metal-NTA complex to cell-free PIPES buffer. The metal-EDTA and metal-NTA ratios were 10:1 for Mg and Ca, and 1:1 for Zn and Cu. Control cultures were established containing 1

mM of Zn or Cu to test for the toxicity of the metals in the $MMNH_3$ medium. W3110 was able to grow in the presence of both (data not shown).

Ammonia concentration was determined using the Krallmann-Wenzel method (13). At specific time points, 0.5 ml of culture samples were taken and centrifuged. Samples (0.25 ml) of the supernatant was transferred to a new tube with the subsequent addition of 10 μl of catalyst solution (3 volumes of 2 mM $MnSO_4$ freshly mixed with 1 volume of acetone), 0.5 ml of phenol reagent, and 0.25 ml of 1.5 % hypochlorite solution (3). The sample mixture was incubated for 6 minutes, and the OD_{636nm} was recorded. This value was compared to a standard calibration curve (1 μM to 5 mM NH_3).

RESULTS

Sequence and phylogenetic analysis. Previous sequence analysis of the gene cluster containing the EDTA transport and metabolism genes showed that the gene encoding EF-Tu, an elongation factor involved in protein synthesis, was located downstream of the EDTA metabolism genes. This gene shows 91% sequence identity to the EF-Tu from *Agrobacterium tumefaciens* (2). Because the EF-Tu sequence can be used as a phylogenetic marker (2), it was speculated that BNC1 was similar to *Agrobacterium tumefaciens*. To test this hypothesis, the sequencing of the 16S rDNA gene was determined. From the sequence of the BNC1 16S rDNA gene, it was found that BNC1 actually is more closely related to *Rhizobium* sp. and *Mesorhizobium* sp. (Fig. 2 and Fig. 3.), and the BNC1 16S rDNA gene is 97% identical with the 16S rDNA gene from *Rhizobium* sp. H-4 and 96% identical with that of *Agrobacterium tumefaciens* str. C58. It is appears that BNC1 is closely related to *Rhizobium*, *Mesorhizobium*, and *Agrobacterium* spp.

Cloning of the gene cluster concerned with EDTA/NTA transport and metabolism. The EDTA/NTA transport system (EppABCD) was cloned into pBlueScript KS(+) vector, producing plasmid pEppABCD coding for the EDTA and NTA transporter. *E. coli* cells harboring pEppABCD were unable to grow on EDTA or NTA even though the genes were expressed. This was expected because *E. coli* does not have any genes homologous to EDTA-metabolizing genes. *E. coli* cells harboring pEmoA (2) were unable to metabolize EDTA, either. When the entire gene cluster involved in transport, metabolism and regulation was introduced into *E. coli* (Fig. 4), the cells gained the ability to degrade EDTA and NTA. Long range PCR with the primers

EDTA-F and EDTA-R yielded a 12-kb product (Fig. 5, lane 4). This product was first cloned into the pPCR2.1 TOPO and subsequently cloned into pBBR1MCS-2, creating pEDTA. Wild-type *E. coli* strain W3110 was transformed with pEDTA, and this strain, W3110(pEDTA), was able to degrade EDTA and NTA.

Growth of W3110(pEDTA). W3110(pEDTA) was able to use NH_3, EDTA, or NTA as the sole nitrogen source in the mineral medium (Fig. 6). In comparison, W3110 grew only on NH_3 or ethylenediamine as the sole nitrogen source (Fig. 7). pEDTA carries genes responsible for the conversion of NTA to glycine and glyoxylate and conversion of EDTA to ethylenediamine and glyoxylate. Since ethylenediamine is not a common metabolite, *E. coli* W3110 must be able to use it as a nitrogen source so that W3110(pEDTA) will be able to use EDTA as its nitrogen source. Apparently, W3110 used ethylenediamine as a nitrogen source. This is not surprising because ethylenediamine is a structural homologue of putrescine, a common polyamine in bacterial cells (9). *E. coli* W3110 must have used putrescine metabolizing enzymes to degrade ethylenediamine. Thus, the acquired ability of W3110(pEDTA) to grow on NTA and EDTA must due to the presence of the EDTA- and NTA-degrading gene cluster.

EDTA degradation studies with W3110(pEDTA). EDTA and NTA degradation with W3110(pEDTA) was further demonstrated by measuring ammonium production from EDTA and NTA degradation. W3110(pEDTA) EDTA, NTA and $MMNH_3$ grown cell suspensions were tested for their production of ammonium from either EDTA or NTA. Cells grown on NTA or EDTA degraded NTA and EDTA faster than cells grown on NH_3 (Fig 8). The results are similar to EDTA and NTA degradation by the EDTA-degrading bacterium BNC1—cells grown on EDTA and NTA degraded

EDTA and NTA faster than cells grown on $MMNH_3$ (Chapter 2 Fig. 3A, and Chapter 3 Fig. 2A). These data suggest that the EppABCD transport system and EDTA metabolizing genes are inducible by EDTA and NTA with EmoR involved in the regulation.

The metabolizing specificity of W3110(pEDTA) for metal-EDTA and metal-NTA was also tested. Cells grown on EDTA were incubated with selected individual metal-EDTA and metal-NTA complexes. The cells produced approximately the same amount of ammonium from $CaEDTA^{2-}$ (290 μM), $MgEDTA^{2-}$ (282 μM), and $ZnEDTA^{2-}$ (150 μM) (Fig. 9A) as BNC1 cells did (310 μM ammonium from both $CaEDTA^{2-}$ and $MgEDTA^{2-}$ and 180 μM ammonium from ZnEDTA) (Chapter 2 Fig 3B). W3110(pEDTA) did not degrade CuEDTA (Fig 9A), nor did BNC1 (Chapter 2 Fig. 3B). W3110(pEDTA) grown on NTA also degraded different metal-NTA complexes to BNC1 cells. W3110(pEDTA) produced 110 μM and 105 μM ammonium from $MgNTA^-$ and $CaNTA^-$, respectively (Fig. 9B). The amount of ammonium produced by W3110(pEDTA) are comparable to the ammonium produced by BNC1: 125 μM and 124 μM from $MgNTA^-$ and $CaNTA^{--}$ degradation (Chapter 3 Fig 2B). W3110(pEDTA) grown NTA did not efficiently degrade Zn and $CuNTA^-$ with only 72 and 47 μM ammonium produced (Fig. 9B), similar to the amount of ammonium produced by BNC1 (92 and 71 μM ammonium, Chapter 3 Fig. 2B).

DISCUSSION

We present here *in vivo* evidence that the EDTA-degrading gene cluster codes for a specific EDTA and NTA transport system, the enzymes involved in degradation, and the regulatory protein. When the entire gene cluster concerned with transport, metabolism and regulation was cloned into *E. coli* W3110, the recombinant cell was able to degrade EDTA and NTA and use them as the sole nitrogen source, comparable to the metabolic activities of BNC1. Previous to this work, the study of EDTA and NTA degradation has been predominately biochemical, with an emphasis on characterizing the periplasmic EDTA/NTA binding protein from the uptake system (Chapter 2 and Chapter 3) and EmoA, EmoB, and IdaA activities (2, 15, 20). The ability of W3110(pEDTA), but not W3110, to release ammonium from EDTA and NTA and to use them as the sole nitrogen source argues strongly that the genes are responsible for EDTA and NTA degradation in *E. coli* and very likely solely responsible for EDTA degradation in bacterium BNC1. To date, we have not successfully knocked out genes in BNC1 due to the ease to which cells lyse. However, sequence comparison and analysis of the newly sequenced BNC1 genome, revealed that there is only a single copy of the EDTA-degrading gene cluster in the genome.

The remaining aspect of EDTA and NTA degradation that has not been studied is the regulatory system in bacterium BNC1. Downstream of *emoA* and *emoB* is *emoR*, which shows sequence homology to LysR type transcriptional regulators. LysR transcriptional regulators contain a helix-turn-helix DNA binding domain and a domain that binds (or recognizes) a co-inducer (22). EmoR hypothetically binds EDTA and NTA and facilitates the activation of transcription by RNA polymerase (22). Work currently is

in progress to clone and purify EmoR so that binding of EmoR for EDTA and NTA can be analyzed.

Cloning and expression of the entire EDTA-degrading gene cluster in *E. coli* not only demonstrates that the gene cluster is responsible for EDTA and NTA uptake and metabolism *in vivo* but also shows that the EDTA-degrading genes can be transferred into other microorganisms. Genetically engineered microorganisms with radiation resistance and chelating agent degradation abilities are ideal for the bioremediation of the mixed wastes at DOE sites, where radionuclides, heavy metals, and chelating agent coexist (24). Further, it will also help in field applications if the microorganism(s) can be economically delivered into the subsurface environment. BNC1 has not formally been classified. On the basis of its 16S rDNA sequence, it is closely related to *Rhizobium*, *Mesorhizobium*, and *Agrobacterium* spp. Thus, it is possible to transfer the EDTA- and NTA-degrading gene cluster into these microorganisms.

Future work will entail cloning the genes into a *Rhizobium* or *Mesorhizobium* sp. to develop a rhizoremediation system (14). Rhizoremediation combines the ability of plant phytoremediation with pollutant degrading capabilities of rhizosphere microorganisms (14). The plant can stimulate the metabolic activity of the rhizosphere because the plant exudant is nutrient rich, and can enhance the growth of rhizosphere microorganisms (14). A *Rhizobium* or *Mesorhizobium* sp. actively expressing the EDTA/NTA metabolism system would therefore potentially be adapted to the rhizosphere of the contaminated sites. These microorganisms are normal rhizosphere microorganisms and they also form nodule with leguminous plants. The growth of plants infected with a strain expressing the EDTA/NTA catabolic genes in contaminated sites

offers a direct delivery system, since alfalfa roots can penetrate the soil up to 100 meters (8). More studies must be done to verify that this system could persist in contaminated environments long enough to be effective. Also, it must be determined whether the plants and the genetically modified microorganism can survive in particular contaminated sites that contain high amounts of radionuclides, heavy metals, and chelating agents. In preliminary work to detemine the concentration of NTA at which alfalfa plants can survive, and it was found that the plants can survive at concentrations of NTA up to 10 mM (17), a concentration higher than what would be expected in the environment, suggesting that this is a promising model for studying the rhizoremediation of EDTA and NTA.

Characterization of the EDTA and NTA metabolism system of BNC1 provides evidence that it can be targeted to mixed wastes containing both chelating agents. Although BNC1 can efficiently mineralize EDTA and NTA, its application in the field may be hindered due to the lack of an efficient delivery system. The application of BNC1 directly to the environment may be possible through infection of alfalfa roots (becasue BNC1 is most closely related to the plant symbiots *Rhizobium* and *Mesorhizobium*), which can be grown directly at the site. The ability of BNC1 to infect plant roots has not been tested but sequence analysis suggests that it does not have genes concerned with nodule formation and nitrogen fixation. Thus, we are interested in cloning the entire gene cluster into a *Rhizobium* or *Mesorhizobium* sp. that can infect alfalfa roots so that the organism can be delivered into the subsurface to clean up EDTA and NTA. Since microbial activities are likely enhanced from root extrudes, the process is rhizoremediation (14).

ACKNOWLEGEMENTS

This research was funded by the Natural and Accelerated Bioremediation Research (NABIR) program, Biological and Environmental Research (BER), U.S. Department of Energy (grant #DE-FG03-01ER63081). JH was also supported by the National Science Foundation (NSF) Integrative Graduate Education and Research Training (IGERT) program at Washington State University (grant DGE-9972817). We thank Mike Mortimer, Drs. Mike Kahn, Linda Thomashow, Jim Petersen, and Harvey Bolton Jr. for their helpful discussions and ideas.

REFERENCES

1. **Altschul, S., T. Madden, S. Schaffer, J. Zhang, Z. Zhang, W. Miller, and D. Lipman.** 1997. Gapped BLAST and PSI-BLAST: a new generation of protein database search programs. Nucleic Acids Res. **25:**3389-3402.
2. **Bohuslavek, J., J. Payne, Y. Liu, H. Bolton, and L. Xun.** 2001. Cloning, sequencing, and characterization of a gene cluster involved in EDTA degradation from the bacterium BNC1. Appl. Environ. Microbiol. **67:**688-695.
3. **Bonicke, R., and B. Lisboa.** 1959. Uber das Vorkommen von Acylamidasen in Mycobacterien: I. Mitteilung: Die enzymatische Desamidierung aromatischer und aliphatischer Caronsaureamide. Zbl. Bakt. I.ABt Orig. **175:**403-421.
4. **Boos, W., and J. M. Lucht.** 1996. Periplasmic binding protein-dependent ABC transporters, p. 1175-1209. *In* R. Curtis III, E. Ingraham, E. C. C. Lin, K. B. Low, B. Magasanik, W. S. Rezinikoff, M. Riley, M. Schaechter, and H. Umbarger (ed.), Escherichia coli and Salmonella: cellular and molecular biology. American Society of Microbiology, Washington, D. C.
5. **Cleveland, J., and T. Rees.** 1981. Characterization of plutonium in Maxey Flats radioactive trench leachates. Science **212:**1506-1509.
6. **Felsenstein, J.** 1993. PHYLIP-(Phylogeny Inference Package), version 3.572c. Department of Genetics, University of Washington, Seattle.
7. **Higgins, C.** 1992. ABC transporters: from microorganisms to man. Annu. Rev. Cell Biol **8:**67-113.
8. **Kahn, M.** 2004. Personal communication.

9. **Karahalios, P., P. Mamos, D. Vynios, D. Papaioannou, and D. Kalpacis.** 1998. The effect of acylated polyamine derivatives on polyamine uptake mechanism, cell growth, and polyamine pools in Escherichia coli, and the pursuit of structure/activity relationships. Eur. J. Biochem. **251:**998-1004.

10. **Ketterer, M., K. Hafer, and J. Mietslski.** 2004. Resolving Chernobyl vs. global fallout contributions in soils from Poland using plutonium atom ratios measured by inductively coupled plasma mass spectrometry. J. Environ. Radioact. **73:**183-201.

11. **Klem, M.** 1988. Inventory of chemicals used at Hanford production plants and support operations (1944-1980). Westinghouse Hanford Company.

12. **Kovach, M., P. Elzer, D. Hill, G. Robertson, M. Farris, R. Roop, and K. Peterson.** 1995. Four new derivatives of the broad-host-range cloning vector pBBR1MCS, carrying different antibiotic-resistance cassettes. Gene **166:**175-176.

13. **Krallmann-Wenzel, U.** 1985. An improved method of ammonia determination, applicable to amidases and other ammonia-producing enzyme systems of *Mycobacteria*. Am. Rev. Respir. Dis. **131:**432-434.

14. **Kuiper, I., E. Lagendijk, G. Boemberg, and B. Lugtenberg.** 2004. Rhizoremediation: A beneficial plant-microbe interaction. Mol. Plant-Microbe. Interact. **17:**6-15.

15. **Liu, Y., T. Louie, J. Payne, J. Bohuslavek, H. Bolton, and L. Xun.** 2001. Identification, purification, and characterization of iminodiacetate oxidase from the EDTA-degrading bacterium BNC1. Appl. Environ. Microbiol. **67:**696-701.

16. **Miljotknk, K., E. Jorgensen, V. Fredriksen, L. Hojbjerg, C. Kindskov, and F. Oemig.** 1999. Remediation of mixed contamination soil and tar/PAH contaminated soil. Miljoproject **503:**1-10.

17. **Mortimer, M.** 2004. Personal communication.

18. **Nortemann, B.** 1992. Total degradation of EDTA by mixed cultures and a bacterial isolate. Appl. Environ. Microbiol. **58:**671-676.

19. **Page, R.** 1996. TREEVIEW: An application to display phylogenetic trees on personal computers. Computer Applications in the Biosciences **12:**357-358.

20. **Payne, J., H. Bolton, J. Campbell, and L. Xun.** 1998. Purification and characterization of EDTA monooxygenase from the EDTA-degrading bacterium BNC1. J. Bacteriol. **180:**3823-3827.

21. **Peterka, M., R. Peterkova, and Z. Likovsky.** 2004. Chernobyl: prenatal loss of four hundred male fetuses in the Czech Republic. Reprod. Toxicol. **18:**75-79.

22. **Schell, M.** 1993. Molecular biology of the LysR family of transcriptional regulators. Annu. Rev. Microbiol. **47:**597-626.

23. **Tan, Z., X. Xu, E. Wang, J. Gao, E. Martinez-Romero, and W. Chen.** 1997. Phylogenetic and genetic relationships of Mesorhizobium tianshanese and related rhizobia. Int. J. of Syst. Microbiol. **47:**874-879.

24. **Toste, A., B. Osborn, K. Polach, and T. Lechner-Fish.** 1995. Organic analyses of an actual and simulated mixed waste: Hanford's organic complexant revisited. J. Radioanal. Nucl. Chem. **194:**25-34.

25. **Xun, L., R. Reeder, A. Plymale, D. Girvin, and H. Bolton.** 1996. Degradation of metal-nitrilotriacetate complexes by nitrilotriacetate monooxygenase. Environ. Sci. Technol. **30:**1752-1755.

Figure 1. PCR amplification of the 16S rDNA gene from BNC1. Primers GBO1 and GBO2 were used to amplify the 16S rDNA gene form BNC1. Lane 1, DNA 1 kb ladder standard; Lane 2, BNC1 16S rDNA gene.

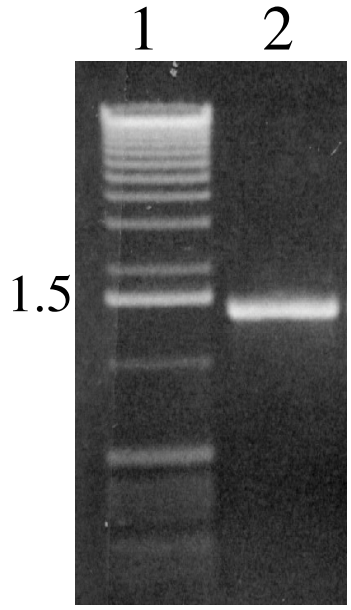
1
2
1.5

Figure 2. Maximum likelihood dendrogram indicating the phylogenetic relationship between BNC1 and the 10 closely related organisms on the basis of the 16S rDNA gene sequence. The 10 most related sequences were identified with the BNC1 sequence from a Megablast search (1). Bootstrap values were calculated with a maximum likelihood comparison with 1000 bootstrap replicates.

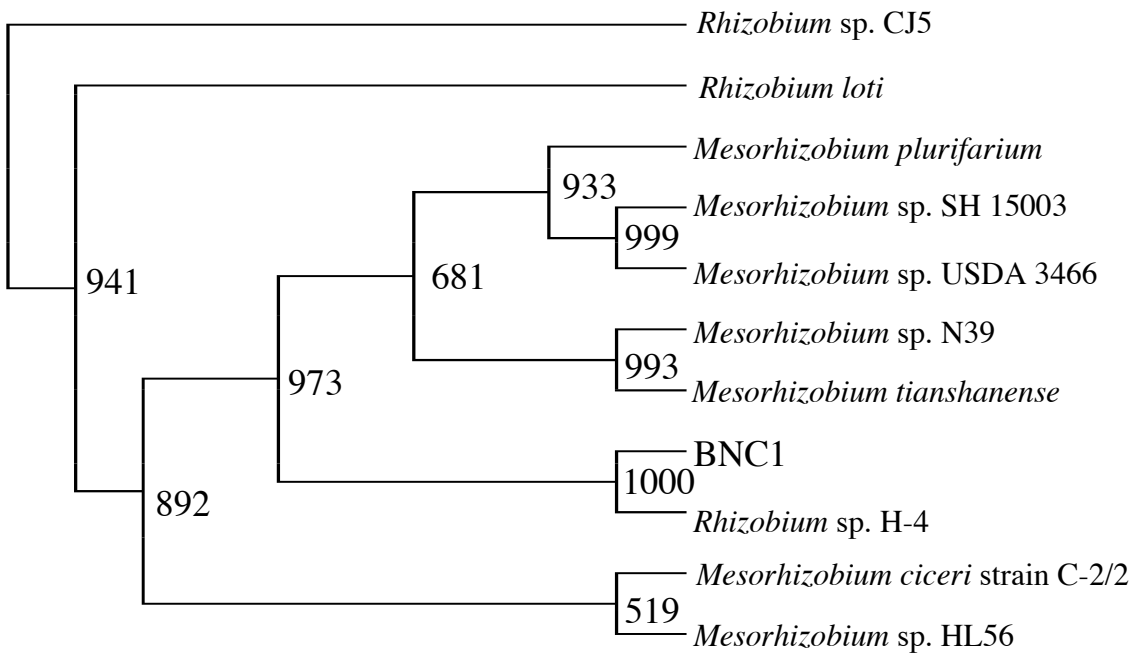
Rhizobium sp. CJ5
Rhizobium loti
Mesorhizobium plurifarium
933
Mesorhizobium sp. SH 15003
999
Mesorhizobium sp. USDA 3466
941
681
Mesorhizobium sp. N39
993
Mesorhizobium tianshanense
973
BNC1
1000
892
Rhizobium sp. H-4
Mesorhizobium ciceri strain C-2/2
519
Mesorhizobium sp. HL56

Figure 3. Phylogenetic tree of species most closely related to BNC1 obtained using TreeView (19). The numbers on the branches represents the confidence interval determined by a bootstrap analysis with 1000 replications.

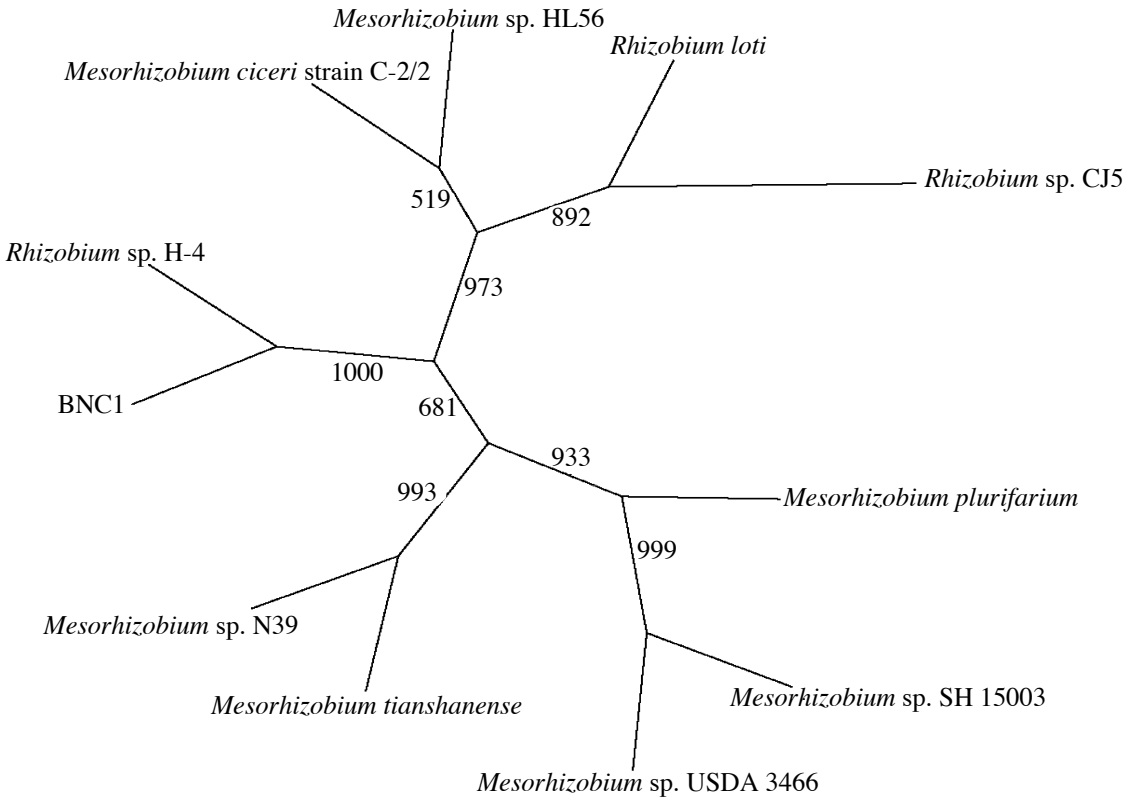
Mesorhizobium sp. HL56
Rhizobium loti
Mesorhizobium ciceri strain C-2/2
Rhizobium sp. CJ5
519
892
Rhizobium sp. H-4
973
1000
BNC1
681
933
993
Mesorhizobium plurifarium
999
Mesorhizobium sp. N39
Mesorhizobium tianshanense
Mesorhizobium sp. SH 15003
Mesorhizobium sp. USDA 3466

Figure 4. Cloning of entire EDTA-degrading gene cluster. Long range PCR with primers EDTA-F and EDTA-R was done to amplify the gene cluster. The PCR product was cloned into pPCR2.1 TOPO. The gene cluster in pTOPO-EDTA was cut with *XbaI* and *NsiI* and ligated into pBBR1MCS-2. The final plasmid pEDTA was transformed into W3110, creating W3110(pEDTA).

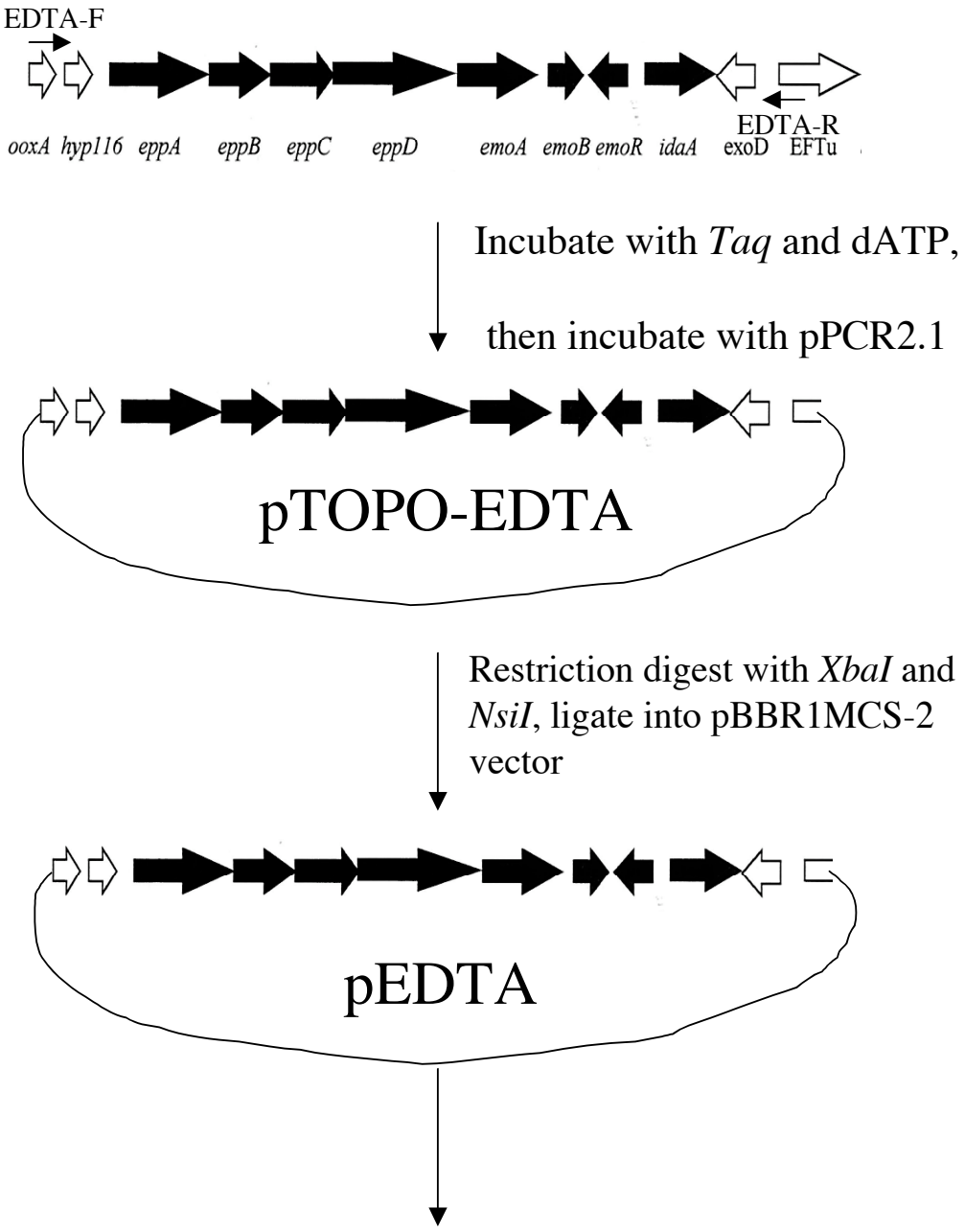
EDTA-F
ooxA hyp116 eppA eppB eppC eppD emoA emoB emoR idaA exoD EFTu
EDTA-R
Incubate with *Taq* and dATP,
then incubate with pPCR2.1
pTOPO-EDTA
Restriction digest with *XbaI* and *NsiI*, ligate into pBBR1MCS-2 vector
pEDTA
Transform into *E. coli* W3110

Figure 5. The cloned EDTA gene cluster was analyzed by restriction digestion. Lane 1 and 5, DNA 1 kb standard ladder; lane 2, digested pEDTA; lane 3, digested pBBR1MCS-2; lane 4, digested 12-kb PCR product. Lanes 2-4, samples digested with both *XbaI* and *NsiI*.

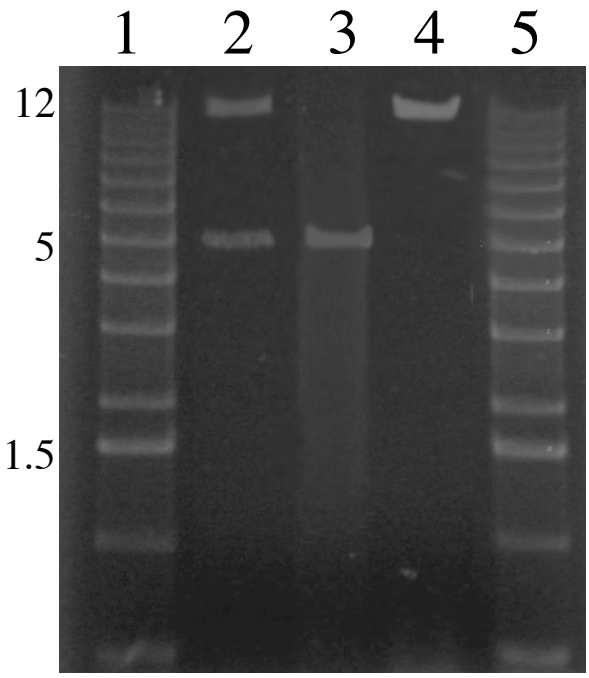
1
2
3
4
5
12
5
1.5

Figure 6. Growth curves of W3110(pEDTA). (A) Growth in MMEDTA medium. (B) Growth in MMNTA medium. (C) Growth in $MMNH_3$ medium.

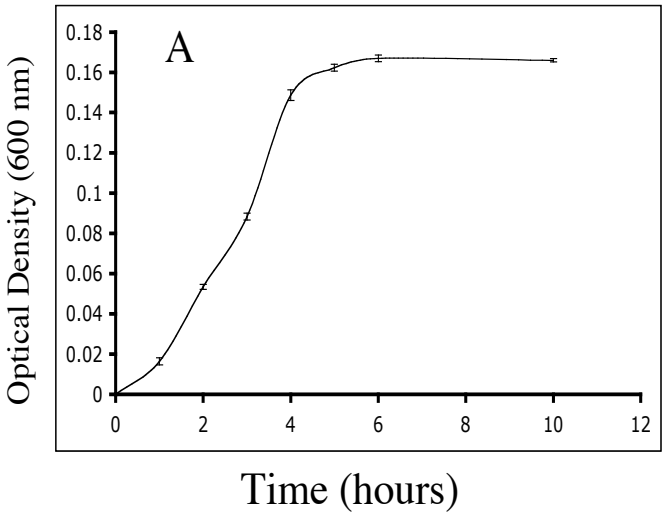
A
Optical Density (600 nm)
0.18
0.16
0.14
0.12
0.1
0.08
0.06
0.04
0.02
0
0
2
4
6
8
10
12
Time (hours)

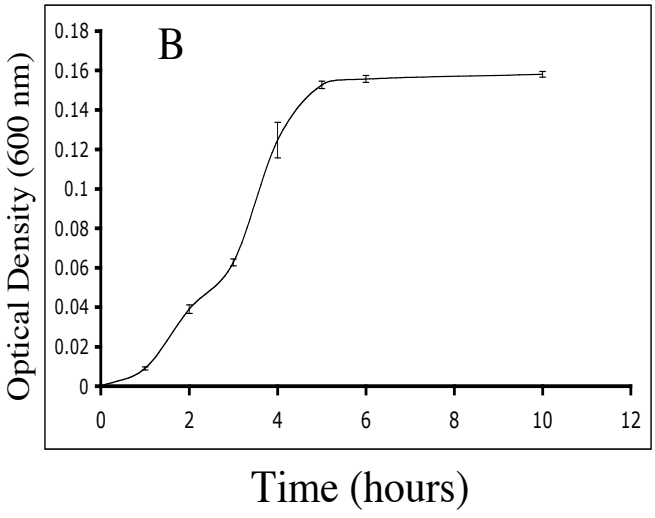
B
Optical Density (600 nm)
0.18
0.16
0.14
0.12
0.1
0.08
0.06
0.04
0.02
0
0
2
4
6
8
10
12
Time (hours)

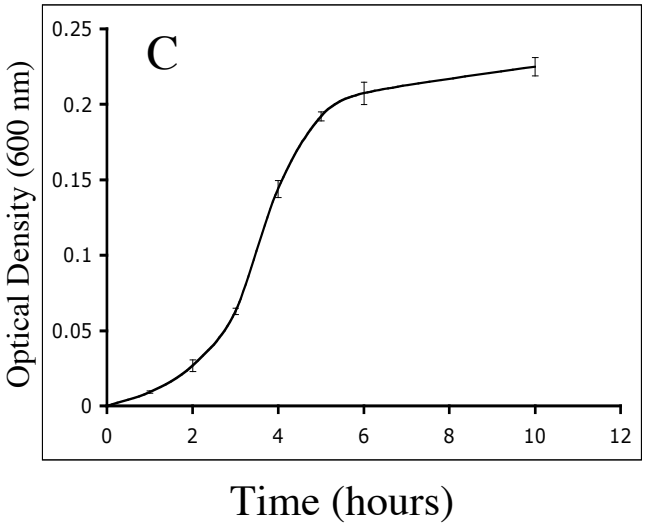
C
Optical Density (600 nm)
0.25
0.2
0.15
0.1
0.05
0
0
2
4
6
8
10
12
Time (hours)

Figure 7. Control growth curves with W3110. W3110 grown in: MMED (black solid line), MMEDTA (grey dashed line), and MMNTA media (black dashed line).

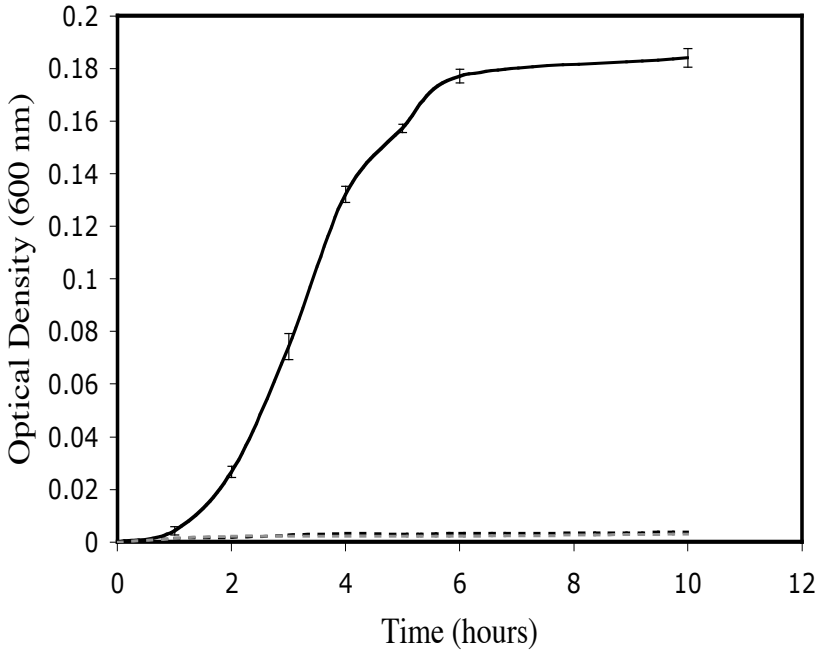
Optical Density (600 nm)
0.2
0.18
0.16
0.14
0.12
0.1
0.08
0.06
0.04
0.02
0
0
2
4
6
8
10
12
Time (hours)

Figure 8. Comparison of $CaEDTA^{2-}$ and $MgNTA^{-}$ degradation by EDTA/NTA grown W3110(pEDTA) cells versus $MMNH_3$ grown W3110(pEDTA) cells. MMEDTA, MMNTA or $MMNH_3$ grown cells were suspended in PIPES buffer at turbidity of 0.4. $CaEDTA^{2-}$ or $MgNTA^{-}$ (1 mM) was added to start EDTA/NTA degradation, monitored by ammonium production. (A) Comparison of $CaEDTA^{2-}$ degradation by MMEDTA grown cells (solid line) and $MMNH_3$ grown cells (dashed line). (B) Comparison of MgNTA degradation by MMNTA grown cells (solid line) and $MMNH_3$ grown cells (dashed line). Data points are averages of three samples with standard deviation (error bars).

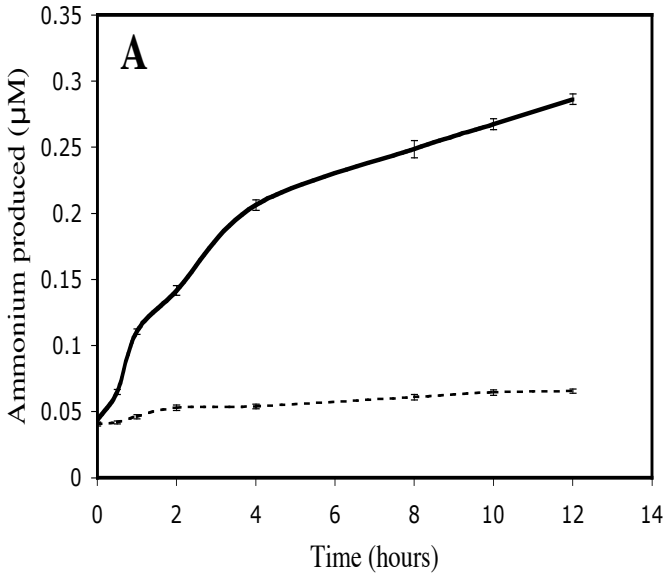
A
Ammonium produced (µM)
0.35
0.3
0.25
0.2
0.15
0.1
0.05
0
0
2
4
6
8
10
12
14
Time (hours)

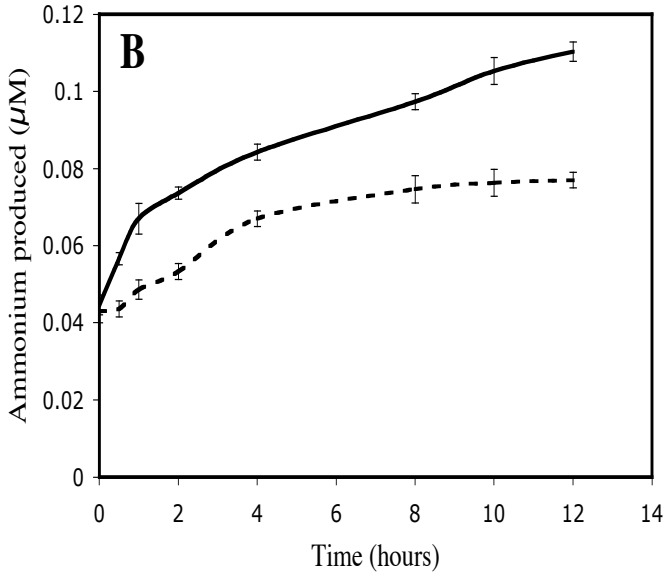
B
Ammonium produced (µM)
0.12
0.1
0.08
0.06
0.04
0.02
0
0
2
4
6
8
10
12
14
Time (hours)

Figure 9. Degradation of different metal-EDTA and metal-NTA complexes by W3110(pEDTA). EDTA and NTA grown cells were suspended in PIPES buffer at turbidity of 0.4. Metal-EDTA or metal-NTA (1 mM) was added to start EDTA/NTA degradation, which was monitored by ammonium production. (A) Ammonium production by EDTA grown cells incubated with $CaEDTA^{2-}$ (black solid line), $MgEDTA^{2-}$ (grey solid line), $ZnEDTA^{2-}$ (black dashed line), and $CuEDTA^{2-}$ (grey dashed line). (B) Ammonium production by NTA grown cells incubated with $MgNTA^{-}$ (black solid line), $CaNTA^{-}$ (gray solid line), $ZnNTA^{-}$ (black dashed line), and $CuNTA^{-}$ (grey dashed line). (C) Ammonium production by cell suspensions without the addition of metal-EDTA or metal-NTA.

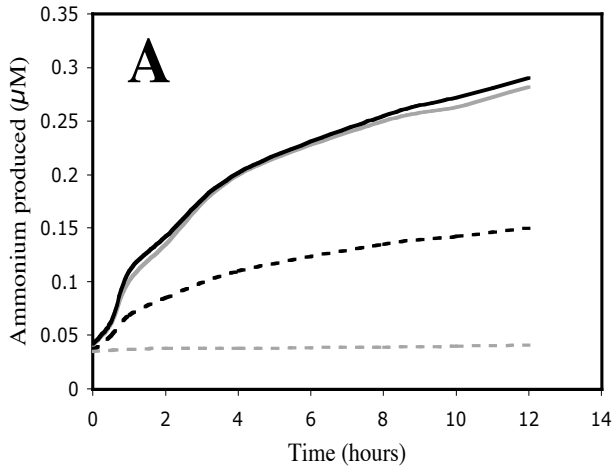
A
Ammonium produced (μM)
0.35
0.3
0.25
0.2
0.15
0.1
0.05
0
0
2
4
6
8
10
12
14
Time (hours)

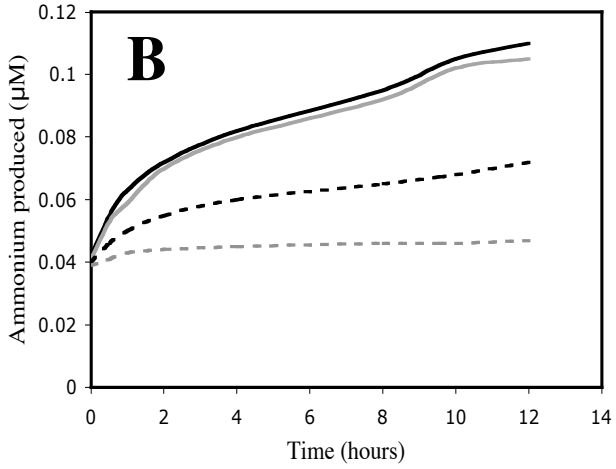
B
Ammonium produced (μM)
0.12
0.1
0.08
0.06
0.04
0.02
0
0
2
4
6
8
10
12
14
Time (hours)

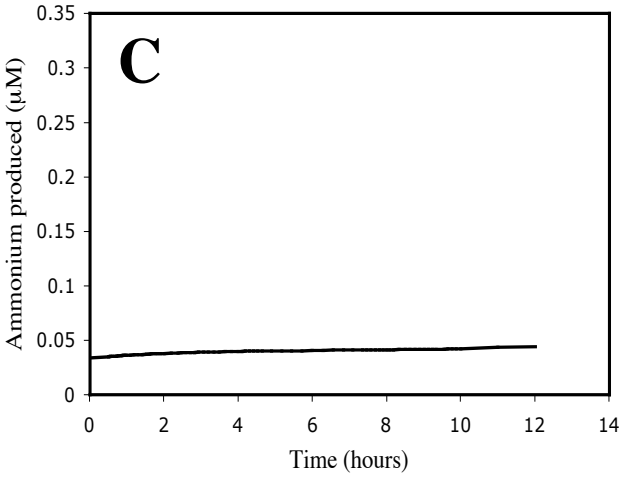
C
Ammonium produced (μM)
0.35
0.3
0.25
0.2
0.15
0.1
0.05
0
0
2
4
6
8
10
12
14
Time (hours)

CHAPTER FIVE

CONCLUSIONS AND FUTURE DIRECTIONS

Ethylenediaminetetraacetate (EDTA) and nitrilotriacetate (NTA) have been used in many industrial processes for their excellent chelating capacities. They have also been used at several Department of Energy sites in nuclear waste processing and decontamination procedures, and the sites are often co-contaminated with both the chelating agents and radionuclides. Unfortunately, EDTA and NTA have been shown to enhance the solubility and transport of radionuclides in the groundwater. To decrease the enhanced mobility of radionuclides, bacterial degradation of EDTA and NTA has been studied. BNC1 has been extensively characterized for its ability to mineralize both EDTA and NTA.

Chapter one summarizes previous work on EDTA and NTA degradation from our lab and others. Chapter two describes the study of the inducible ABC-type transporter responsible for EDTA uptake into the cytoplasm. Whole cells degradation and RT-PCR analysis provided evidence that EDTA uptake is an EDTA inducible process. RT-PCR analysis also demonstrated that *eppABCD* are co-transcribed with *emoA* on a single mRNA. EppA, the periplasmic binding protein of the system, was shown to preferentially bind to $CaEDTA^{2-}$ and $MgEDTA^{2-}$, but not to $CuEDTA^{2-}$. Therefore, the recalcitrance of certain metal-EDTA species is due to the inefficient binding of the metal-EDTA complex by EppA. The low affinity of EppA for $ZnEDTA^{2-}$ allows us to speculate either that $ZnEDTA^{2-}$ is inefficiently transported by EppABCD or that respeciation with another metal must occur before transport occurs. More work must be

done to understand the exact mechanism of $ZnEDTA^{2-}$ transport. Future work also entails studying more metal-EDTA complexes, specifically $Fe(III)EDTA^{-}$, since it is a major species in the environment. Work is also being done in regards to EmoR, the Lys-R type regulator, to understand its role in regulating the expression of the EDTA transporter.

The ability of EppABCD to transport NTA is described in chapter three. Inducible degradation of different metal-NTA species follows the same trend as the metal-EDTA species reported in chapter 2. $MgNTA^{-}$ and $CaNTA^{-}$ are degraded at the fastest rate, $ZnNTA^{-}$ at a slower rate, and marginal $CuNTA^{-}$ is degraded. The binding affinity of EppA for different metal-NTA complexes is parallel to those of metal-EDTA, which demonstrates that there might be a specific trend for what EppA binds. Future work includes studying the binding of more metal-NTA species. Also competition experiments with EDTA and NTA should be done with whole cells to demonstrate which is the preferred substrate of BNC1.

Chapter four describes preliminary work for developing a field applicable system for bioremediation of mixed wastes. The 16S rDNA gene of BNC1 shows the highest identity with *Rhizobium* and *Mesorhizobium* sp.; therefore, we propose to create a genetically modified organism for rhizoremediation. The entire EDTA/NTA transport and metabolism system was cloned into *E. coli* W3110 (generating W3110(pEDTA)), and this strain was able to grow with EDTA and NTA as its sole nitrogen source. Because EDTA and NTA are highly hydrophilic, they cannot enter the cell by diffusion. *E. coli* W3110(pEDTA) growing on EDTA and NTA is further evidence that EppABCD is responsible for EDTA and NTA cellular uptake. Future work includes transferring the

pEDTA plasmid into a *Rhizobium* or *Mesorhizobium* sp. The recombinant bacterium will be tested for its ability to metabolize EDTA and NTA. Our work with *E. coli* W3110(pEDTA) bodes well for a *Rhizobium* sp. recombinant strain to degrade them as well. Once confirmed, the bacterium can then infect alfalfa roots for delivery into the subsurface, creating a field applicable system for bioremediation.

This dissertation presents a better understanding of the EDTA and NTA transport system of BNC1. Future work will need to address if $ZnEDTA^{2-}$ and $ZnNTA^{-}$ are directly transported inside the cell, or if the metal-chelates must respeciate in order for cellular uptake of EDTA to occur. Future work also includes developing a genetically modified organism that can be targeted directly to EDTA and NTA mixed wastes.

APPENDIX I

ATTRIBUTION PAGE

I preformed all experiments described in this dissertation except for the BNC1 whole cell uptake experiments in Chapter 2. The following is a summary of my research contribution and those who helped complete the research.

Chapter 2.

All experiments were done by me except for the BNC1 whole cell uptake experiments, which were done by Andy Plymale. Dr. Lisa Gloss helped set up fluorescence experiments, and Gerhart Munski helped set up microcalorimetry experiments. All the writing was done by me with input and editing from Dr. Xun, and editing by Dr. Bolton.

Chapter 3.

All the experiments were done by me alone. All the writing was done by me with input and editing from Dr. Xun.

Chapter 4.

All the experiments were done by me alone. All writing was done by me with input and editing from Dr. Xun.